DEVELOPMENT OF CATHODIC ELECTROCATALYSTS FOR USE IN LOW TEMPERATURE H_2/O_2 FUEL CELLS WITH AN ALKALINE ELECTROLYTE

Contract No. NASW-1233

Q-6

Sixth Quarterly Report
Covering October 1, 1966
Through December 31, 1966

by

J. Giner
J. Parry
L. Swette
R. Cattabriga

for
National Aeronautics and Space Administration
Headquarters, Washington, D. C.

DEVELOPMENT OF CATHODIC ELECTROCATALYSTS FOR USE IN LOW TEMPERATURE H_2/O_2 FUEL CELLS WITH AN ALKALINE ELECTROLYTE

CONTRACT OBJECTIVES

The research under contract NASW-1233 is directed towards the development of an improved oxygen electrode for use in alkaline H_2/O_2 fuel cells. The work is being carried out for the National Aeronautics and Space Administration, with Mr. E. Cohn as technical monitor. Principal investigators are Dr. J. Giner, and Dr. J. Parry.

NOTICE

This report was prepared as an account of Government sponsored work, Neither the United States, nor the National Aeronautics and Space Administration (NASA), nor any person acting on behalf of NASA:

A) Makes any warranty or representation, expressed or implied, with respect to the accuracy, completeness, or usefulness of the information contained in this report, or that the use of any information, apparatus, method, or process disclosed in this report may not infringe privately owned rights; or

B) Assumes any liabilities with respect to the use of, or for damages resulting from the use of any information, apparatus, method or process disclosed in this report.

As used above, "person acting on behalf of NASA" includes any employee or contractor of NASA, or employee of such contractor, to the extent that such employee or contractor of NASA, or employee of such contractor prepared, disseminates, or provides access to, any information pursuant to his employment or contract with NASA or his employment with such contractor.

Requests for copies of this report should be referred to:

National Aeronautics and Space Administration
Office of Scientific and Technical Information
Attn: AFSS-A
Washington, D.C. 20546

Development of Cathodic Electrocatalysts for Use in Low Temperature H_2/O_2 Fuel Cells with an Alkaline Electrolyte

Contract No. NASW-1233

Q-6

Sixth Quarterly Report
Covering October 1, 1966
Through December 31, 1966

for
National Aeronautics and Space Administration
Headquarters, Washington, D. C.

CONTENTS

		Page No.
	ABSTRACT	i
	Part 1 – The Testing of Interstitial Compounds of Fe	
I.	INTRODUCTION	1
II.	MATERIAL HANDLING	2
III.	INDUCTION METHODS	3
IV.	ACTIVITY TESTS	8
V.	DISCUSSION	12
VI.	ALTERNATE PLASTIC BINDERS	13
	A. Vydax (duPont)	13
	B. KEL-F (3M)	13
	C. FEP Fluorinated Ethylene Propylene (duPont)	13
	Part 2 – Solid Electrodes	
I.	INTRODUCTION	14
II.	EXPERIMENTAL	17
III.	RESULTS	18
IV.	DISCUSSION	19
V.	Pt/Os ALLOYS	21
	REFERENCES	22

ABSTRACT

Carbides, nitrides, nitrocarbides, and carbonitrides of iron have been examined for catalytic activity in the oxygen reduction reaction in 2N KOH at 75°C. Thirty-three compounds were tested, and a summary of their activities is given in Table III of this report.

The activities were very dependent on the way in which the catalysts were inducted, i.e. initially exposed to oxygen. A sample of χ -Fe_2C (#11C) when exposed directly to air showed a current of 3 ma/ cm^2 at 600 mv vs. RHE; this increased to 42 ma/ cm^2 at 600 mv when the catalyst was first immersed in petroleum ether. The petroleum ether was replaced successively by diethyl ether, acetone, and methanol, the catalyst being covered by solvent at all times until the methanol was allowed to evaporate slowly in air.

Except for catalysts containing silver, the maximum activity observed reproducibly was 40 ma/ cm^2. Two compounds, samples #5N (ϵ -Fe_3N + γ' -Fe_4N) and 6N (ϵ-Fe_3N + ζ -Fe_2N), exceeded this value initially with activities of 53 and 58 ma/ cm^2 at 600 mv vs. RHE, but these performances could not be repeated. The general pattern of activity was nitrides > carbonitrides > carbides $\geq$ nitrocarbides. Some exceptions to this sequence are apparent in Table III. Despite some internal inconsistencies in the results, the measurements reported here define the ultimate level of activity of this group of catalysts with sufficient precision and show that it is below the level of practical usefulness required of an oxygen electrocatalyst in a H_2/ O_2 fuel cell.

Current voltage curves from slow potential sweeps (50 mv/ min) and fast potential sweeps (500 mv/ sec) were recorded for oxygen reduction in 2N KOH at 25°C with 9 samples in each of the alloy systems Au/ Pd, Au/ Pt, and Au/ Ag. The experimental techniques and methods of measurement were carefully controlled to give precise information on surfaces having a composition identical to that of the bulk phase. Tafel plots (E vs. log i) were derived from the current voltage curves, and

within the range of linearity of these plots, comparisons were made of potentials corresponding to selected values of current density (E_i). It can be shown that these E_i values reflect the catalytic activity of the surface.

The order of activity was Au/Pd> Au/Pt > Au/Ag; for the 1:1 alloys the following E_i values were recorded for i = 50 $\mu a/cm^2$: Au/Pd - 926 mv, Au/Pt - 878 mv, Au/Ag - 856 mv vs. RHE. The Au/Pd exhibits a shallow maximum of activity over the range 70/30 - Au/Pd to 30/70 Au/Pd; the Au/Pt and Au/Ag alloys show, with some scatter, a steady transition from the activity of one pure component to the other. The enhanced activity of the Au/Pd alloys is not unexpected and has been reported in the literature. An interesting feature of these results is that at 25°C pure Pd (E_{50} = 922 mv vs. RHE) is more active than pure Pt (E_{50} = 880 mv vs. RHE). As the temperature was increased from 25°C to 75°C, the activity (E_{50}) of pure Pt increased from 880 to 903 mv, while that of Pd decreased from 922 to 915 mv. In other words, at 75°C and 50 $\mu a/cm^2$ Pd was still somewhat more positive (12 mv) than Pt.

The fast sweep measurements indicated that for the most part the alloys retain the individual characteristics of the component metals with respect to the formation and reduction of oxygen films.

An initial examination of Pt/Os 80/20 alloy in an unannealed condition was carried out. The $E_{1/2}$ value of 850 mv was identical to that of Pt, but this value probably relates to a two-phase system with a surface rich in Pt.

PART 1

THE TESTING OF INTERSTITIAL COMPOUNDS OF Fe

I. INTRODUCTION

The carbides, nitrides, and carbonitrides of iron, nickel, and cobalt are an interesting group of catalysts which have been investigated in detail in connection with the Fischer-Tropsch reaction. [1] [2] Because of their metallic properties and their possible enhanced resistance to oxidation as compared with their parent metals, this class of materials presents attracti possibilities as oxygen reduction electrocatalysts. Previous measurements with porous Ni_3C electrodes showed very high activity for O_2-reduction, at least for short-term measurements. In addition, initial measurements in which an iron rod was carbided on the surface demonstrated that iron carbide had a somewhat higher activity than pure Fe. This point has been investigated in detail, using highly dispersed iron carbide.

During this report period a range of interstitial compounds of Fe in finely divided form was prepared by the Bureau of Mines, as part of a cooperative program. In the finely divided state (BET surface areas in the range 10-27 m^2/g) many of these materials were pyrophoric. Pyrophoric oxidation probably results in the complete oxidation of the sample and, for finely divided materials, the loss of a large proportion of their surface area. Special techniques were developed to induct the materials prior to exposure to oxygen during electrochemical testing. The basis of these techniques was to carry out the initial oxidation process as slowly as possible. Thus it was hoped to limit the extent of oxidation and any significant increase in temperature to avoid appreciable loss of surface area by sintering.

II. MATERIAL HANDLING

The materials were delivered in sealed containers under an atmosphere of CO_2; the first process was to divide the sample into eight approximately equal lots. The subdivision was carried out in a glove box in a nitrogen atmosphere; the individual samples were contained in plastic snap top bottles that were further sealed in paraffin wax as the bottles were brought out of the inert atmosphere. A freshly prepared sample of Raney nickel was subjected to exactly the same procedures as the Bureau of Mines materials up to the stage of wax sealing. The Raney nickel was then exposed to air and on each occasion the sample was pyrophoric, indicating the effectiveness of the glove box in each case. (The surface of Raney nickel is easily passivated by exposure to very small amounts of O_2 and becomes nonpyrophoric.)

Also, during the subdivision of the samples, the resistance of the powder was measured. The sample was contained between two pieces of Pt foil by an O ring 1/2" O.D. and 5/16" I.D. The sample was then compressed at constant pressure in a jig using a torque wrench (Sturtevant Model F-21-1 at 15 inch pounds) and the resistance measured. The resistance of exposed and inducted samples was measured in an attempt to measure the need for, or the effectiveness of, the induction procedure. The method was only used to determine major changes in conductivity (See below).

III. INDUCTION METHODS

The activities found for the initial samples tested were very low (< 2 ma/cm^2). For each of these, no induction process was used since the resistance did not change on exposure to air. Methods of induction were examined in detail for sample 11C; this material is uniquely defined at χ - Fe_2C (Hagg carbide) with no free Fe or Fe_2O_3.* Two factors were considered to be important.

(1) The rate and extent of the initial oxidation of the surface, thought to be dependent on how and at what stage of the electrode fabrication process the catalyst is first exposed to air.

(2) The effect of the sintering process in the preparation of PTFE bonded electrodes (15 mins at 275°C); complete details of electrode manufacture are recorded in a previous report [5].

The experiments carried out are detailed in Table I. The effect of exposure to air when covered with methanol or water is believed to produce slow oxidation of the surface, either by reaction with dissolved O_2 or by progressive exposure to air during evaporation of the liquid layer. Elvax (a duPont polyvinyl resin) was substituted for PTFE as a plastic binder in the tests to investigate the effect of sintering. Elvax electrodes were prepared by dissolving the appropriate quantity of the resin in trichloroethylene at 70 - 80°C; after cooling to 35°C the catalyst was added and the mix distributed on a nickel screen. The electrodes required no sintering and were tested after evaporation of the residual solvent. The results obtained with Elvax bonded Pt electrodes were equivalent to some of the better results obtained with PTFE bonded Pt electrodes, indicating that this was an effective method of catalyst testing. The life of the Pt electrode was, however, limited to about two hours, probably due to oxidation of the Elvax under the test conditions (35%KOH at 75°C). The life of Elvax-bonded electrodes prepared from the interstitial compounds was somewhat longer (3-4 hours). Other plastic binders are being examined in order to obtain longer lived electrodes.

The main conclusion drawn from these experiments, outlined in Table I, was that careful induction of the catalyst produces a more active

* Details of the manufacture and characterization of these catalysts is given in the reports of the Bureau of Mines [3].

TABLE I

Inducting Methods For Catalysts 11-C

		Activity ma/cm^2 at 600 mv
ELVAX ELECTRODES		
1. Electrode made in N_2 then		
(i) Exposed to air slowly		10
(ii) Exposed to air in water		4
(iii) Exposed to air in methanol		4
2. Catalyst inducted by		
(i) Exposure to air slowly	Electrodes made in air	10
(ii) Exposure to air in water		3
(iii) Exposure to air in methanol		32
PTFE ELECTRODES		
3. Electrode made and sintered in N_2		10
4. Electrode made in air sintered in N_2 using catalyst 2 (iii)		12

electrode and also that resistance measurements on the dry powder are not sensitive enough to relate to activity.

The electrodes made with PTFE, in which the catalyst was exposed to air in the first case (#3, Table I) after sintering and in the second case (#4, Table I) before sintering, showed no significant difference. Both were comparable to electrode #1 (i) made with Elvax. However, this cannot be regarded as a conclusive indication that the sintering process is not detrimental, since the test was not conducted with the catalyst in its most active form.

The induction method was further refined by the use of the following techniques:

(1) Slow oxidation in the gas phase

(2) Extension of the liquid phase induction in methanol to a sequence of organic solvents (petroleum, ether, diethyl ether, aceton and methanol), a sequence in which the reactivity and solubility of oxygen increases.

The slow gas phase oxidation was carried out by the Bureau of Mines with a second sample of material 11-C. Three samples of 11-C were supplied: an untreated sample, one that had been oxidized in 0.1% O_2 in N_2 for 100 hours at room temperature, and another in 1% O_2 in N_2 for 100 hours at room temperature. All were tested as Elvax bonded electrodes and compared with further samples that had been subjected to the liquid phase induction described above. The details of the tests and the results are presented in Table II. The uniformity of the results (all except one produced close to 20 ma/ cm^2 at 600 mv) indicates that all attempts, both at Tyco and at the Bureau of Mines, to induct this material were of no consequence. This is in direct contrast to the results reported previously. Further, the activity of the uninducted sample A is higher than previously observed, suggesting that the surface was in some way conditioned prior to the induction processes. The improved efficiency of the extended liquid phase induction process was demonstrated by the induction of the original sample of 11-C to produce an activity of 40 ma/ cm^2 at 500 mv; this compares to 33 ma/ cm^2 observed with simple methanol induction

TABLE II

11C – Oxygen Induction Series (B. O. M).

Sample	A	B	C	A	B	C
B. O. M. Pretreatment	None	Inducted in N_2 with 0. 1% O_2 100 hours	Inducted in N_2 with 1. 0% O_2 100 hours	None	Inducted in N_2 with 0. 1% O_2 100 hours	Inducted in N_2 with 1. 0% O_2 100 hours
Tyco Pretreatment	None	None	None	Catalyst Inducted in Pet. Ether etc.	Catalyst Inducted in Pet. Ether etc.	Catalyst Inducted in Pet. Ether etc.
Binder	10% Elvax	10% Elvax	10% Elvax	10% Elvax	10% Elvax	10% Elvax
Electrode Activity ma/cm^2 at 600 mv	19. 3	18. 2	18. 0	18. 4	14. 4	19. 8

The induction method for the protection of the activity of Raney nickel described in German Patent 1,185,589 (Doehren and Jung to Varta Pertrix-Union G. m. bH) , in which the catalyst was immersed in a polyhydric alcohol such as ethylene glycol, was not successful for induction of catalyst 11-C.

IV. ACTIVITY TESTS

The experimental determination of the activity of these catalysts as plastic bonded floating electrodes was carried out as has been described previously [4]. The measured activities with all relevant information on the method of testing is presented in Table III.

TABLE III

Activity of Interstitial Compounds of Fe

	Sample	Induction	Electrode Type	Activity[1]
1 NC	ϵ-Fe_2X[2] + Fe_3O_4	P[3]	Elvax (10%)	3.2
		P	PTFE (10%)	3.2
2 NC	χ-Fe_2X + ϵ-Fe_2X + C	P	Elvax (i) (10%)	3.5
		P	(ii) (10%)	0.4
		P	PTFE (i) (10%)	68.0
		P	(ii) (10%)	5.2
3 NC	ϵ-Fe_2X	P	Elvax (10%)	1.6
4 NC	ϵ-Fe_2X	P	Elvax (10%)	Anodic[4]
5 NC	θ-Fe_3X	P	Elvax (10%)	5.4
6 NC	χ-Fe_2X	P	Elvax (10%)	1.2
7 NC	θ-Fe_3X	P	Elvax (10%)	Anodic
		P	PTFE (10%)	Anodic
I CP	$Fe(OH)_3$ + Ag_2O (3:1)	None	Elvax (5%)	1.0
II CP	$Fe(OH)_3$ + Ag_2O (1:1)	None	Elvax (10%)	92.0
III CP	$Fe(OH)_3$ + Ag_2O (1:3)	None	Elvax (8%)	59.0

(1) Activity – Current density (ma/cm^2) at 600 mv vs. RHE

(2) X – Carbon or nitrogen

(3) P – Catalyst inducted by exposure to petroleum ether, diethyl ether, acetone, methanol, the last solvent being allowed to evaporate slowly

(4) An anodic current indicates a corrosion rate greater than the oxygen reduction process

TABLE III (Cont.)

	Sample	Induction	Electrode Type	Activity
2 N	γ' -Fe_4N + ϵ-Fe_3N	P	Elvax (10%)	0.6
		None	PTFE (19%)	3
5 N	ϵ-Fe_3N + γ' -Fe_4N	P	Elvax (10%)	0.6
		None	PTFE (10%)	58
6 N	ϵ-Fe_3N + ζ - Fe_2N	P	Elvax (10%) (i)	1.3
		P	(10%) (ii)	2.2
		None	PTFE (19%) (i)	53.0
		None	(19%) (ii)	2.6
8 N	γ' -Fe_4N	P	Elvax (10%)	6.4
9 N	ζ-Fe_2N	P	Elvax (10%)	3.0
		None	PTFE (10%)	27.0
11 N	ϵ-Fe_3N + Ag (3:1)	P	Elvax (10%)	14.8
13 N	ϵ-Fe_3N	P	Elvax (10%)	12.4
			PTFE (10%)	Anodic
15 N	ϵ-Fe_3N + Ag (1:1)	P	Elvax (10%)	19.4
16 N	ϵ-Fe_3N + Ag (1:3)	P	Elvax (10%)	14.0
18 N	ζ-Fe_2N + ϵ-Fe_3N	P	Elvax (10%)	Anodic
2 C	ϵ-Fe_2C + Fe_3O_4	None	Elvax (10%)	Anodic
		P	PTFE (i) (10%)	1.0
		P	(ii) (10%)	11.0
4 C	χ -Fe_2C + Fe_3O_4	None	Elvax (10%)	1.0
6 C	χ -Fe_2C + θ-Fe_3C		Elvax (10%)	
		None	PTFE (19%)	4.0
10 C	θ-Fe_3C + Fe	P	Elvax (10%)	3.4
11 C	χ -Fe_2C + C See separate Table			

TABLE III (Cont.)

	Sample	Induction	Electrode Type	Activity
1 CN	ϵ-Fe_2X	None	PTFE (10%)	1.0
2 CN	ϵ-Fe_2X	P	Elvax (10%)	Anodic
		P	PTFE (10%)	2.9
3 CN	ϵ-Fe_2X	P	Elvax (10%)	Anodic
6 CN	ϵ-Fe_2X + Ag (3:1)	P	Elvax (10%)	7.0
7 CN	ϵ-Fe_2X + Ag (1:1)	P	Elvax (10%)	11.6
8 CN	ϵ-Fe_2X + Ag (1:3)	P	Elvax (10%)	5.4
9 CN	γ'-Fe_4X	P	Elvax (10%)	Anodic
10 CN	γ'-Fe_4X	P	Elvax (10%)	1.9

V. DISCUSSION

The highest activities measured for this series of interstitial compounds of iron, in the range 40-60 ma/ cm^2 at 600 mv vs. RHE, cannot be considered to be of practical usefulness for H_2/O_2 fuel cells. This level of activity does not compare with the preliminary results for Ni_3C (100 ma/ cm^2 at 880 mv) which were obtained for PTFE bonded electrodes for uninducted samples.

Some of the results presented in Table III require qualification in that several of the activity levels are inverted for the Elvax and PTFE bonded electrodes and are not readily reproducible. The most probable reason for this is a degree of uncertainty associated with electrode fabrication, particularly in the case of the Elvax bonded electrodes in which some coating of the catalyst with loss of surface area is possible.

The highest activities were observed for samples #5N and #6N at 53 and 58 ma/ cm^2 at 600 mv vs. RHE respectively, though these figures were not reproduced when checked out at a later date, (giving 1.3 and 2.2 ma/ cm^2). The differences were too great to be accounted for in terms of electrode structure and were attributed to the fact that the subsequent electrodes were made from an inducted powder that had been exposed to air for several weeks. No repeat tests were carried out on freshly inducted material. Taking into account the initial figures for # 5 N and # 6 N, the general picture of order of activity for these materials is nitrides > carbonitrides > carbides $\geq$ nitro carbides. Those materials in which silver was included to increase the conductivity of the electrode structure showed relatively large activities (90 ma/ cm^2) most of which are due to the silver. (Pure silver electrodes should give substantially higher figures $\sim$ 200 ma/ cm^2 at 900 mv). It is considered, however, that the measurements remain a reliable guide to the level of activity though quantitative internal comparisons cannot be made with confidence. A search for alternative plastic binders that would avoid the sintering process and increase the reliability of the electrode fabrication process is being carried out; the work is reported below.

VI. ALTERNATE PLASTIC BINDERS

The main objective in looking at alternate binders is to avoid the sintering process at 275°C associated with the PTFE bonded electrodes. The requirements of the binder are that it should be hydrophobic and inert; ideally the particulate form of the PTFE dispersions should be retained to prevent the partial coating of the catalyst that is inevitable with dissolved materials. The initial examination has considered alternative fluorinated polymers since they offer the best properties in terms of being inert and nonwetting.

A. Vydax

Tetrafluoroethylene (a low molecular weight PTFE) in a Freon solvent (duPont).

Electrodes were made from a paste of Pt black and Vydax; 75% by weight polymer was needed to obtain even a fragile electrode structure. These electrodes were not sintered and were waterproof, but no successful electrochemical tests were possible.

B. KEL-F (3 M)

Polychlorotrifluoroethylene in Xylene.

The electrodes made with this material were not waterproof and disintegrated on complete evaporation of the xylene.

C. FEP Fluorinated Ethylene Propylene (duPont)

This material is available as an aqueous dispersion and is very similar in characteristics to PTFE. It is, unlike PTFE,thermoplastic and softens at a much lower temperature than PTFE. Attempts were made to prepare electrodes with low sintering temperatures. Electrodes prepared at 275°C showed slightly higher activity at low current density and approximately the same performance at high current density. FEP is, therefore, a practical alternative to the present method with PTFE, offering the advantage of sintering at 150°C. Electrodes dried at 100°C in a vacuum oven, however, showed very little activity. This experiment is being pursued to check whether this is due to incomplete removal of the wetting agent.

Further experiments are being carried out with polyethylene.

PART 2

SOLID ELECTRODES

I. INTRODUCTION

This report describes the examination of the activity of Au/Pt, Au/Pd, and Au/Ag alloys for the cathodic reduction of O_2. The interest lies in the changes in electronic configuration and lattice parameter with composition and the differences in the extent of the adsorbed oxygen film on the parent metals in the potential range 800-1200 mv vs. RHE. These factors have been discussed in a previous report[5].

Compared to the earlier survey of metals and alloys in which we were seeking to define only the level of activity, this study requires greater experimental precision. The improvements to the apparatus were described in the previous report[5], along with some results for the Au/Pd system. The results were termed provisional at the time because of two unexpected features in the experimental curves. These were (1) an unusual cathodic peak in the limiting current during the return sweep (increasing potential) at 250-500 mv; and (2) an anodic current, also observed with gold, at potentials > 900 mv, which varied with time and immediate past history of the system. Both these factors were important in considering our present objectives. The peak in the limiting current was undesirable because it prevented precise definition of $E_{1/2}$ (the significance of $E_{1/2}$ as a measure of activity was described in the Fourth Quarterly Report of this contract,) and because it was an indication of an impurity in solution that was actively involved in the oxygen reduction reaction. The anodic current was undesirable because it occurred in the potential region where the O_2 reduction process is activation controlled. The activation controlled region (Tafel region) of the current voltage curve is that part where the surface reaction, which is dependent on the catalytic activity of the electrode, controls the over-all rate of the reduction reaction. Measurement of the rate, the current density per real square centimeter of the surface

as a function of potential, in this region is a means of assessing the activity of the electrocatalyst. Therefore, the presence of a simultaneous anodic process of any magnitude restricts precise determination of the electrocatalytic activity toward the O_2 reduction process (further discussion below). Prior to making the experimental measurements on the three systems, the possible causes of the anodic current and the cathodic peak were investigated.

Gold was chosen as the electrode material for the investigation since it allows the most sensitive measurements of side reactions. The anodic current occurred at all potentials > 800 mv under N_2. Under O_2 the anodic current was not observed until higher potentials (~ 950 mv), but it was assumed that the anodic reaction occurred simultaneously at the lower potentials affecting the magnitude of the observed cathodic current. The anodic current usually increased with time and frequently showed a sharp increase after the determination of a current voltage curve under O_2.

Several explanations were considered: electrolyte leakage between the electrode and mount, impurities in solution, peroxide oxidation or platinum contamination of the electrode surface.

Electrolyte leakage was eliminated since it is an accidental occurrence and is accompanied by a marked sloping of the curve obtained in N_2. This was not observed.

An explanation in terms of impurities in solution was not consistent with the increase of the anodic current with time and in the presence of O_2. However, this behavior does correspond to the accumulation in the electrolyte of H_2O_2 (or more precisely HO_2^-) produced by the incomplete reduction of O_2. This is particularly the case when the electrode material is not a good peroxide decomposition catalyst. To check the effect of peroxide accumulation, hydrogen peroxide was added to the electrolyte to make a 10^{-3}M solution. The anodic current increased by a factor of 10^3. If it is assumed that the current is diffusion controlled then the anodic currents usually observed correspond to a solution 10^{-6}M in peroxide. This condition is considered feasible under the normal operating conditions, particularly since the electrode is at low positive potentials for quite long periods during the slow sweep measurements. A large gold scavenger electrode was introduced to the

system and maintained at a potential of 1 v vs. RHE, in order to consume accumulated peroxide. However, this electrode was not as efficient as was expected in the oxidation of HO_2^-, and did not reduce the magnitude of the anodic current possibly because of poor transport of OH^- to its surface.

The anodic currents have been minimized by working with fresh electrolyte for every determination, by conducting the measurements in the shortest possible time and by using a restricted potential range for the slow sweep studies (see below) thereby reducing the amount of peroxide produced.

The cathodic peak in the limiting current of O_2 reduction to HO_2^- is considered to be a catalytic peak. It did not appear when the potential was maintained above 300 mv vs. RHE suggesting that the effect was possibly due to the complete reduction of O_2 to water catalyzed by the metal deposited at the low potential.

Kronenberg[6] has reported that a 1 M solution of KOH contained 1-10 ppm of Fe, Ag, Cu and Cr. For iron a 5 ppm impurity level corresponds to a 10^{-4} M solution. Electrolytic purification of potassium will be undertaken in order to prepare ultra pure KOH.

One of the sources of impurities that was considered was the counter electrode. Initially, Pt was excluded from the system because of its possible dissolution and deposition on the surface of the work electrode, thereby changing its character, including oxygen film formation at lower potentials. Measurements carried out with a graphite counter electrode indicated that it contained leachable impurities. Gold was excluded on the same basis as Pt. Any gold deposited on the working electrode would not show the difference in activity expected of Pt but could give rise to a continuously changing surface roughness. The system subsequently used for the counter electrode was a massive piece of Ag/Pd alloy charged with H_2. The anodic process that occurs to complement the cathodic reduction of O_2 is hydrogen oxidation, and since this occurs at < 100 mv vs. RHE, no metal dissolution can occur. (At inert electrodes the anodic reaction is O_2 evolution at very high positive potentials.)

II. EXPERIMENTAL

The following alloy systems were examined at 10% increments of composition: Au/Pd, Au/Pt, and Au/Ag. The experimental methods, described below, were carried out with rotating electrodes with the configuration described by Makrides and Stern (Fig. 1). This configuration is the most convenient for the present studies in that the electrodes are readily mounted in a leak tight manner without the electrolyte coming into contact with any plastic mounting other than PTFE. Transport of the reacting species (O_2) is fast enough to both the walls and the base of the cylinder to study between one and two decades of current in the activation controlled region of the oxygen reduction reaction.

The two experimental techniques were (1) fast potential sweeps at 50 mv/min carried out in the presence of a N_2 saturated solution (2 N KOH at 25°C) to determine the extent of surface oxidation of the alloys and (2) slow sweeps at 50 mv/min in an O_2 saturated solution to define the current voltage relationship for the O_2-reduction reaction. The fast sweeps are shown in Figs. 2 to 13. The potential range for these fast sweeps was limited for the gold palladium alloys to 400 mv → 1600 mv vs. RHE to avoid the absorption of H_2 by palladium at low positive potentials. Changes in lattice parameter associated with H_2 uptake can significantly increase the specific surface by cycling, and because subsequent oxidation of the H_2 masks the surface oxidation processes being studied. Particular precautions were taken to prevent surface roughening and changes of surface composition of the alloys. The samples were repolished for each experiment; in addition, the number of potential cycles applied to the electrode before the recorded measurements was restricted. All the measurements presented in Figs. 3 to 13 were taken on the fourth sweep, the first three being used to set up and align the trace on the oscilloscope. For the slow sweep, the electrode was again polished and the potential range restricted to 600-1000 mv to prevent surface composition changes and the accumulation of peroxide as discussed above. A typical example of a slow sweep curve is shown in Fig. 14.

III. RESULTS

The complete series of results is presented in the form of E-log i curves in Figs. 15 to 45. The linearity of the E log i curves for over a decade of current confirm that in this particular region the reaction is activation controlled.

The activities of the complete range of alloys are presented in Figs. 46 and 47 as the potential corresponding to a particular current density; the current was normalized for the real surface area of the electrodes using the double layer capacities which were measured by means of a fast triangular sweep technique. Also shown in Fig. 48 are the activities defined in terms of potential at a constant current density (per geometric square centimeter). The pattern of activity is the same.

IV. DISCUSSION

The observed order of activity is Au/Pd > Au/Pt > Au/Ag. The Au/Pt and Au/Ag alloys show, with some small scatter, a smooth transition from the activity observed for gold and that of the second component. The Au/Pd alloys show an activity pattern with a shallow but quite definite activity maximum in the region of 30-40% gold. These results confirm the enhanced activity reported in the literature for the Au/Pd alloy[7]. The surprising feature of the results is that at 25°C the activity of pure Pd is greater than that of pure Pt; this was confirmed in a second measurement of the activities.

The activity pattern is the same at 75°C (Fig. 49), though the difference in activity is not as great as at 25°C. These figures may be compared with the previous results which were also determined at 75°C.

	E (mv) at i = 50 $\mu a/cm^2$ (Fig. 49)	$E_{1/2}$ from 4th Quarterly Report
Pd	915	835
Pt	903	845

Although the difference is small, greater confidence is placed in the present results, since they were obtained under more carefully defined conditions and because the $E_{1/2}$ values were determined using the equation

$$\eta = \eta_{act} + \frac{Z'}{Z\alpha}\ 0.018$$

which applies rigorously only to electrodes with the same limiting current density.

An important reason why Pd has not been extensively used in practice is that it is known to corrode at a significant rate at positive potentials in KOH (or in acid) at 75°C and above. The anodic current observed at 1000 mv was 3 $\mu a/cm^2$ for Pd compared to 1 $\mu a/cm^2$ for Pt, though no great significance

should be attached to the absolute value of these figures. It is therefore of considerable interest to note that the activity of Pd is maintained or even enhanced in the gold alloys up to 70% Au, particularly since it might be expected that the corrosion resistance of the alloys would be better than that of pure Pd, as it is for the Ni alloys of Mn and Co[4]. The level of activity, compared to Pt, shown by these gold alloys of palladium warrants further examination in a practical form as finely divided catalysts. We will investigate methods of preparing alloy blacks in order to make up PTFE bonded electrodes.

The fast sweeps of Figs. 2 to 13, are primarily of interest in terms of the formation and reduction of the adsorbed oxygen films at the more positive potentials.

A significant feature is that separate peaks exist for the O_2 desorption process (cathodic current) on the Au/Pd and Au/Pt alloys, the relative magnitudes changing with the alloy composition. This indicated that, for the most part, the component metals retain their individual characteristics with respect to oxide reduction, and do not exhibit any composite properties. The behavior of the Ag/Au system is quite different in this respect but this is to be expected for two metals that have identical electronic configuration.

V. Pt/Os ALLOYS

An initial examination of a Pt/Os 80/20 alloy in an unannealed condition was carried out, Fig. 50. The $E_{1/2}$ = 850 mv vs. RHE was identical with that of pure Pt. Subsequently, when the sample was polished after annealing, some unmelted Os metal was exposed so that the percentage of alloyed Os was considerably less than 20% in the above sample. The measurements will be repeated when single phase alloys have been prepared.

REFERENCES

1. J. F. Shulty, L. J. E. Hofer, E. M. Cohn, K. C. Stein, and R. B. Anderson, Bulletin 578, 1959, Bureau of Mines, Synthetic Liquid Fuels from Hydrogeneration of CO.
2. J. C. Shultz, L. J. E. Hofer, K. C. Stein and R. B. Anderson, Bulletin 612, 1963, Bureau of Mines, Carbides, Nitrides and Carbonitrides of Iron as Catalysts in the Fischer Tropsch Synthesis.
3. Monthly Progress Reports to NASA, August-December 1966, Bureau of Mines, Pittsburgh Coal Research Center.
4. Fourth Quarterly Report, Contract No. NASW-1233, June 1966.
5. Fifth Quarterly Report, Contract No. NASW-1233, September 1966.
6. M. L. Kronenberg, J. Electro anal. Chem. (12) 168 (1966).
7. J. H. Fishman and E. F. Rissman, Extended Abstracts, Spring Meeting of the Electrochemical Society, San Francisco, May 1965.

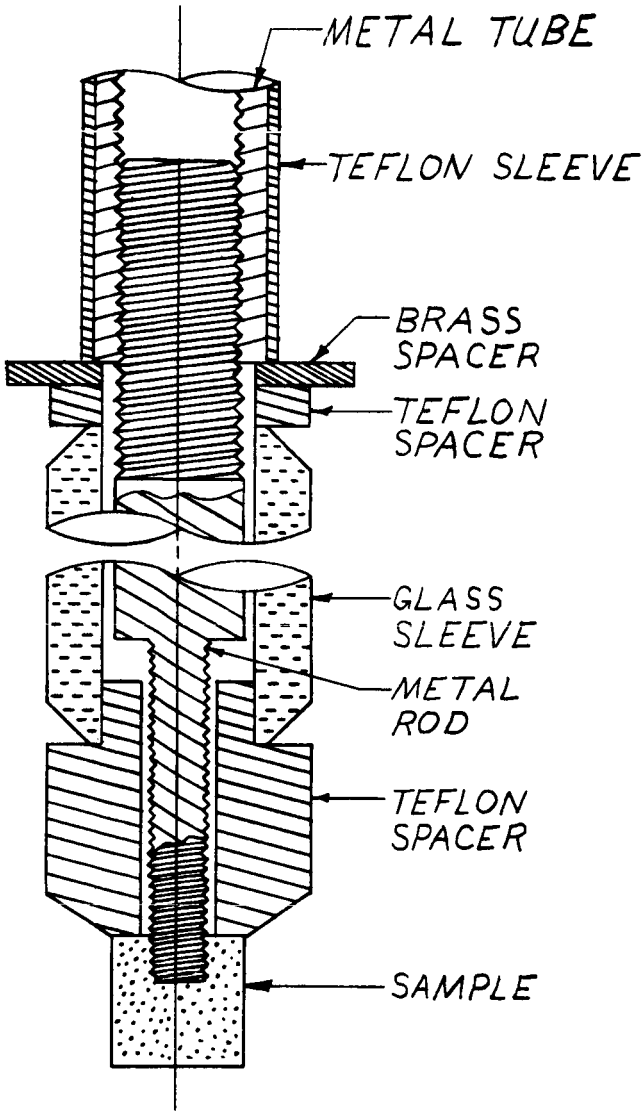

Fig. 1 "Makrides-Stern" holder

GOLD - PALLADIUM ALLOYS (SHORT-SWEEPS)

GOLD

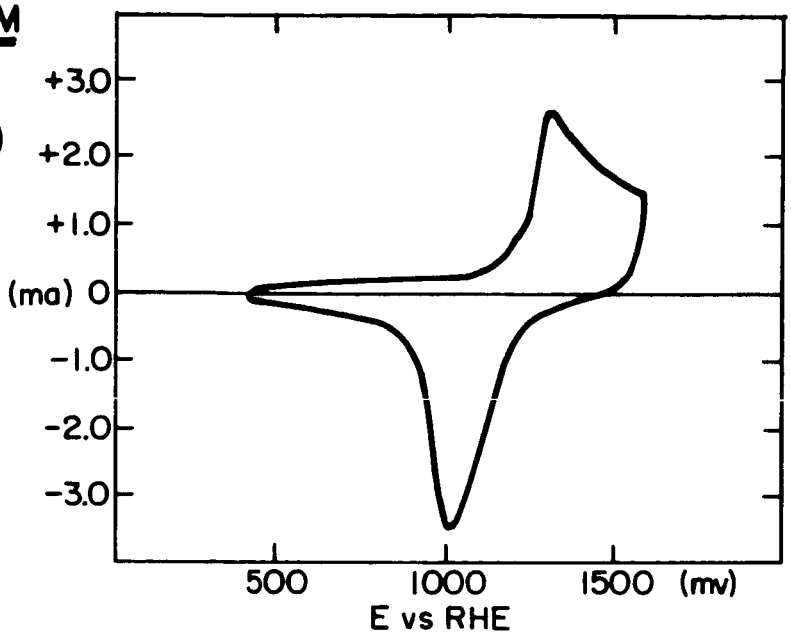

Au - Pd 90 - 10

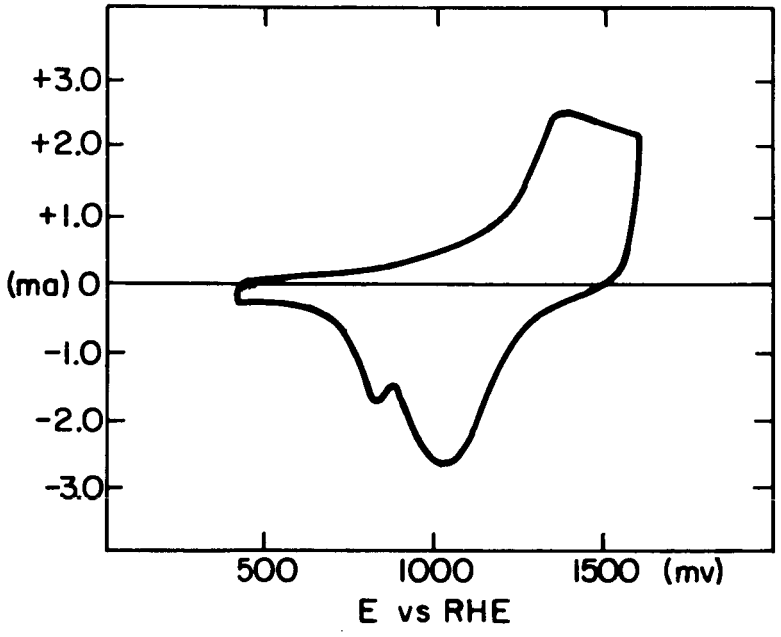

Au - Pd 80 - 20

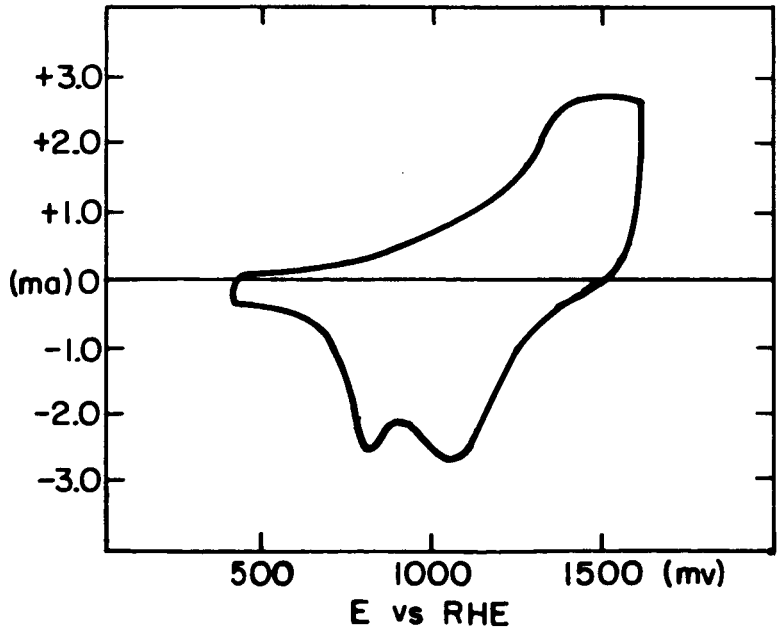

Fig. 2

Au-Pd
70-30

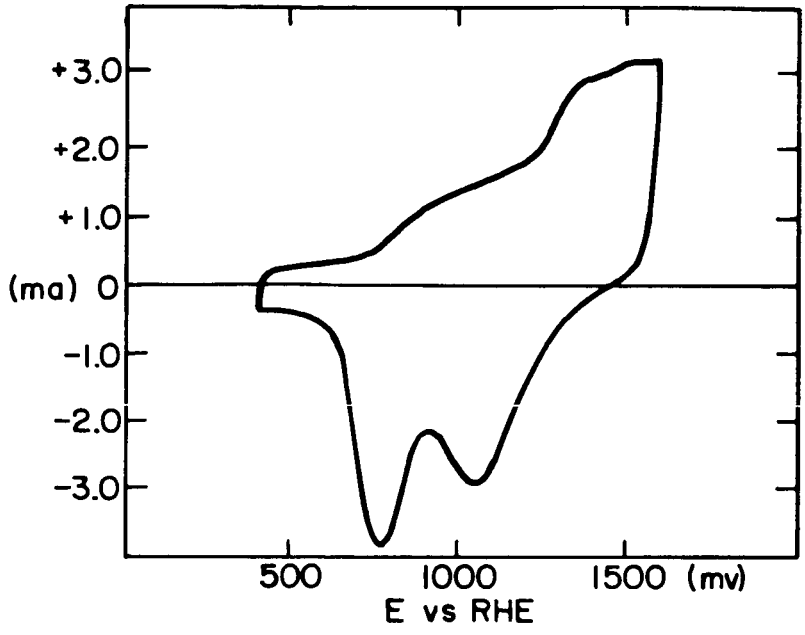

Au-Pd
60-40

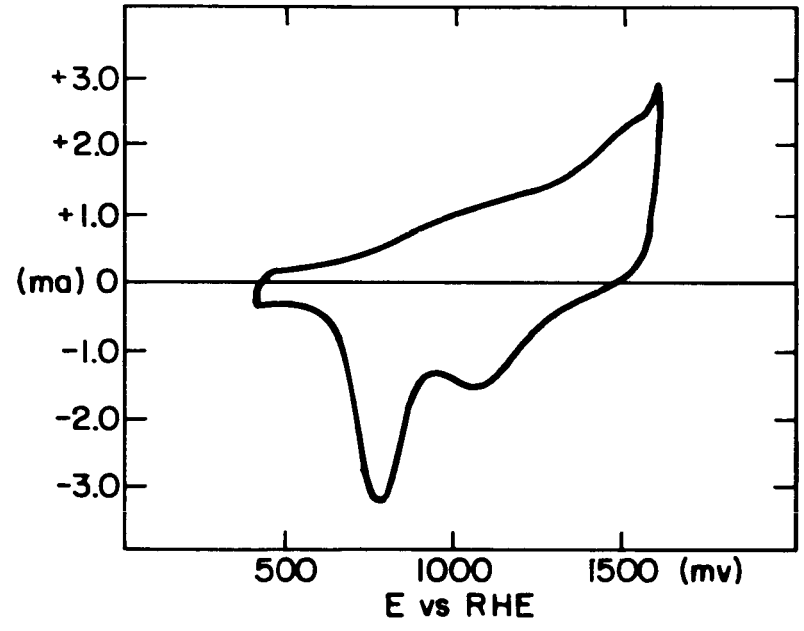

Au-Pd
50-50

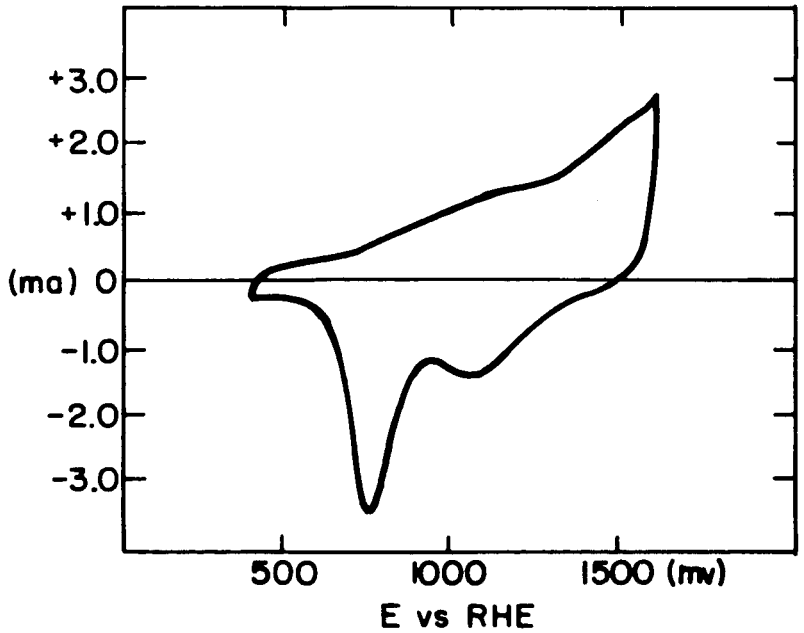

Fig. 3

Au - Pd
40 - 60

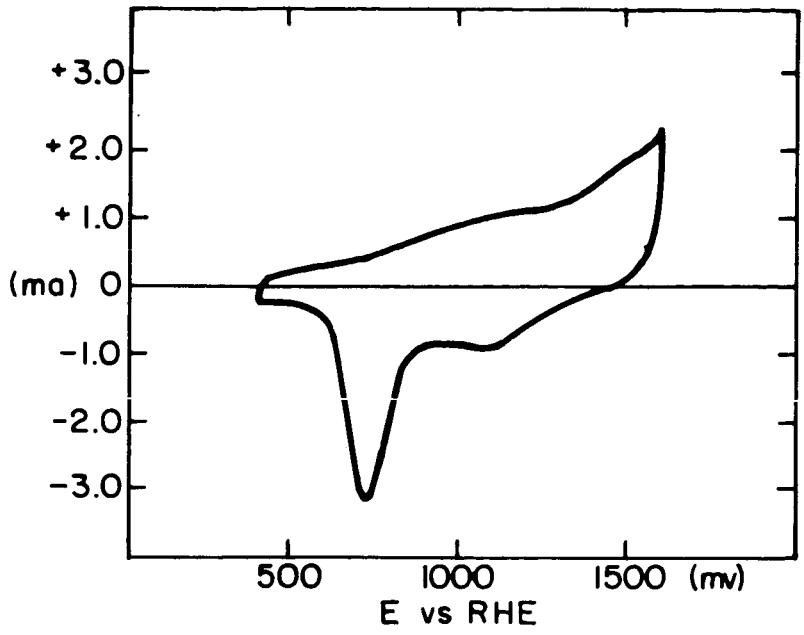

Au-Pd
30-70

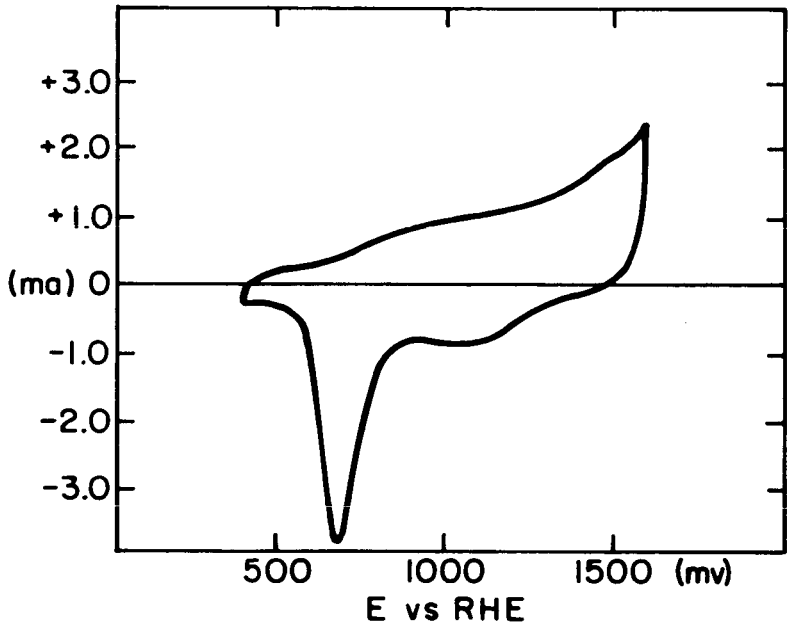

Au-Pd
20-80

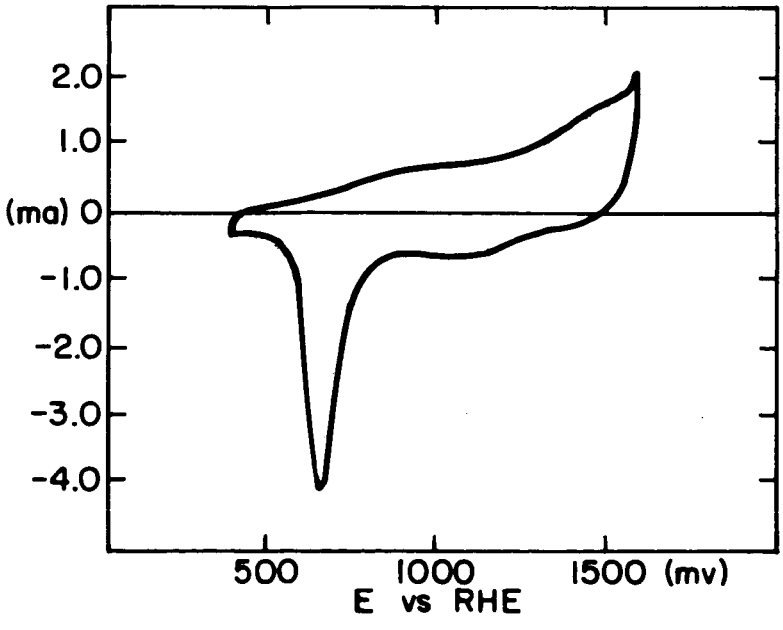

Fig. 4

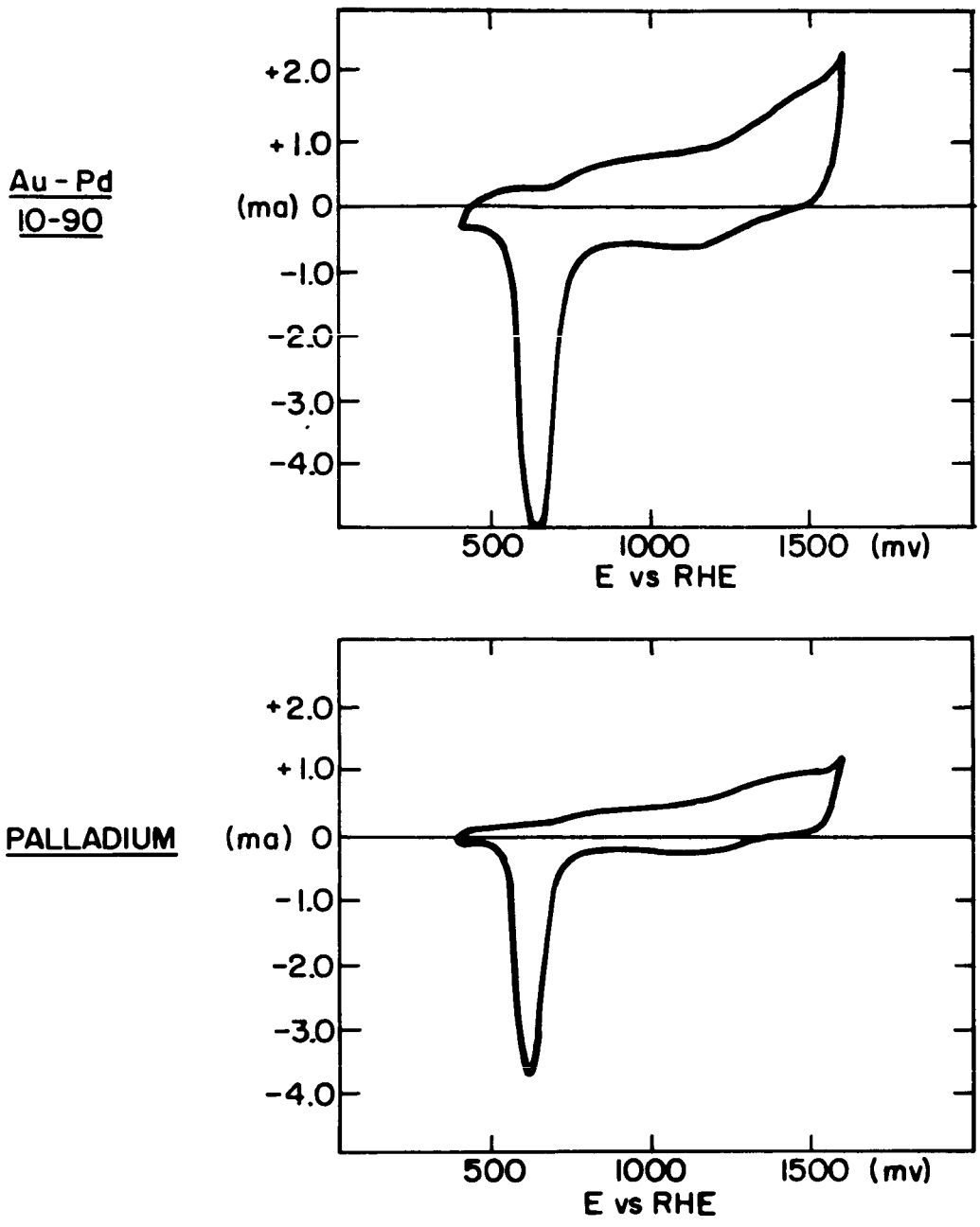

Fig. 5 All of the above measurements (Au-Pd Series) were made under the following conditions:

N_2 - Saturated 2N KOH, 25°C
500 mv/sec, 4th sweep recorded
E vs Rev. H_2 elec., Pd-Ag/H_2 counter electrode
Makrides-Stern electrode holder-rotated at 600 RPM
Geometric areas approx. 1.5 cm^2

GOLD-PLATINUM ALLOYS

GOLD

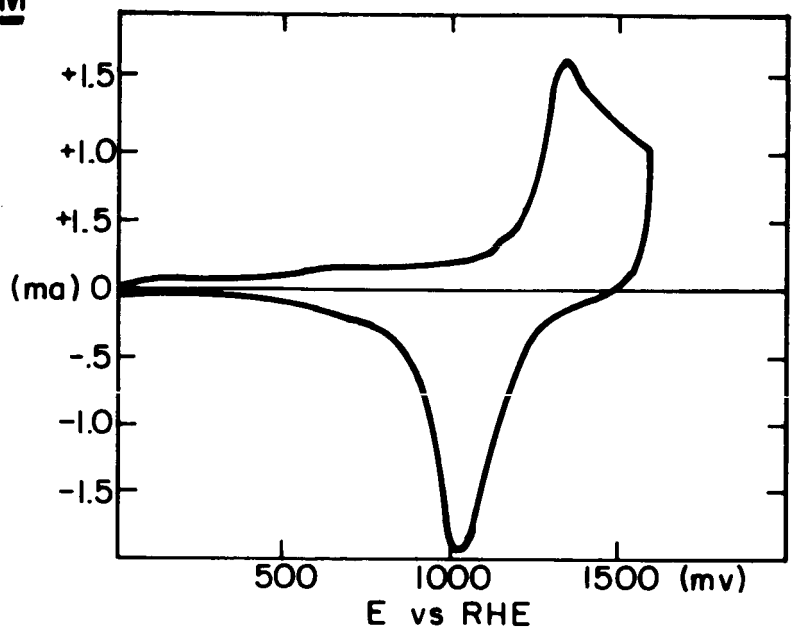

Au-Pt
90-10

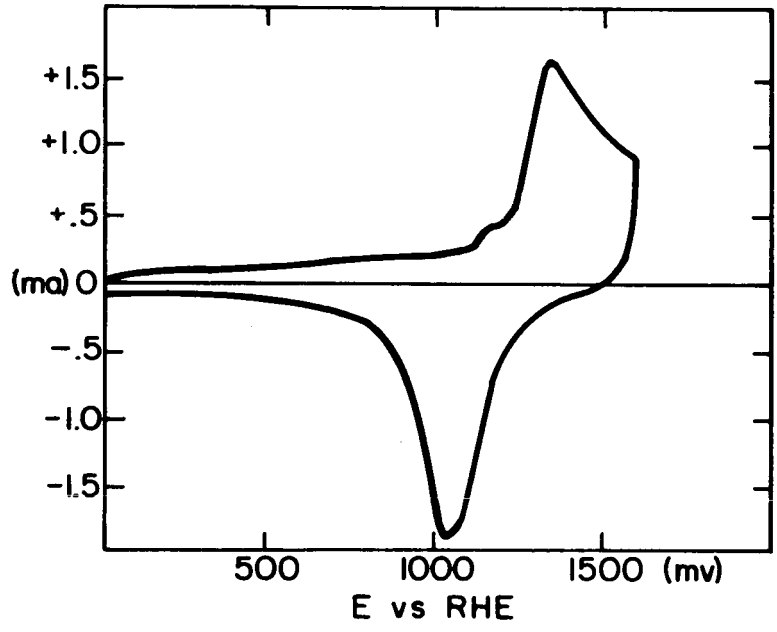

Au-Pt
80-20

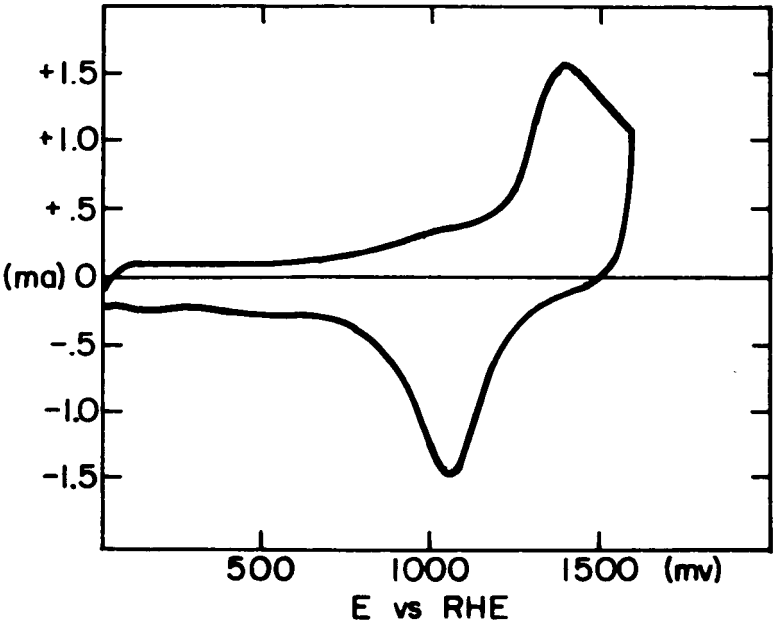

Fig. 6

Au-Pt
70-30

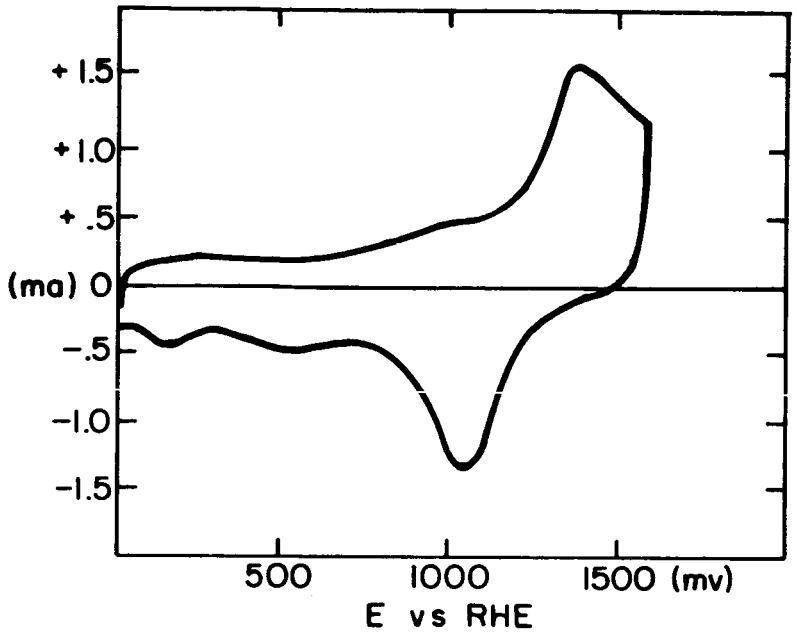

Au-Pt
60-40

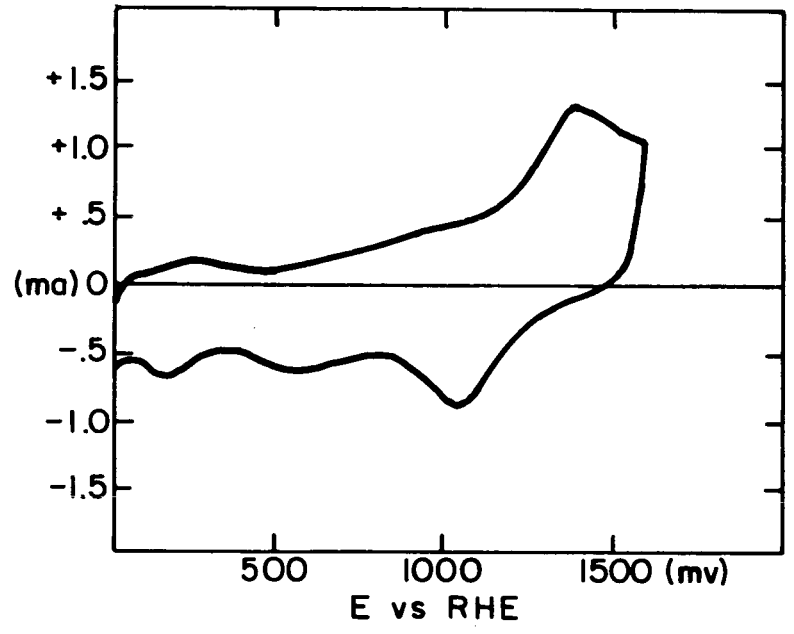

Au-Pt
50-50

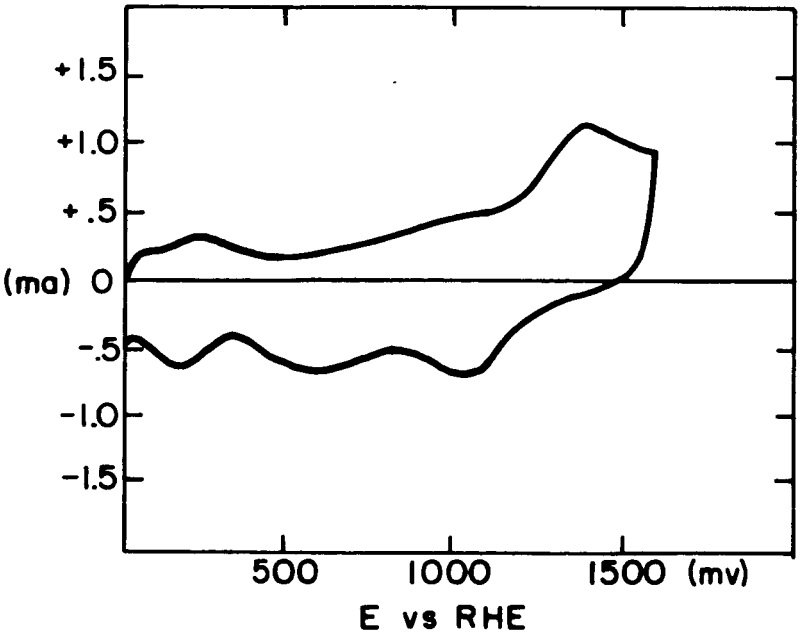

Fig. 7

Au-Pt
40-60

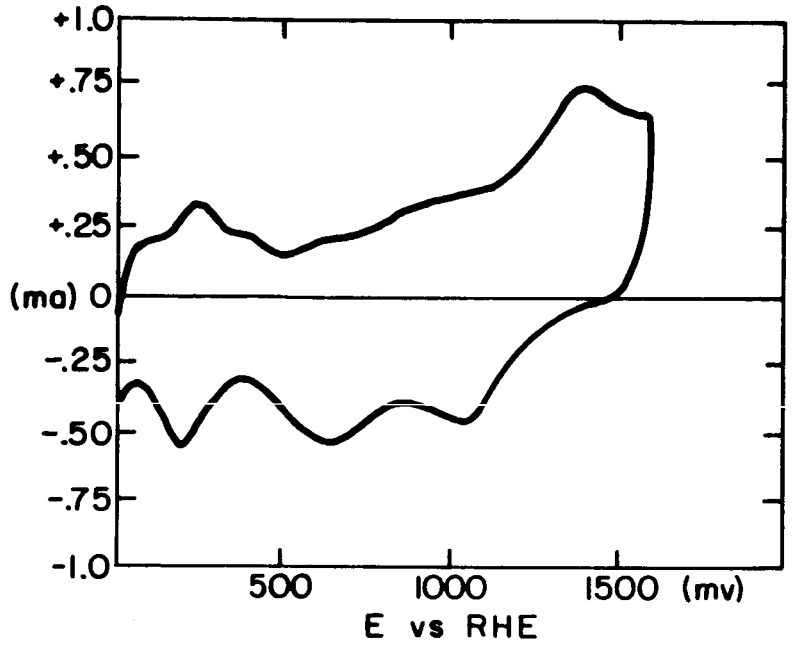

Au-Pt
30-70

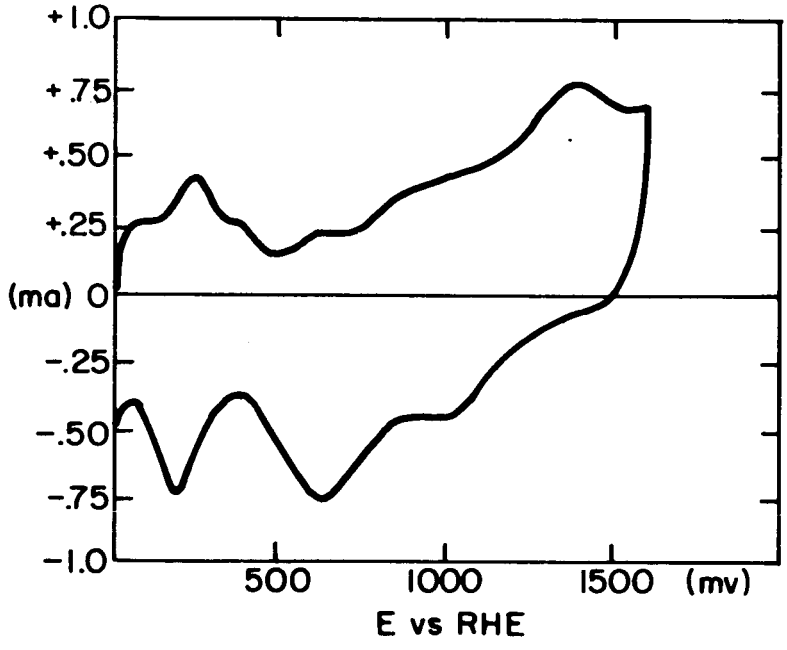

Au-Pt
20-80

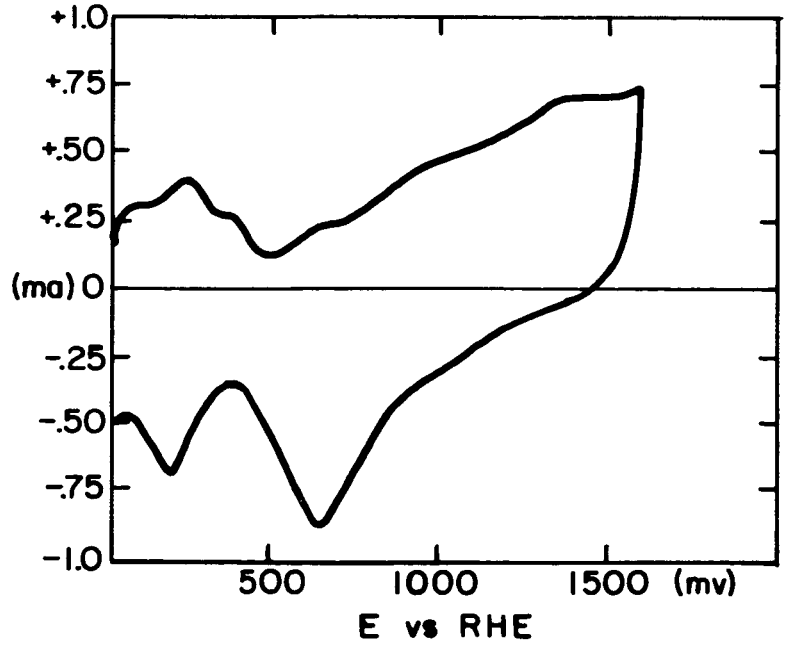

Fig. 8

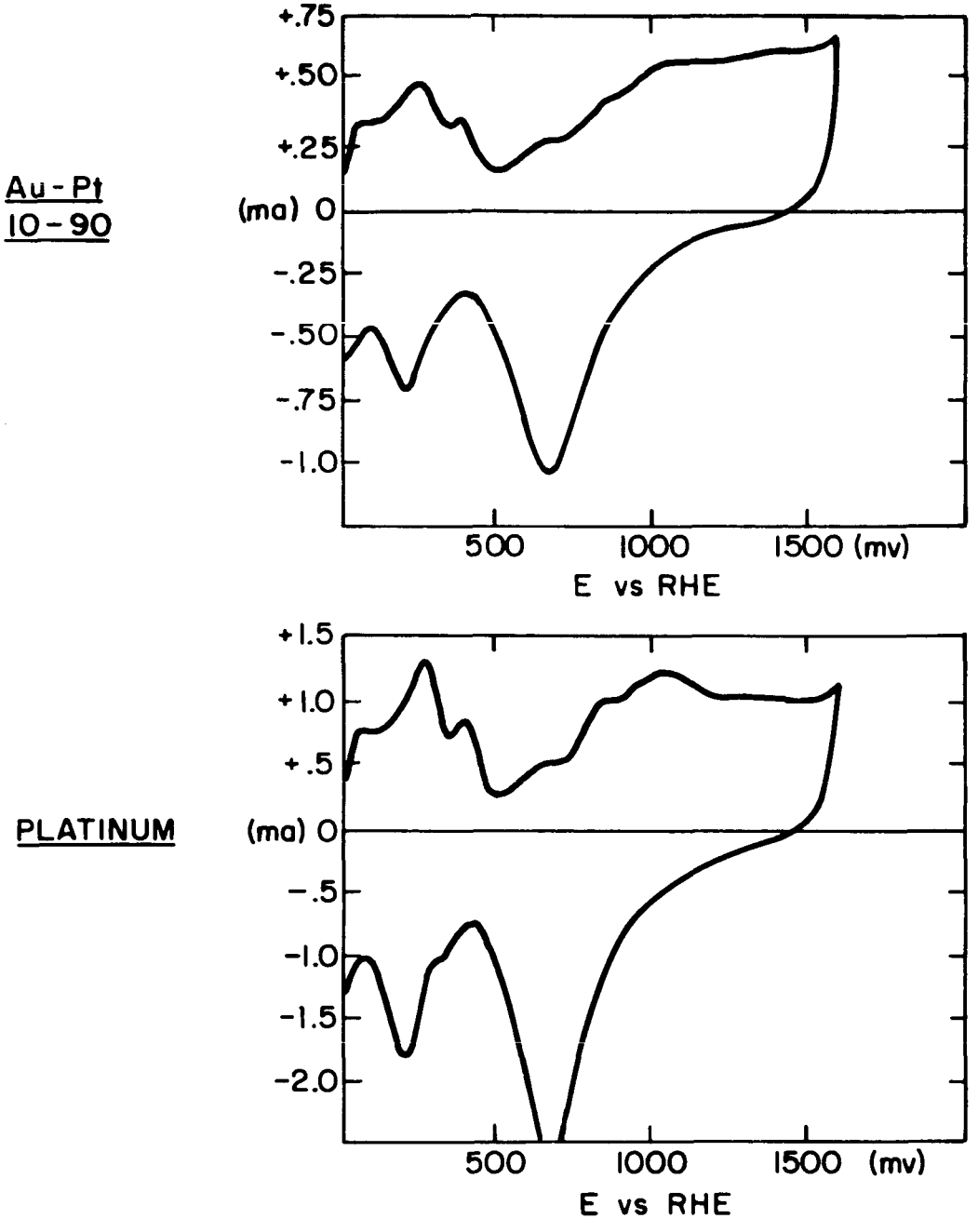

Fig. 9 All of the above measurements (Au-Pt Series) were made under the following conditions:

N_2-Saturated 2N KOH, 25°C
500 mv/sec, 4th sweep recorded
E vs Rev. H_2 Elec., Pd-Ag/H counter electrode
Makrides-Stern electrode holder-rotated at 600 RPM
Geometric areas approx. 1.5 cm^2

GOLD-SILVER ALLOYS

GOLD

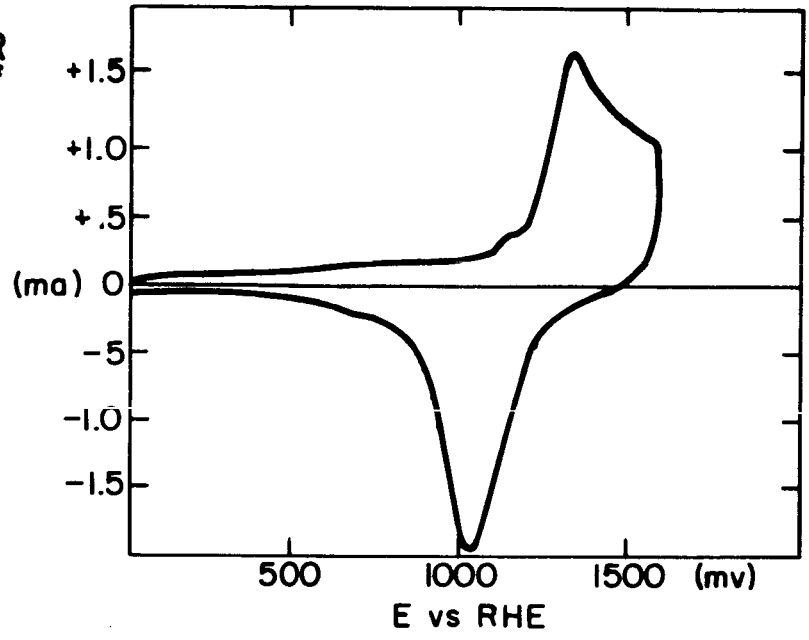

Au - Ag
90-10

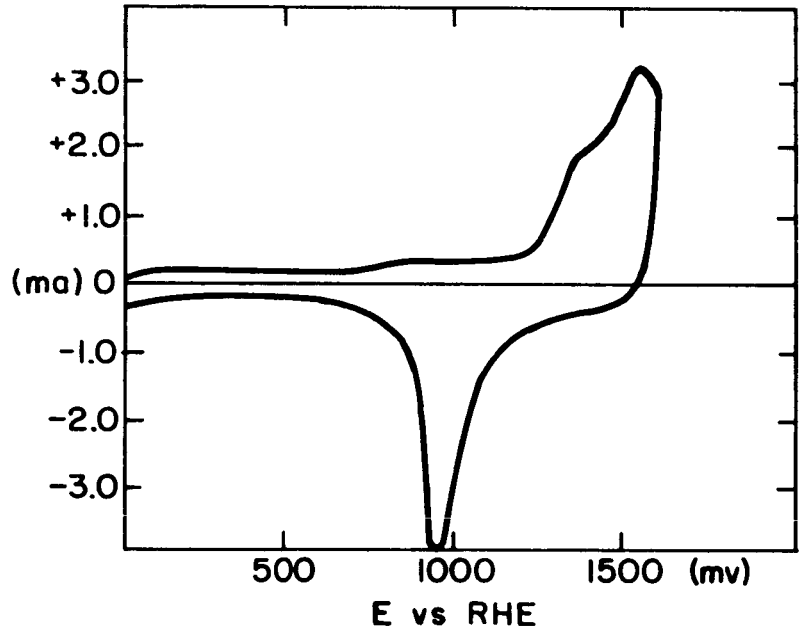

Au - Ag
80-20

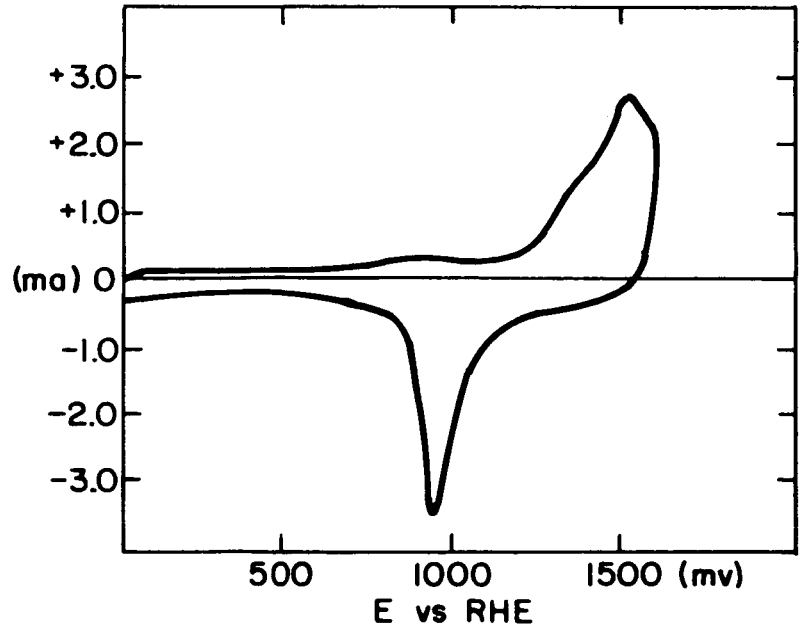

Fig. 10

Au-Ag
70-30

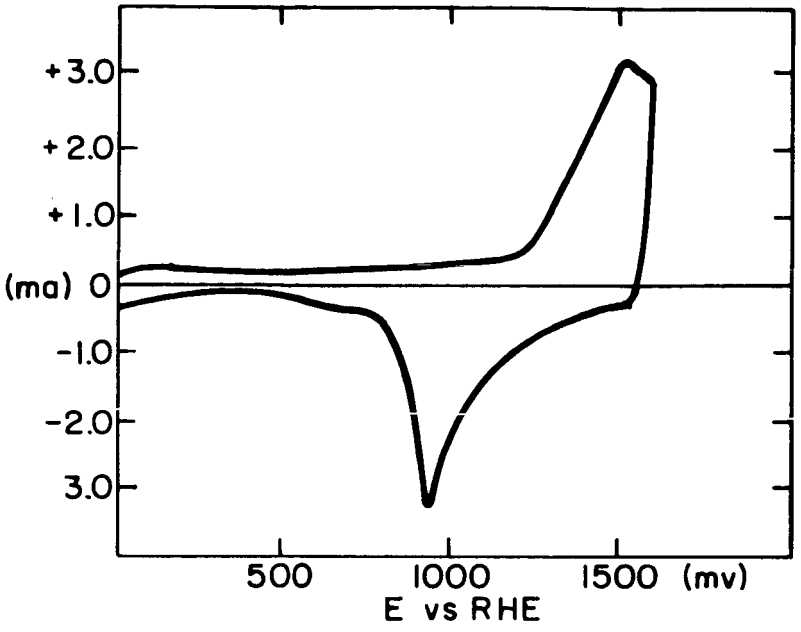

Au-Ag
60-40

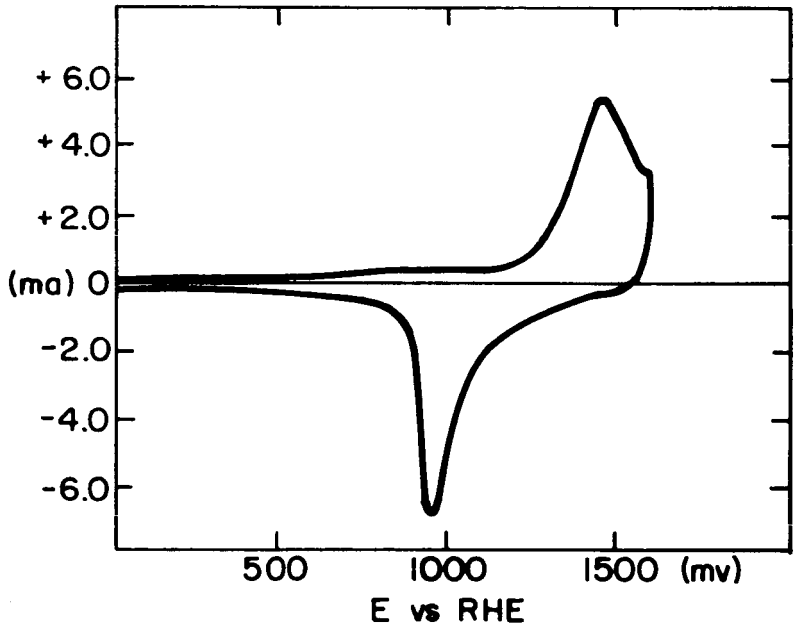

Au-Ag
50-50

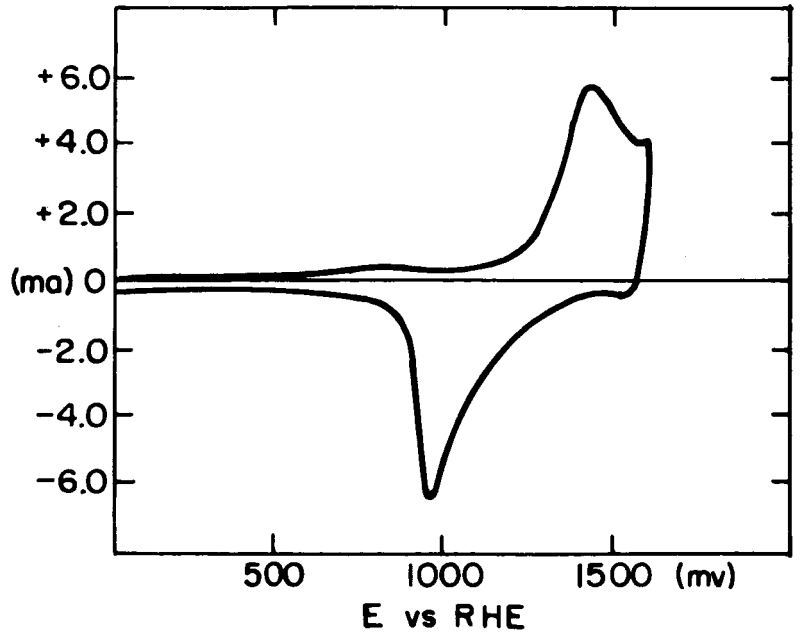

Fig. 11

Au-Ag
40-60

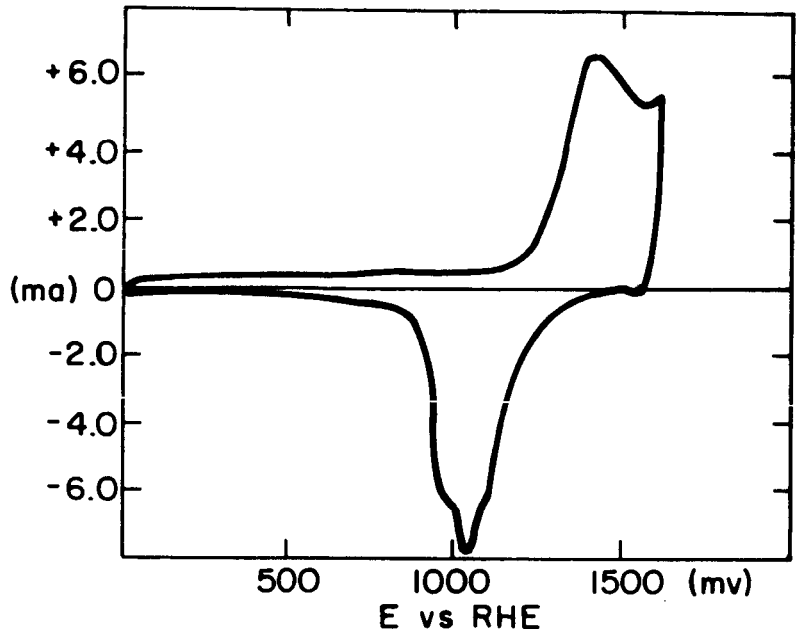

Au-Ag
50-70

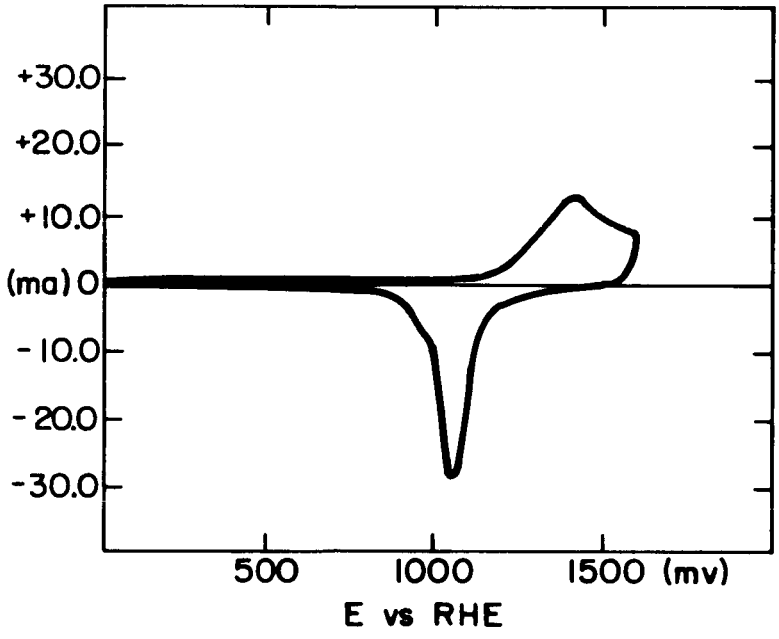

Au-Ag
20-80

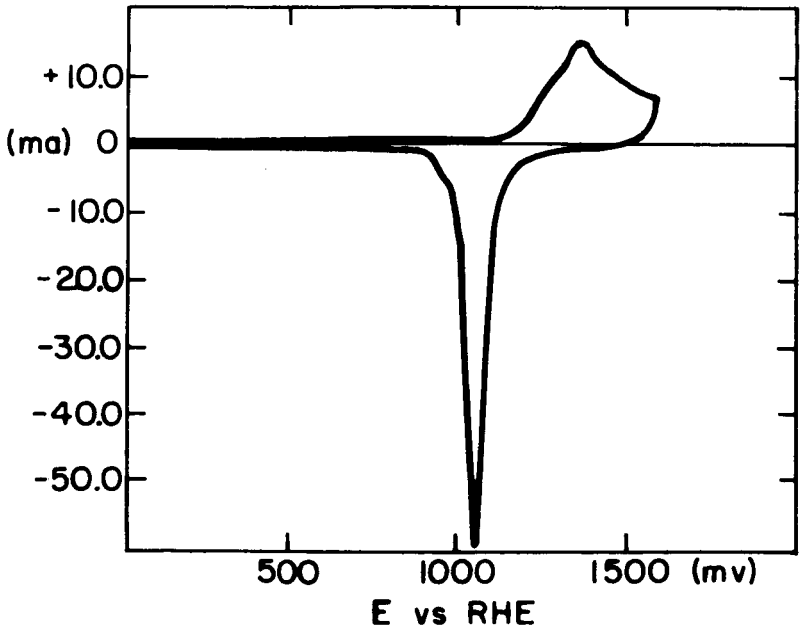

Fig. 12

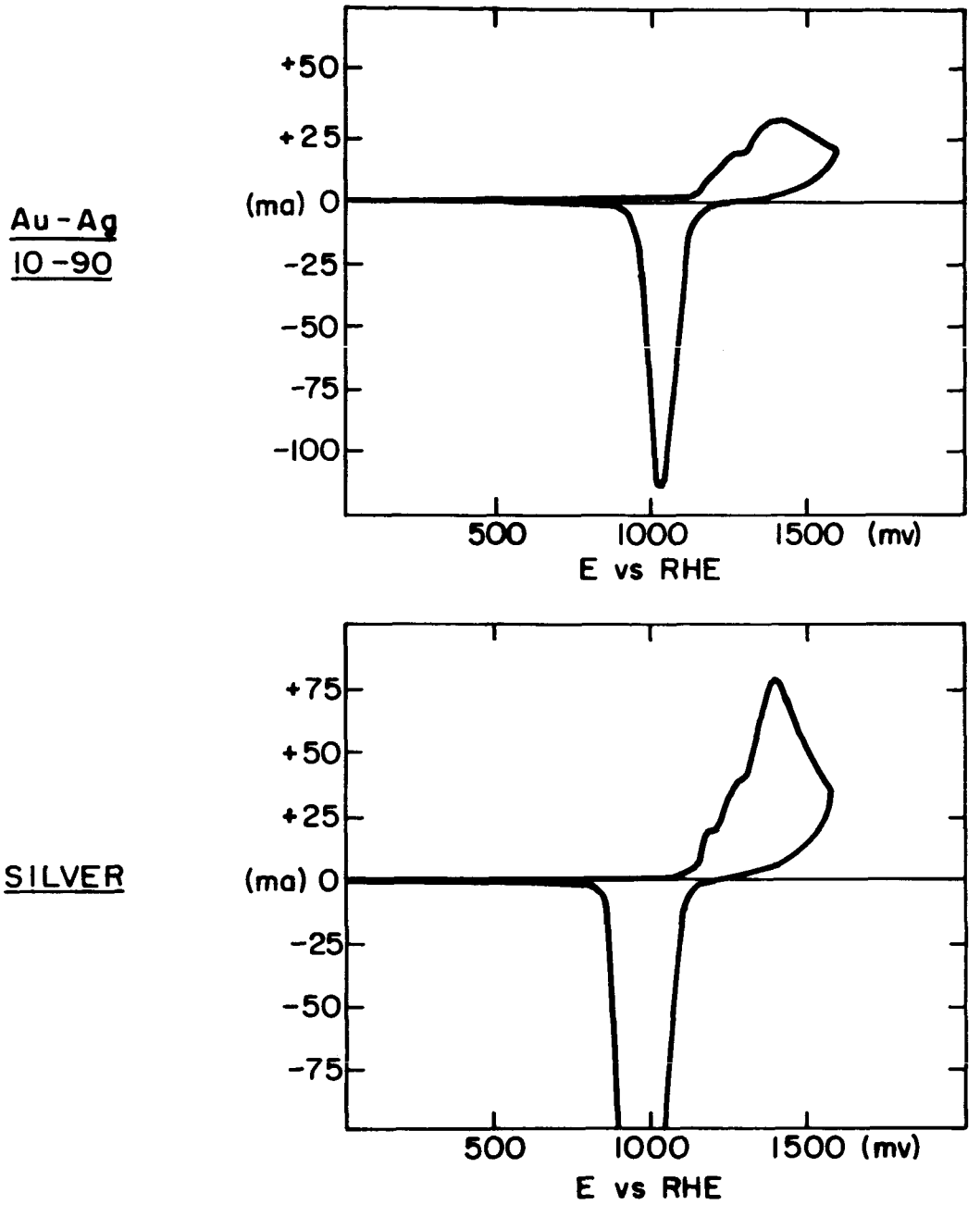

Fig. 13 All of the above measurements (Au-Ag Series) were made under the following conditions:

N_2 - Saturated 2N KOH, 25°C
500 mv/sec, 4th sweep recorded
E vs Rev. H_2 elec., Pd-Ag/H_2 counter electrode
Makrides-Stern electrode holder-rotated at 600 RPM
Geometric areas approx. 1.5 cm^2

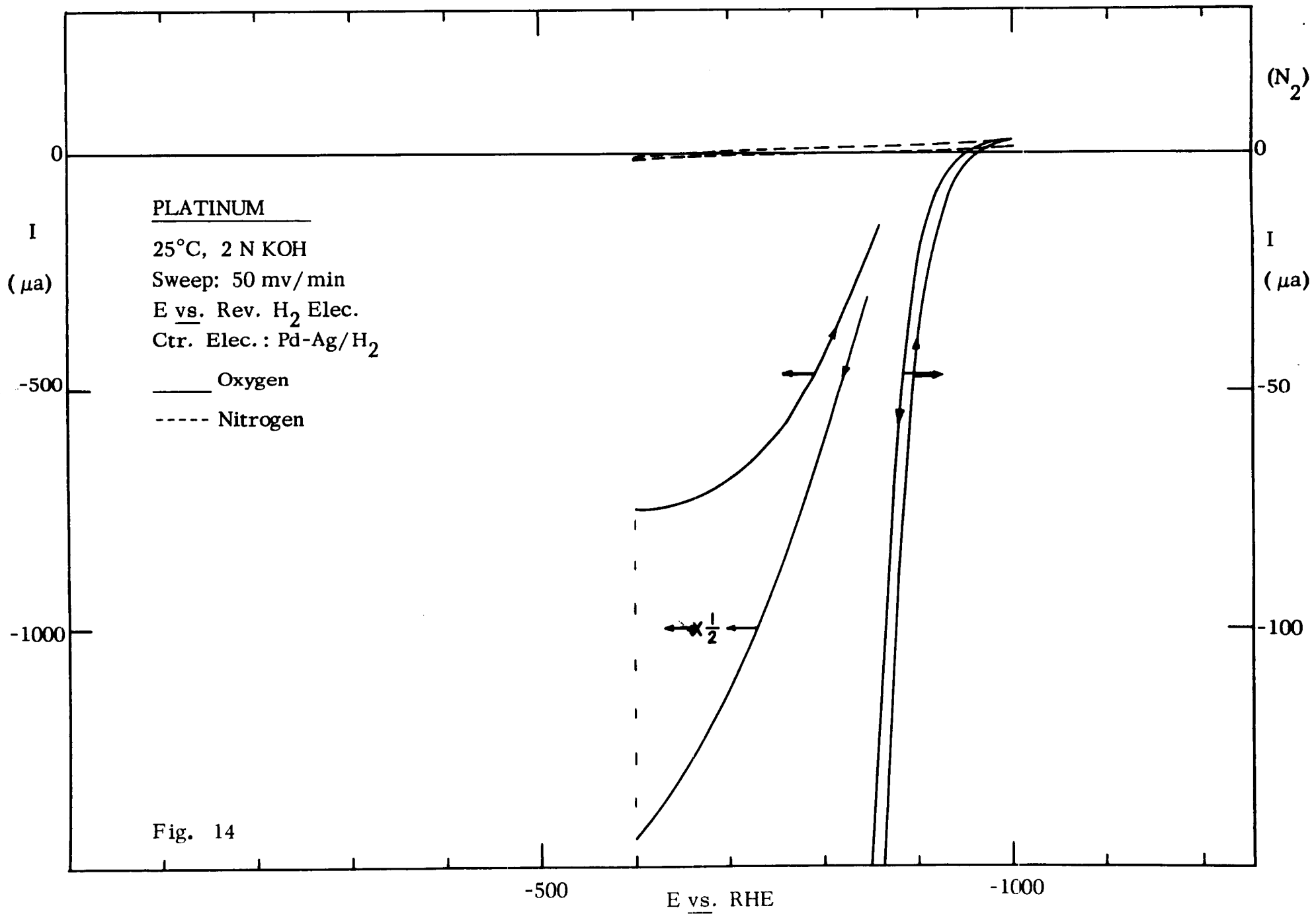
PLATINUM
25°C, 2 N KOH
Sweep: 50 mv/min
E vs. Rev. H_2 Elec.
Ctr. Elec.: Pd-Ag/H_2
Oxygen
Nitrogen
I (μa)
0
-500
-1000
(N_2)
0
-50
-100
$\frac{1}{2}$
-500
E vs. RHE
-1000

Fig. 14

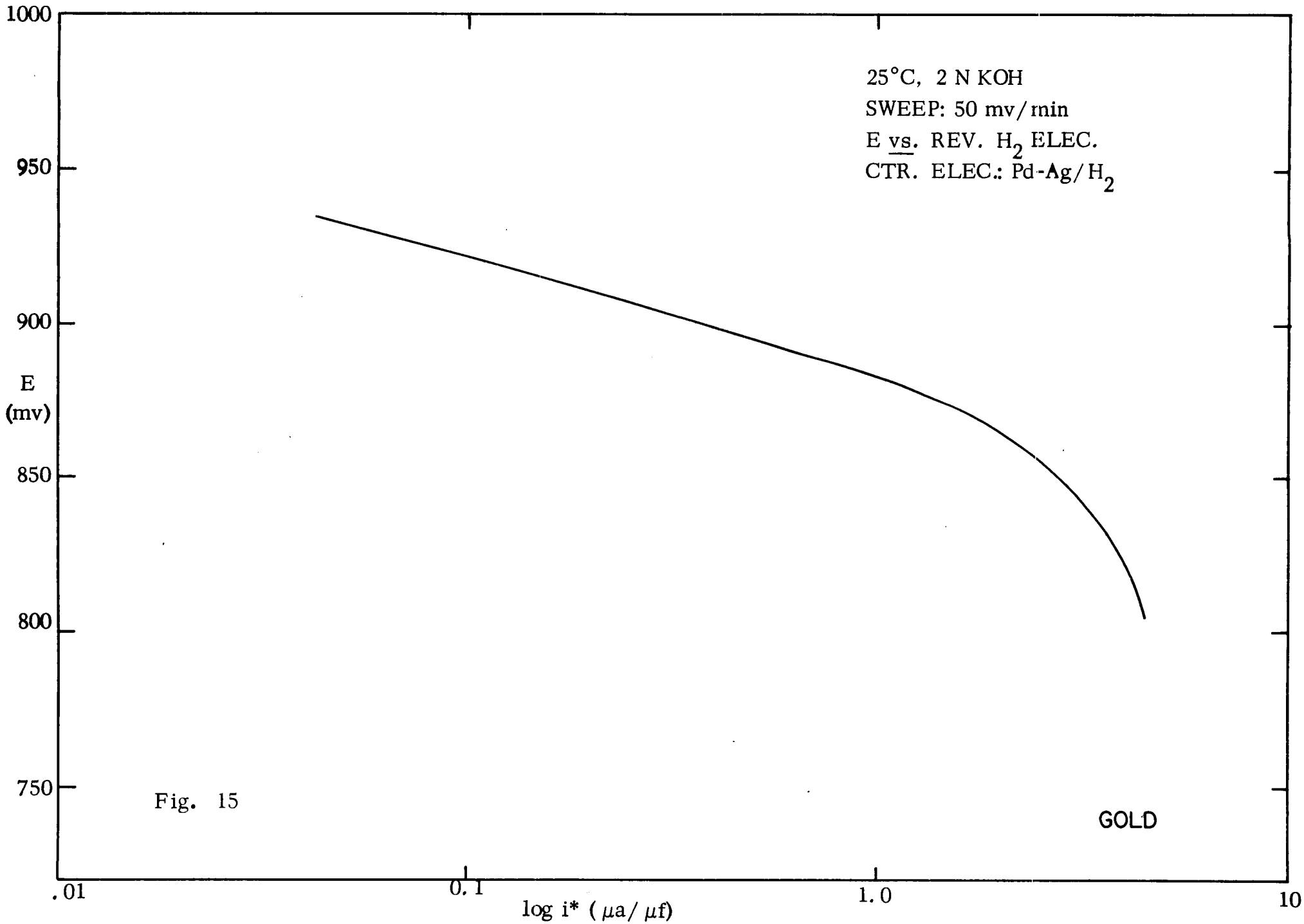
1000
950
900
E
(mv)
850
800
750
25°C, 2 N KOH
SWEEP: 50 mv/min
E vs. REV. H2 ELEC.
CTR. ELEC.: Pd-Ag/H2
GOLD
.01
0.1
1.0
10
log i* (μa/μf)

Fig. 15

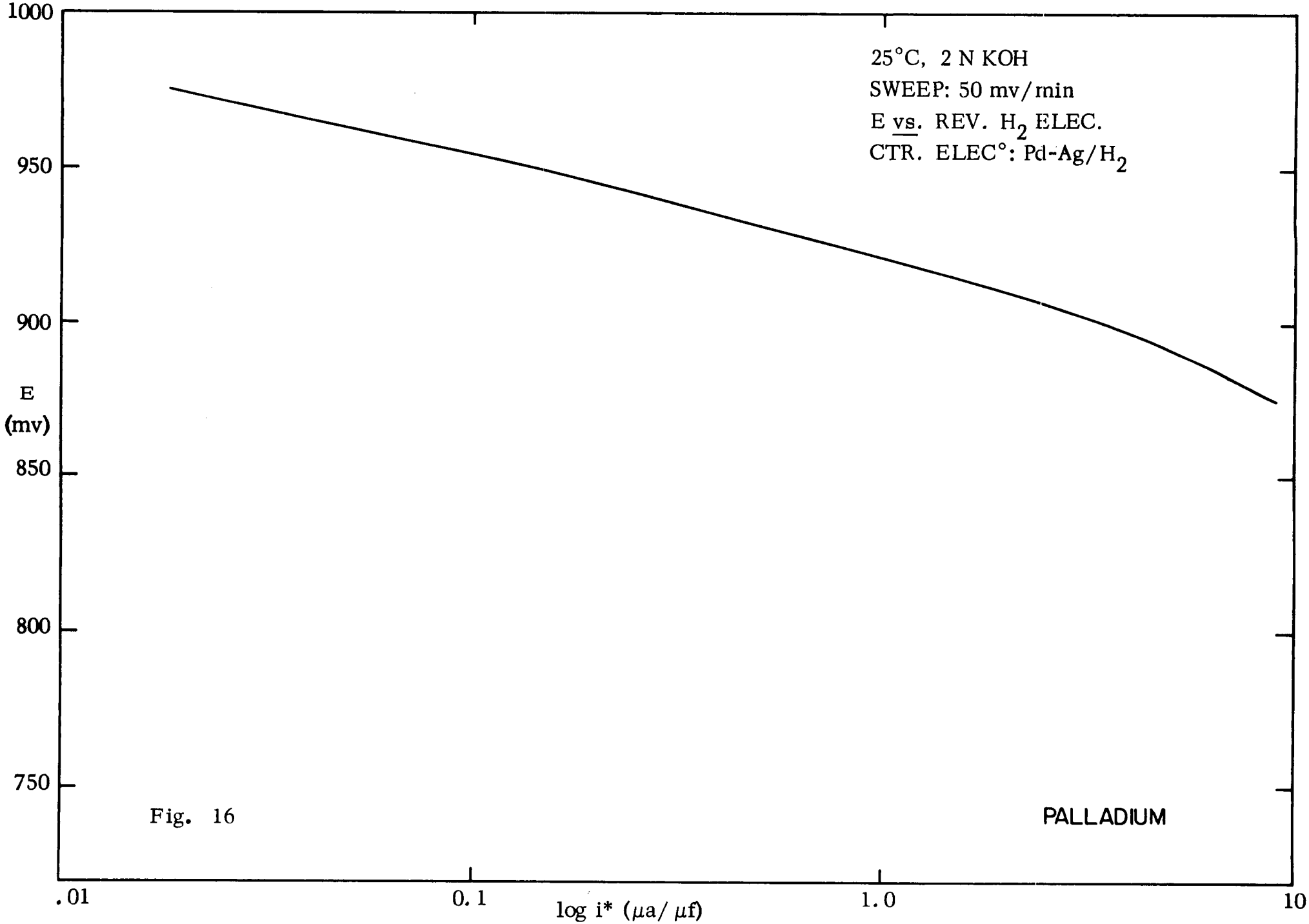
1000
950
900
E
(mv)
850
800
750
25°C, 2 N KOH
SWEEP: 50 mv/min
E vs. REV. H2 ELEC.
CTR. ELEC°: Pd-Ag/H2
PALLADIUM
.01
0.1
1.0
10
log i* (μa/ μf)

Fig. 16

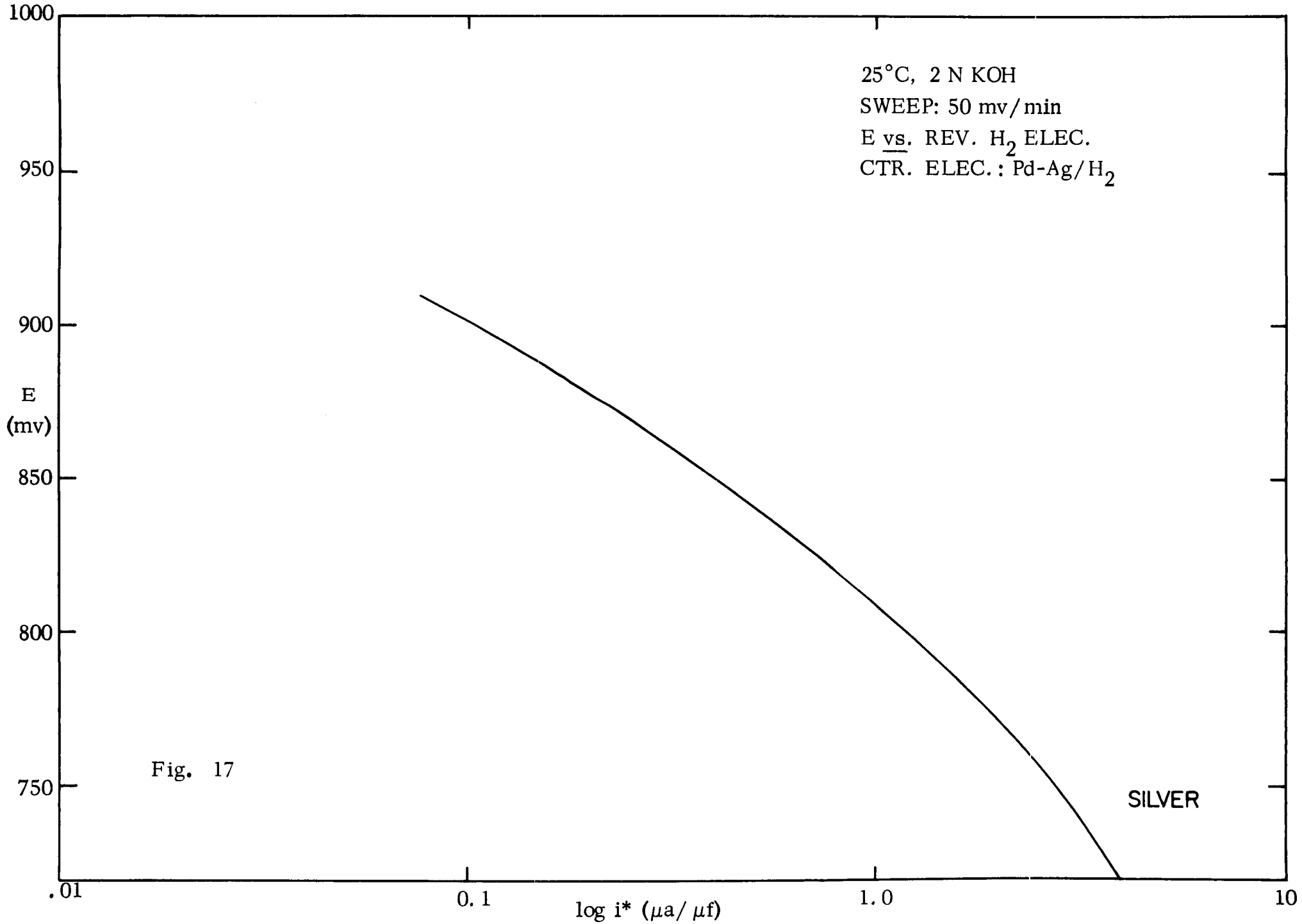
1000
950
900
850
800
750
E
(mv)
25°C, 2 N KOH
SWEEP: 50 mv/min
E vs. REV. H_2 ELEC.
CTR. ELEC.: Pd-Ag/H_2
SILVER
.01
0.1
1.0
10
log i* (μa/ μf)

Fig. 17

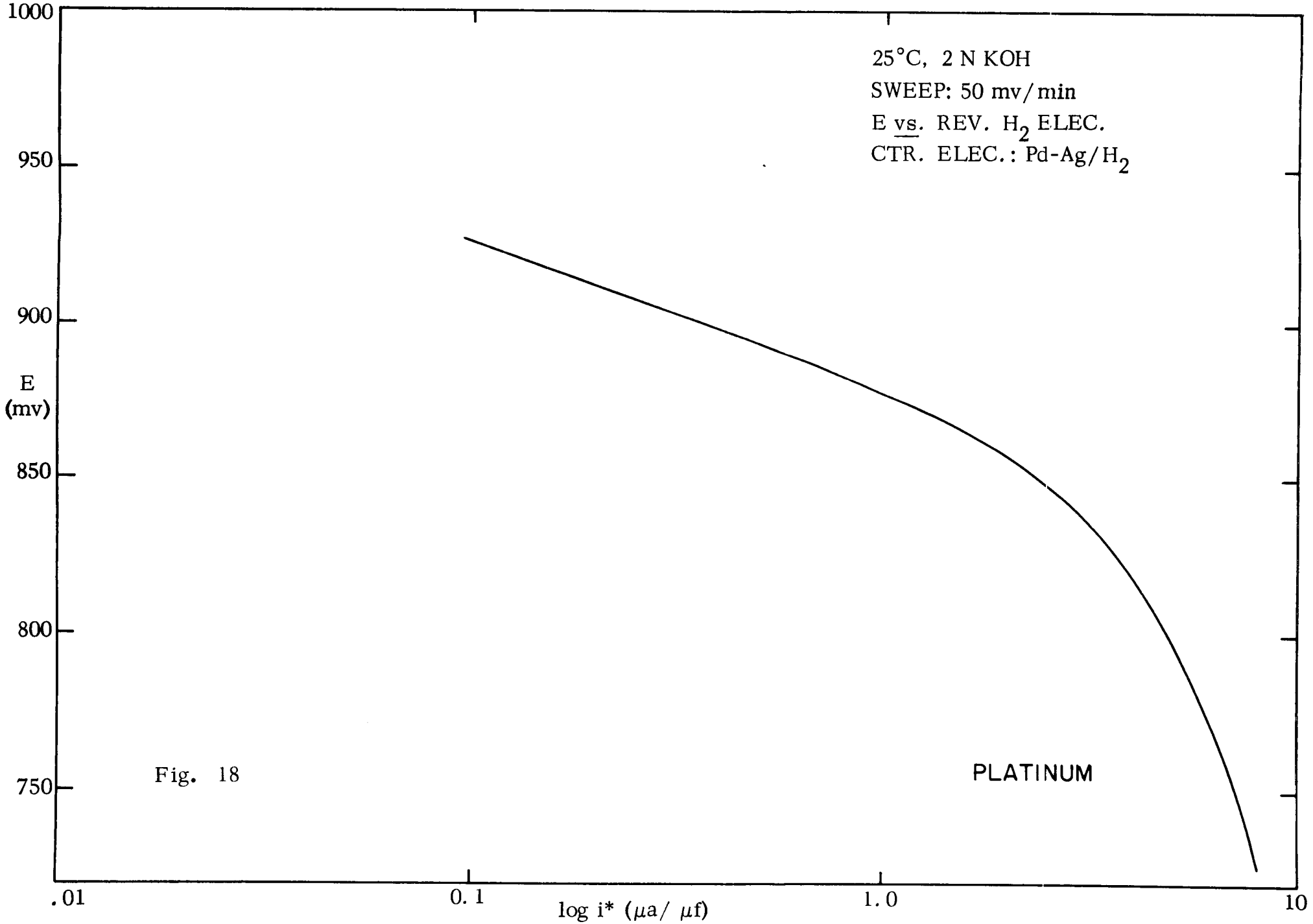
1000
950
900
E
(mv)
850
800
750
25°C, 2 N KOH
SWEEP: 50 mv/min
E vs. REV. H_2 ELEC.
CTR. ELEC.: Pd-Ag/H_2
PLATINUM
.01
0.1
1.0
10
log i* (μa/ μf)

Fig. 18

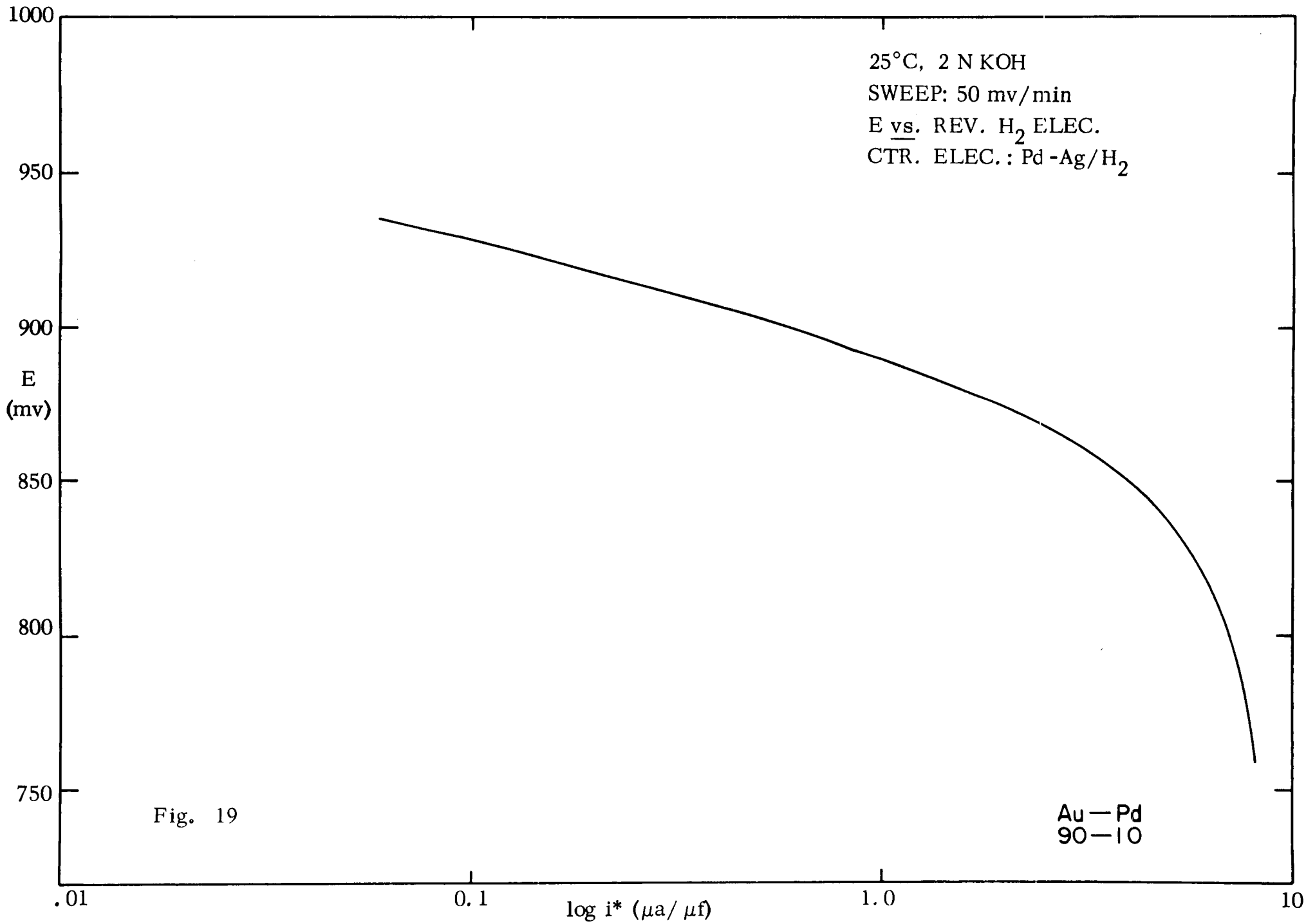
1000
950
900
E
(mv)
850
800
750
25°C, 2 N KOH
SWEEP: 50 mv/min
E vs. REV. H_2 ELEC.
CTR. ELEC.: Pd-Ag/H_2
Au—Pd
90—10
.01
0.1
1.0
10
log i* (μa/ μf)

Fig. 19

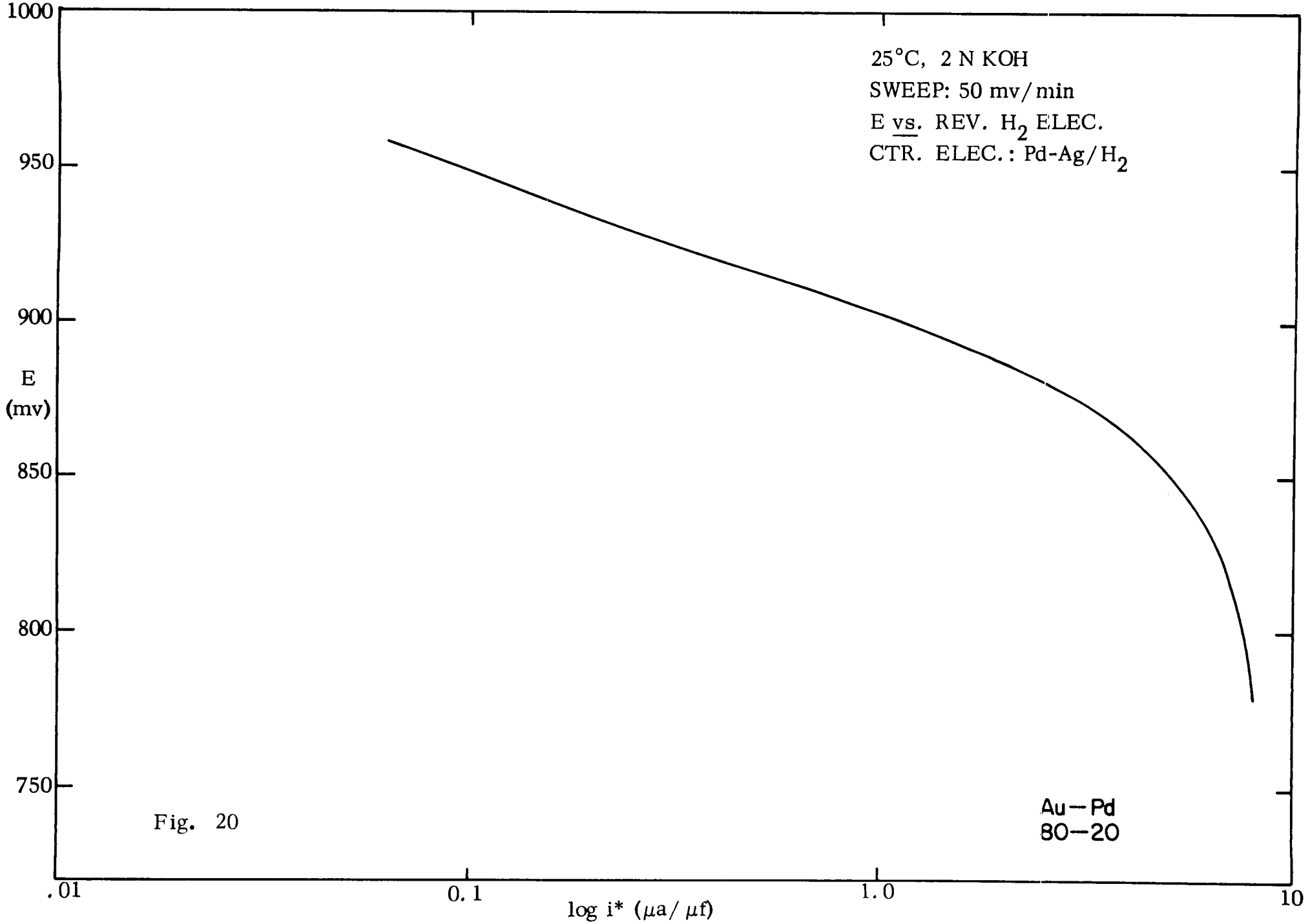
25°C, 2 N KOH
SWEEP: 50 mv/min
E vs. REV. H_2 ELEC.
CTR. ELEC.: Pd-Ag/H_2
1000
950
900
850
800
750
E
(mv)
.01
0.1
1.0
10
log i* (μa/ μf)
Au—Pd
80—20

Fig. 20

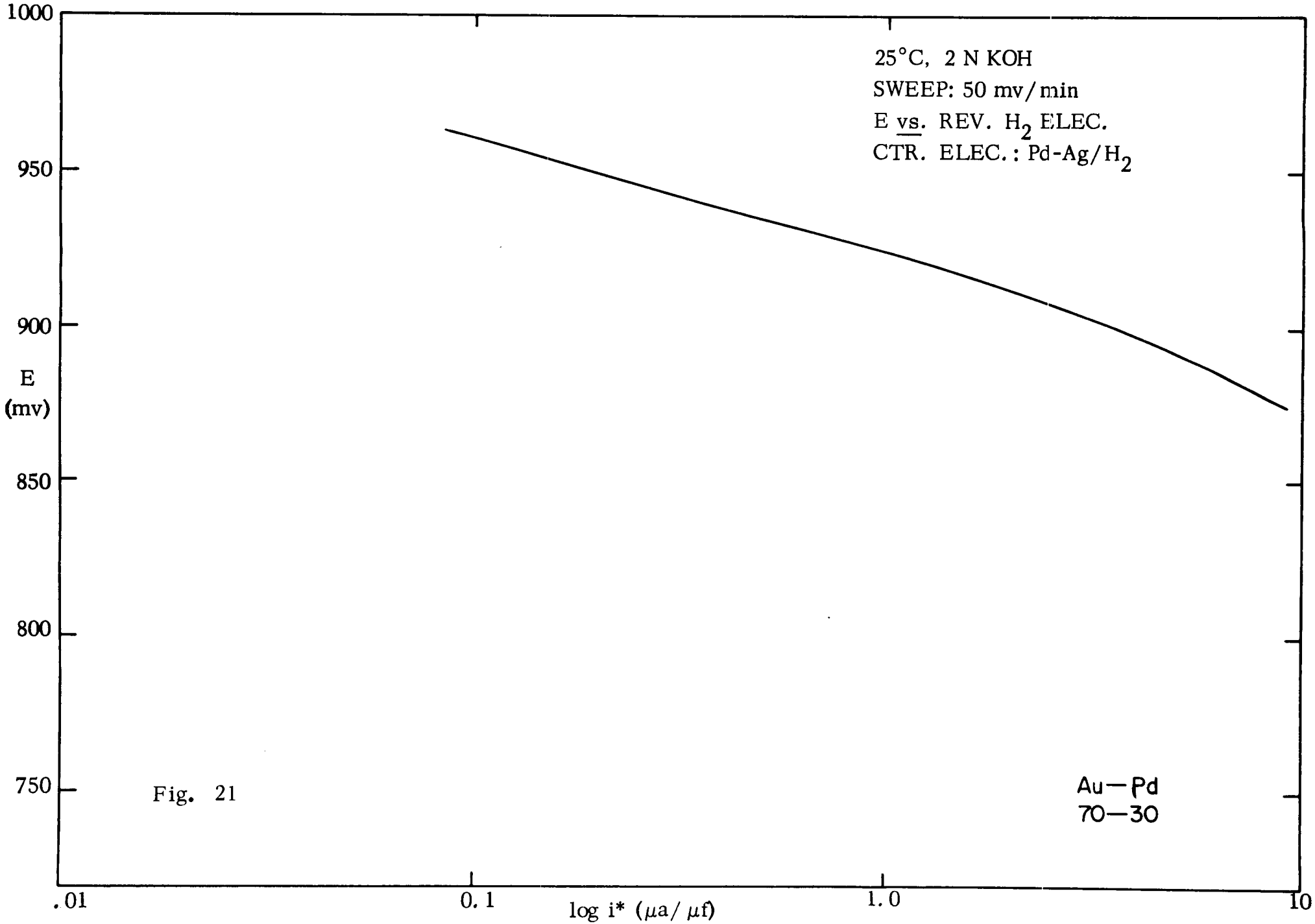
1000
950
900
E
(mv)
850
800
750
25°C, 2 N KOH
SWEEP: 50 mv/min
E vs. REV. H2 ELEC.
CTR. ELEC.: Pd-Ag/H2
Au—Pd
70—30
.01
0.1
1.0
10
log i* (μa/μf)

Fig. 21

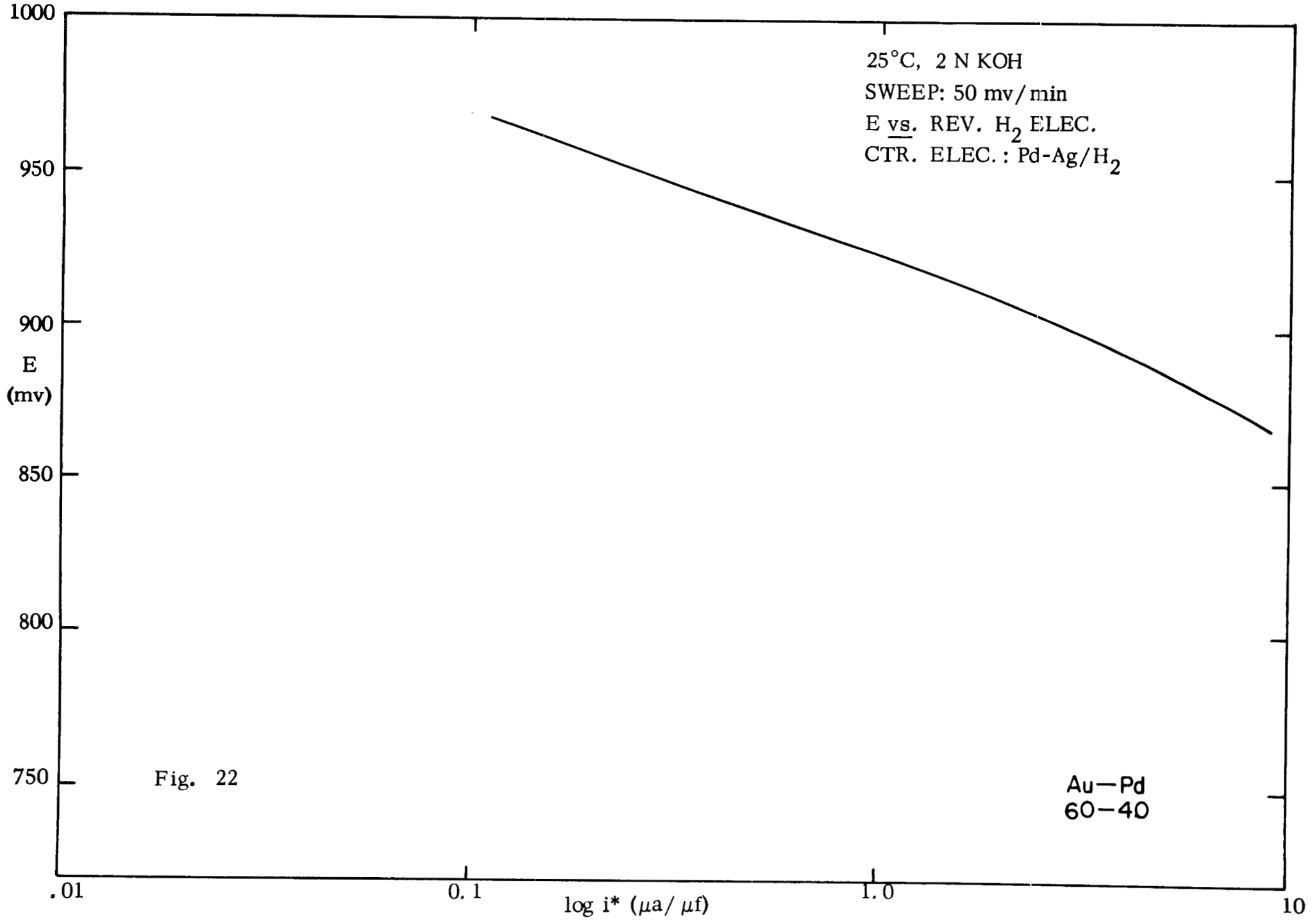
1000
950
900
E
(mv)
850
800
750
25°C, 2 N KOH
SWEEP: 50 mv/min
E vs. REV. H_2 ELEC.
CTR. ELEC.: Pd-Ag/H_2
Au—Pd
60—40
.01
0.1
1.0
10
log i* (μa/μf)

Fig. 22

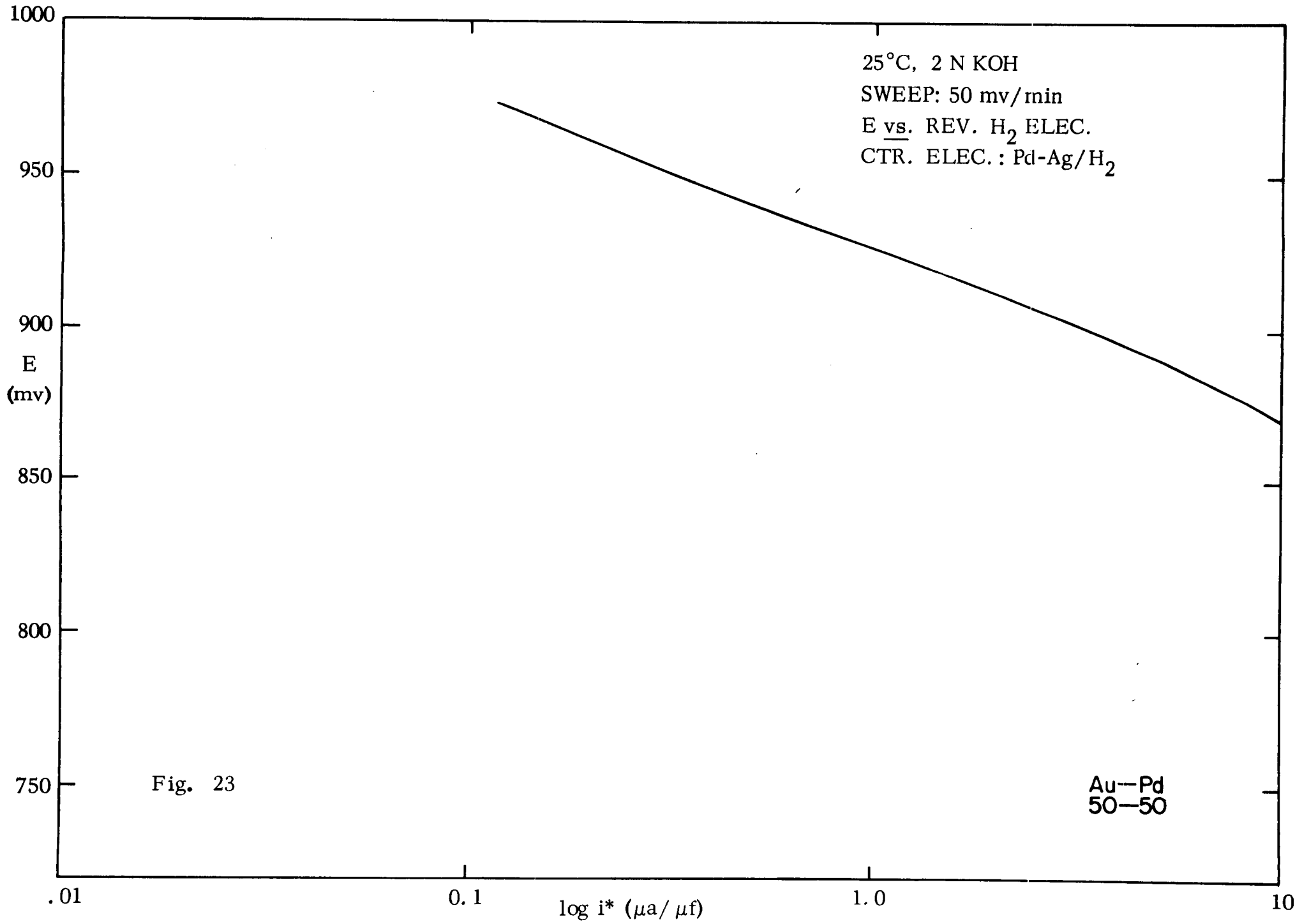
25°C, 2 N KOH
SWEEP: 50 mv/min
E vs. REV. H_2 ELEC.
CTR. ELEC.: Pd-Ag/H_2
1000
950
900
850
800
750
E
(mv)
.01
0.1
1.0
10
log i* (μa/ μf)
Au—Pd
50—50

Fig. 23

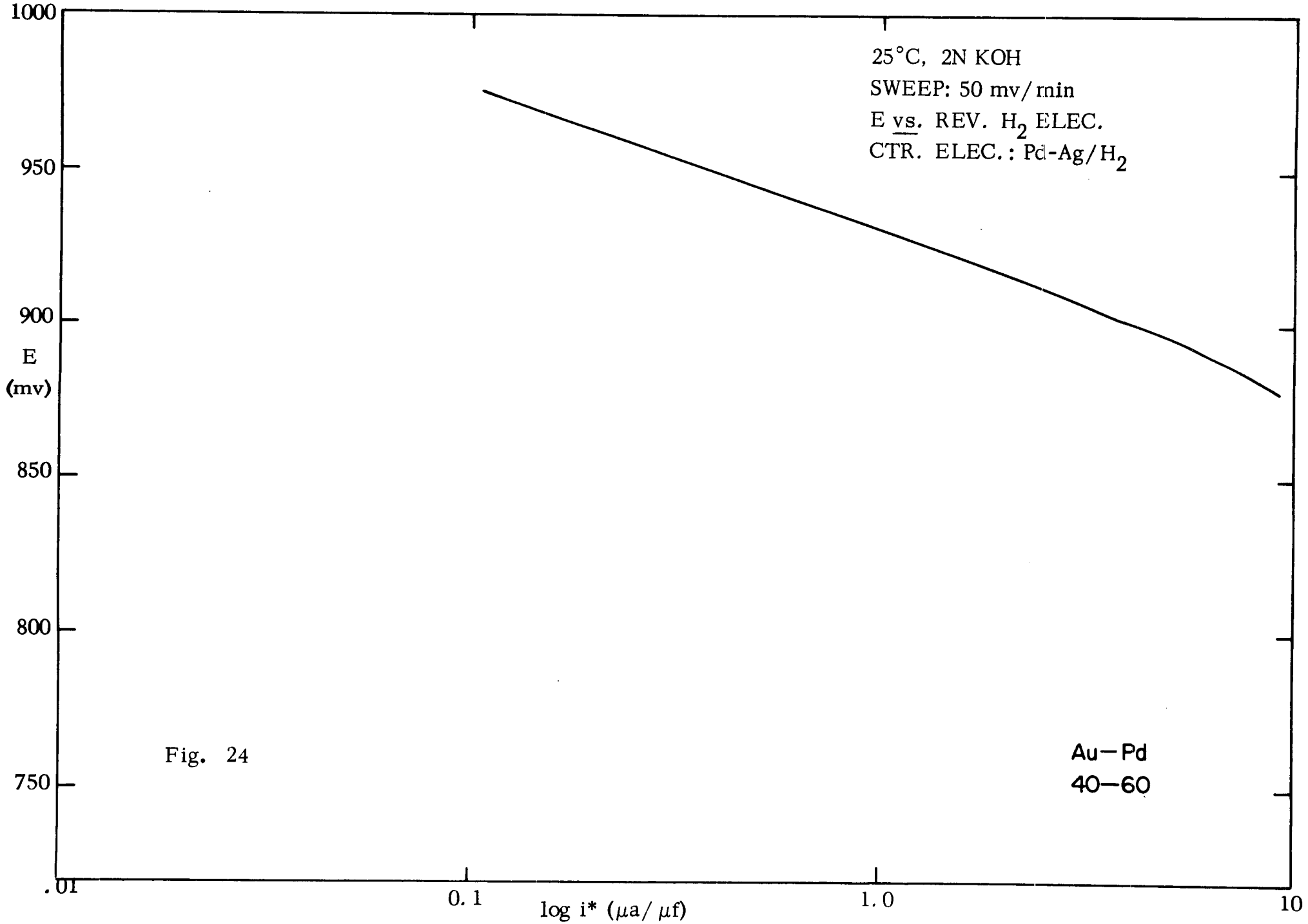
1000
950
900
E
(mv)
850
800
750
25°C, 2N KOH
SWEEP: 50 mv/min
E vs. REV. H2 ELEC.
CTR. ELEC.: Pd-Ag/H2
Au—Pd
40—60
.01
0.1
1.0
10
log i* (μa/μf)

Fig. 24

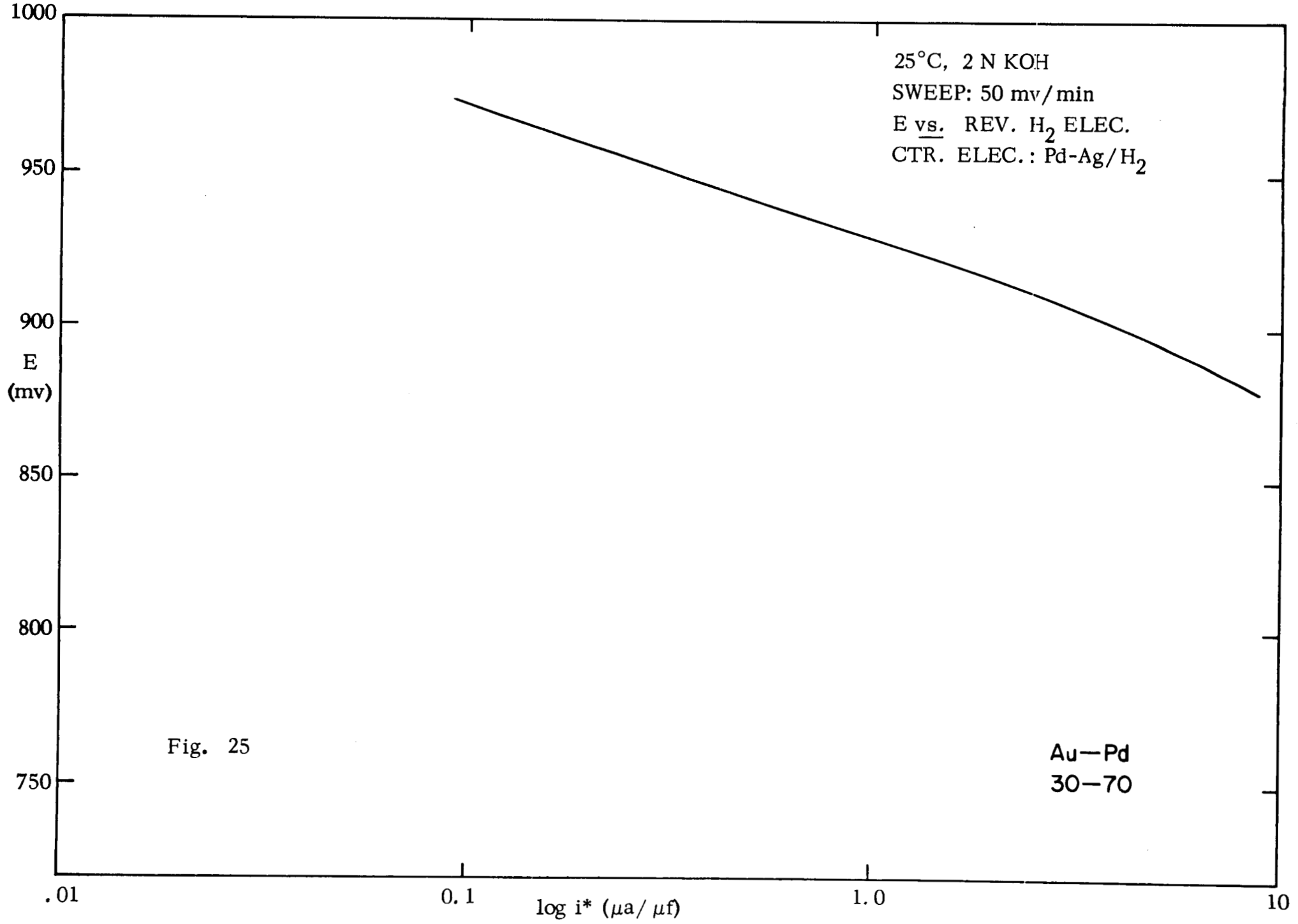
1000
950
900
E
(mv)
850
800
750
25°C, 2 N KOH
SWEEP: 50 mv/min
E vs. REV. H2 ELEC.
CTR. ELEC.: Pd-Ag/H2
Au—Pd
30—70
.01
0.1
1.0
10
log i* (μa/μf)

Fig. 25

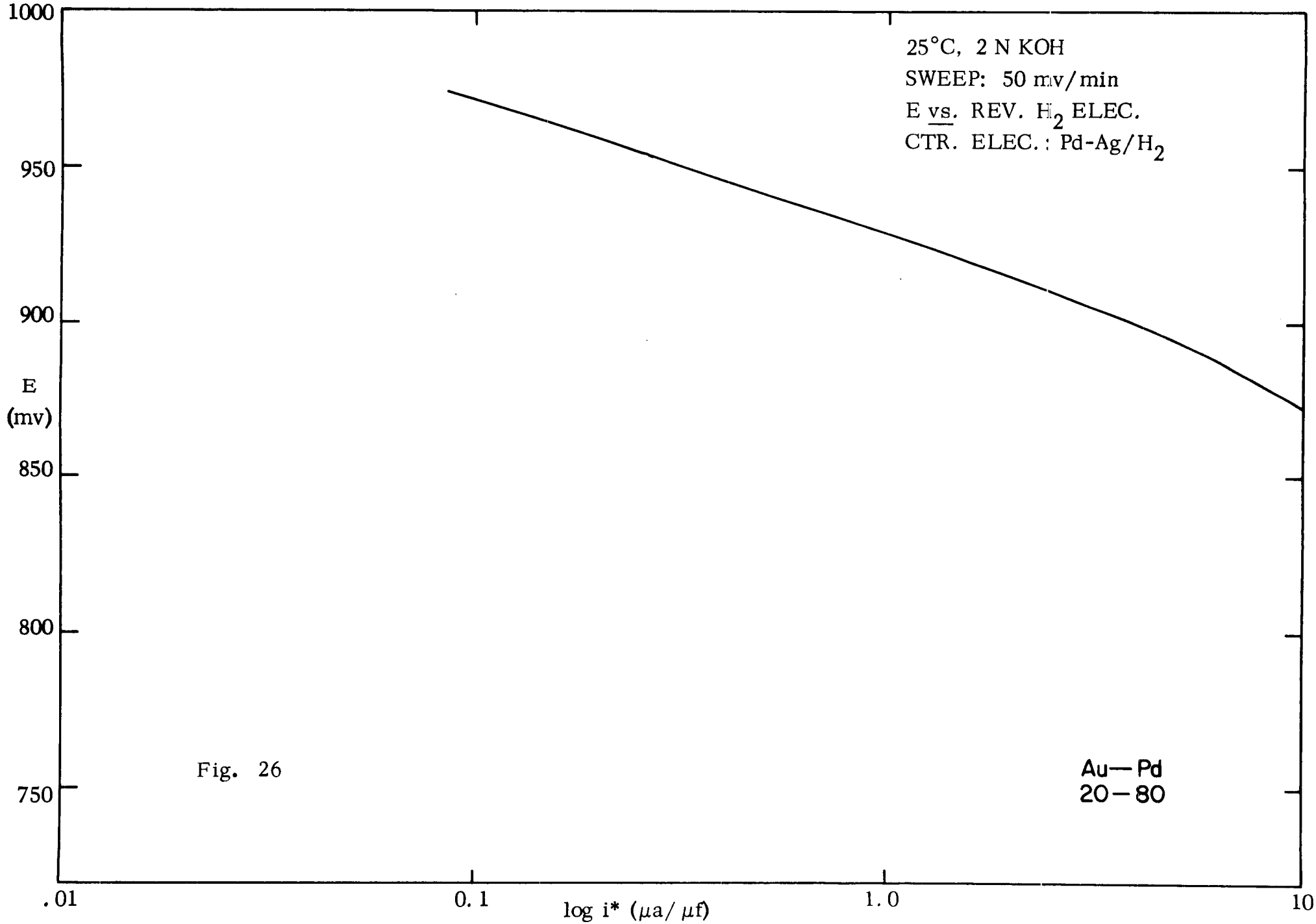
25°C, 2 N KOH
SWEEP: 50 mv/min
E vs. REV. H_2 ELEC.
CTR. ELEC.: Pd-Ag/H_2
1000
950
900
850
800
750
E
(mv)
.01
0.1
1.0
10
log i* (μa/μf)
Au—Pd
20—80

Fig. 26

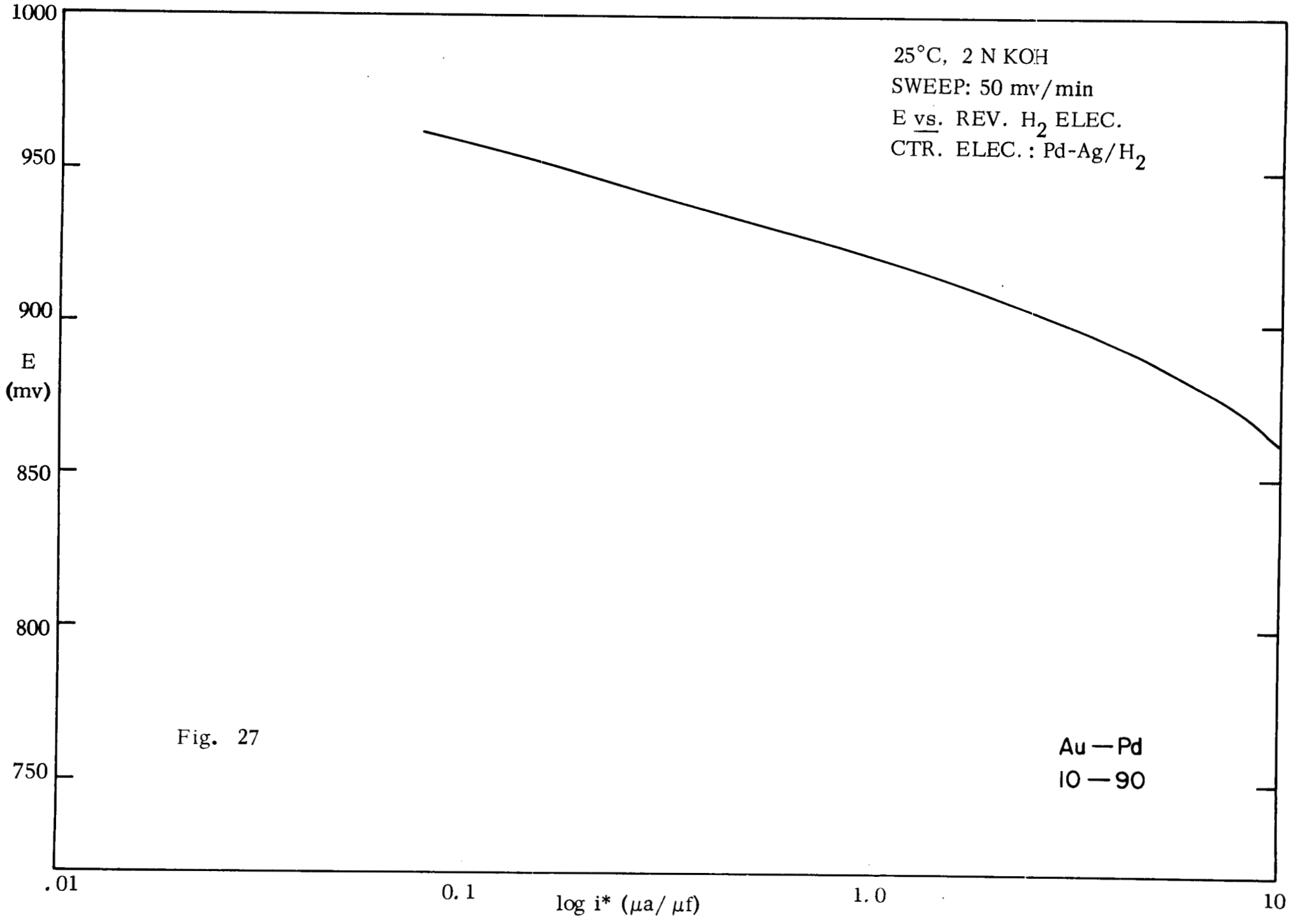
1000
950
900
E
(mv)
850
800
750
25°C, 2 N KOH
SWEEP: 50 mv/min
E vs. REV. H_2 ELEC.
CTR. ELEC. : Pd-Ag/H_2
Au — Pd
10 — 90
.01
0.1
1.0
10
log i* (μa/ μf)

Fig. 27

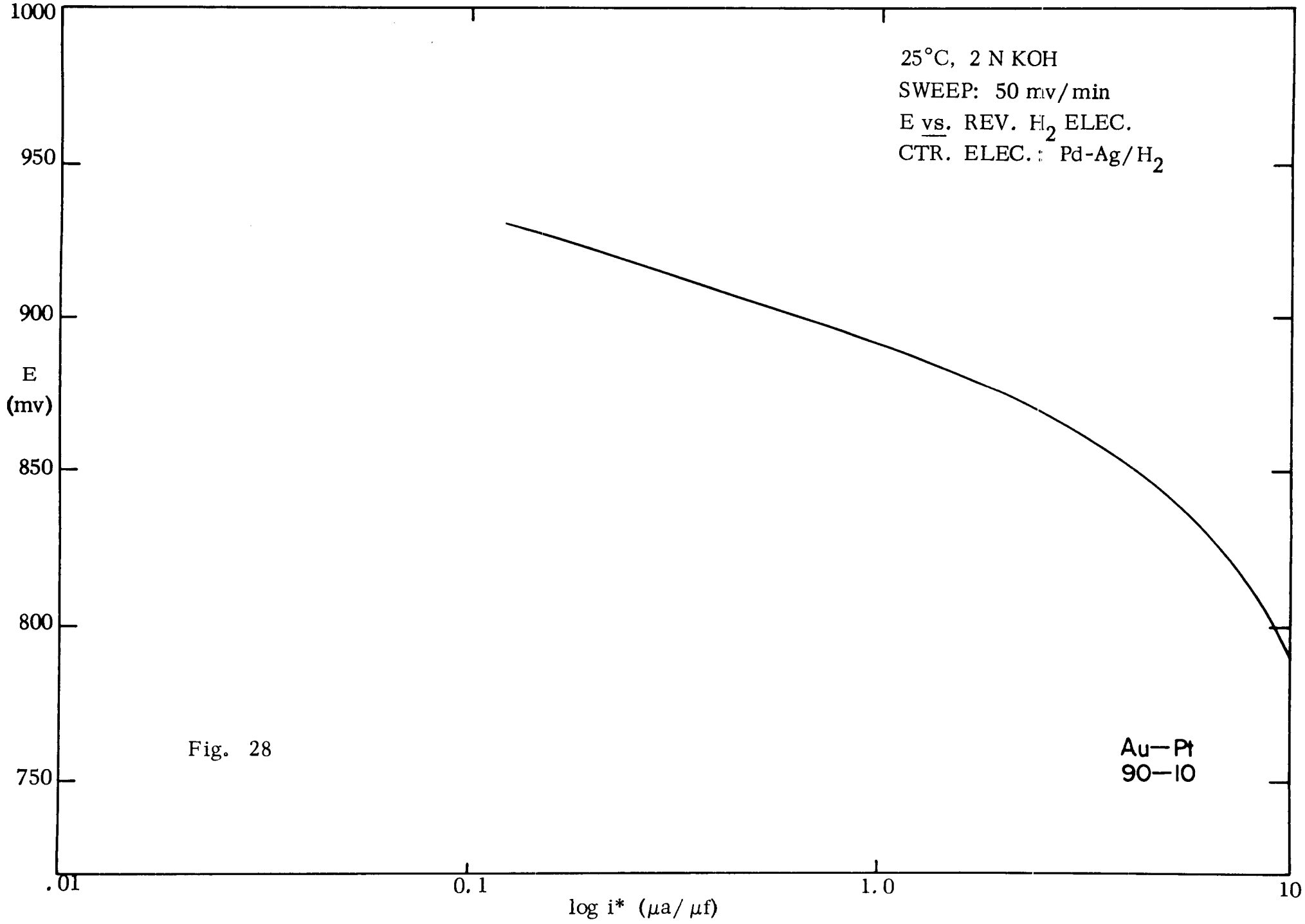
1000
950
900
E
(mv)
850
800
750
25°C, 2 N KOH
SWEEP: 50 mv/min
E vs. REV. H_2 ELEC.
CTR. ELEC.: Pd-Ag/H_2
Au—Pt
90—10
.01
0.1
1.0
10
log i* (μa/ μf)

Fig. 28

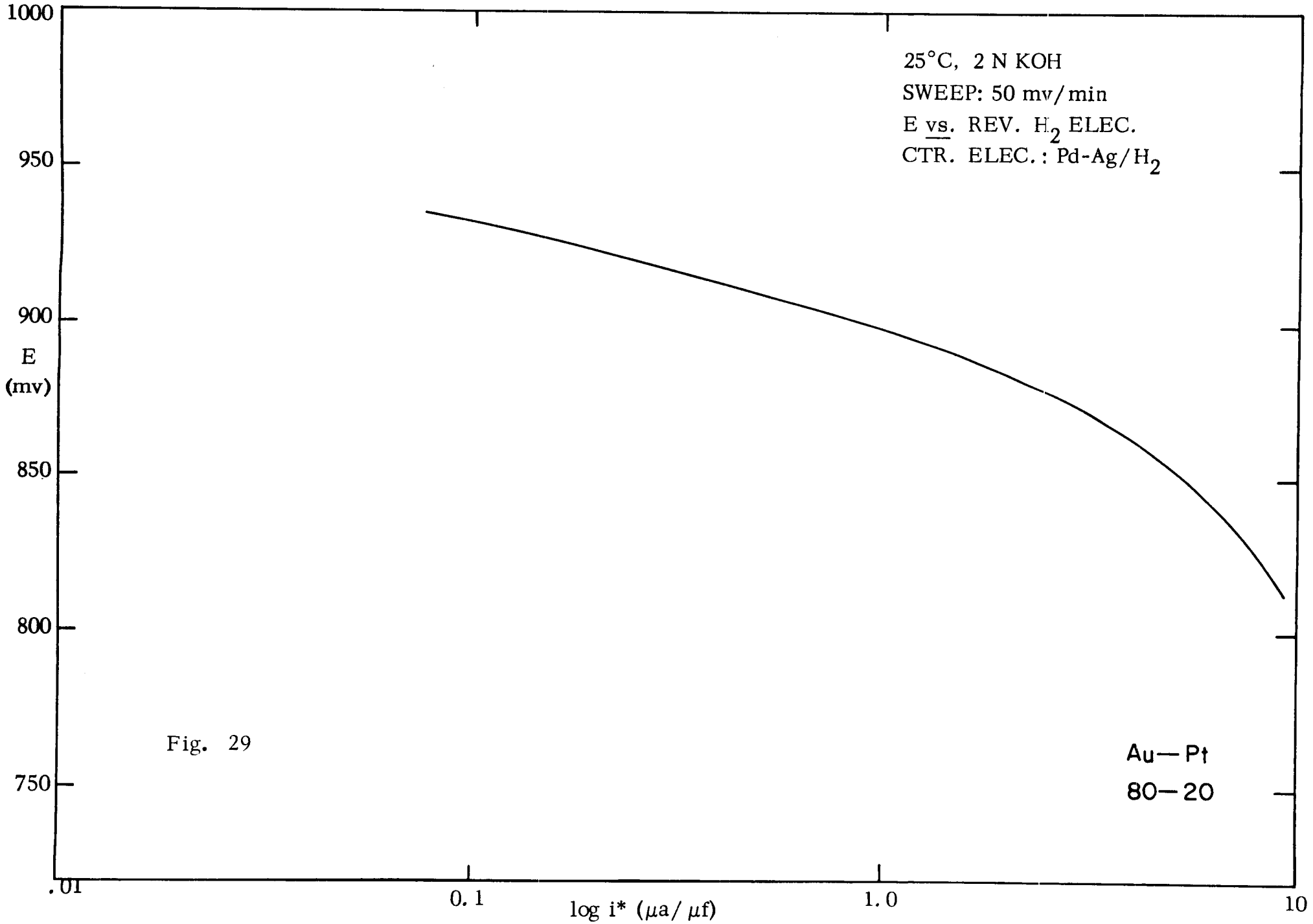
1000
950
900
E
(mv)
850
800
750
25°C, 2 N KOH
SWEEP: 50 mv/min
E vs. REV. H_2 ELEC.
CTR. ELEC.: Pd-Ag/H_2
Au—Pt
80—20
.01
0.1
1.0
10
log i* (μa/μf)

Fig. 29

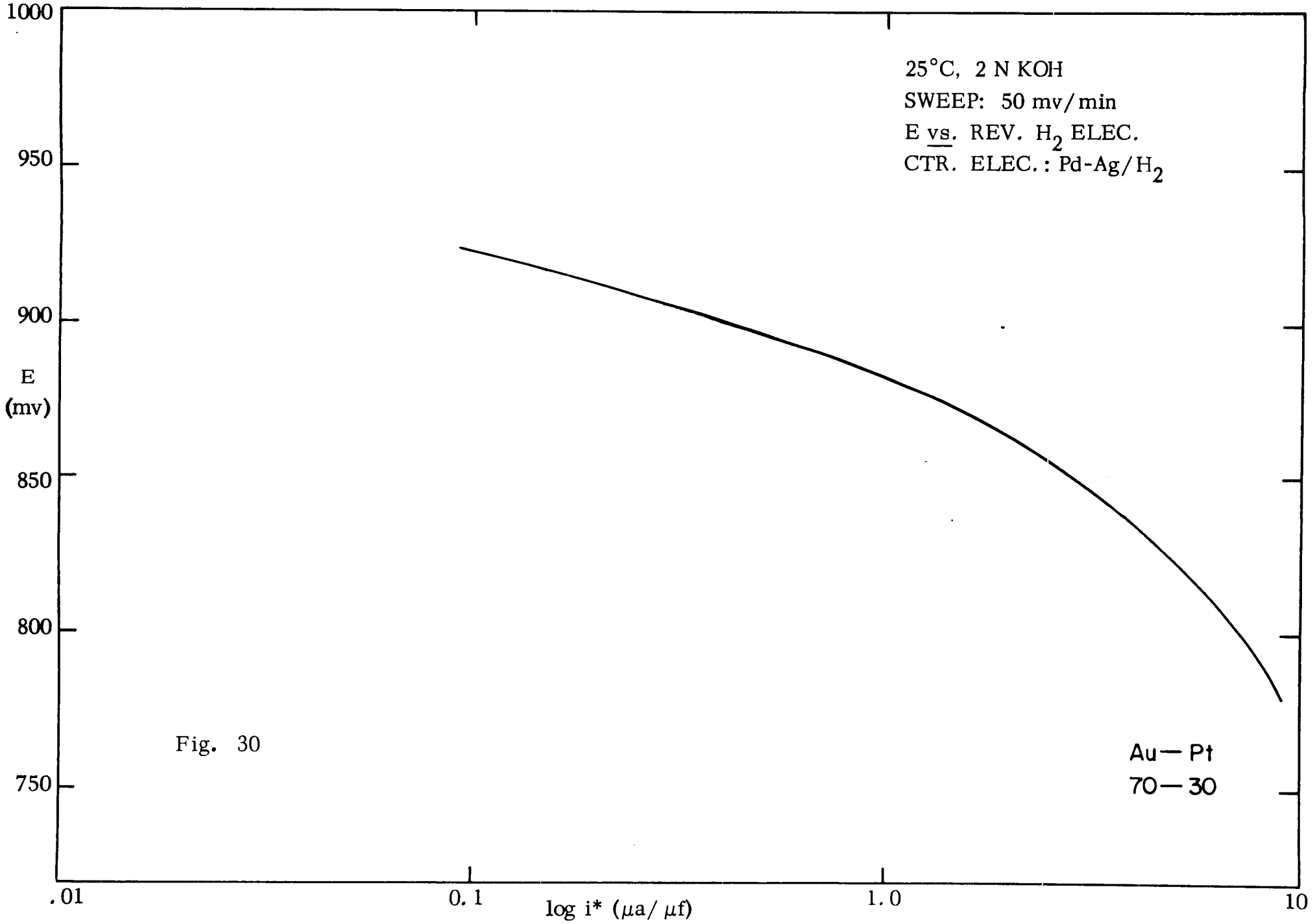
1000
950
900
E
(mv)
850
800
750
25°C, 2 N KOH
SWEEP: 50 mv/min
E vs. REV. H_2 ELEC.
CTR. ELEC.: Pd-Ag/H_2
Au—Pt
70—30
.01
0.1
1.0
10
log i* (μa/ μf)

Fig. 30

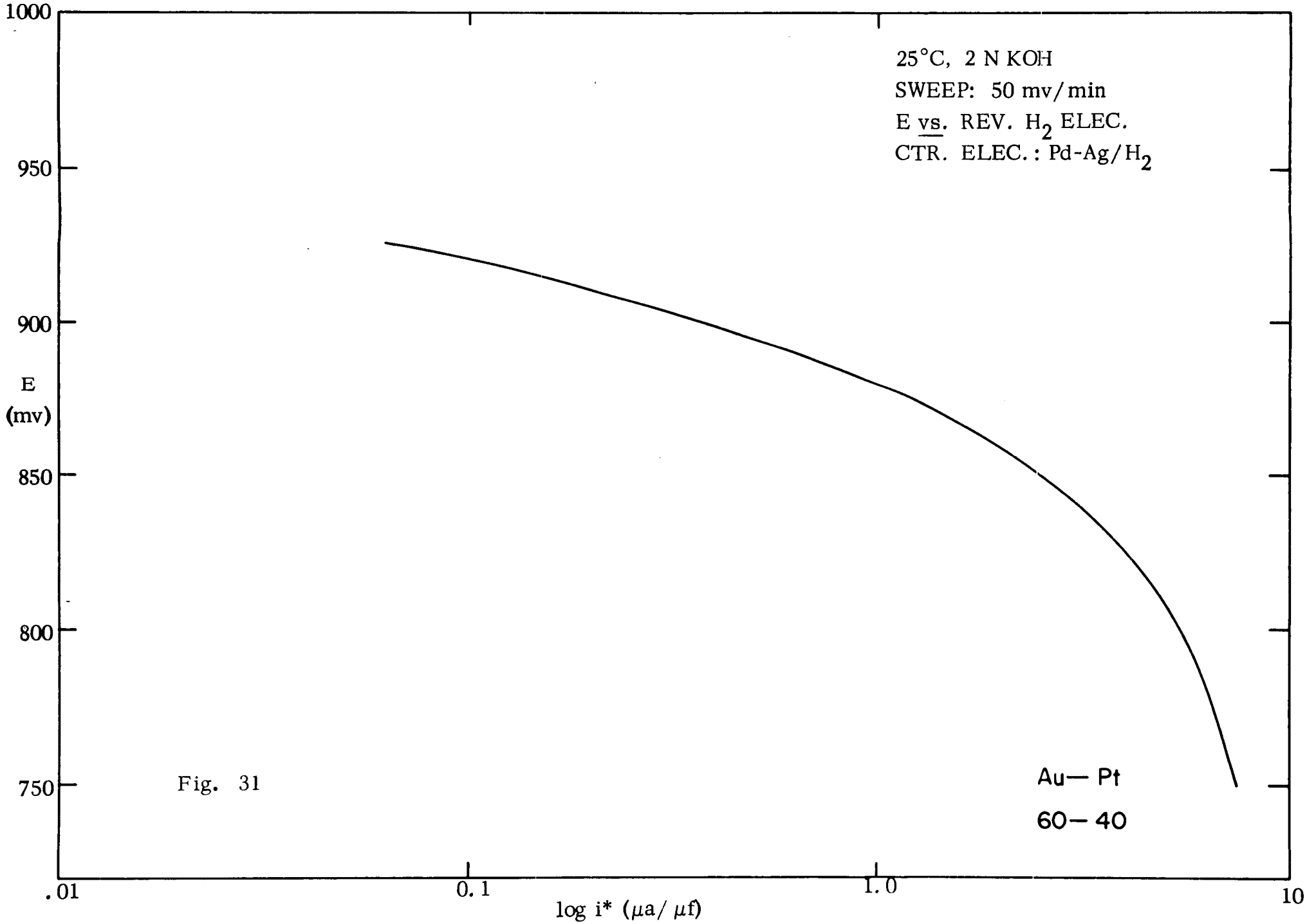
1000
950
900
E
(mv)
850
800
750
25°C, 2 N KOH
SWEEP: 50 mv/min
E vs. REV. H2 ELEC.
CTR. ELEC.: Pd-Ag/H2
Au— Pt
60— 40
.01
0.1
1.0
10
log i* (μa/ μf)

Fig. 31

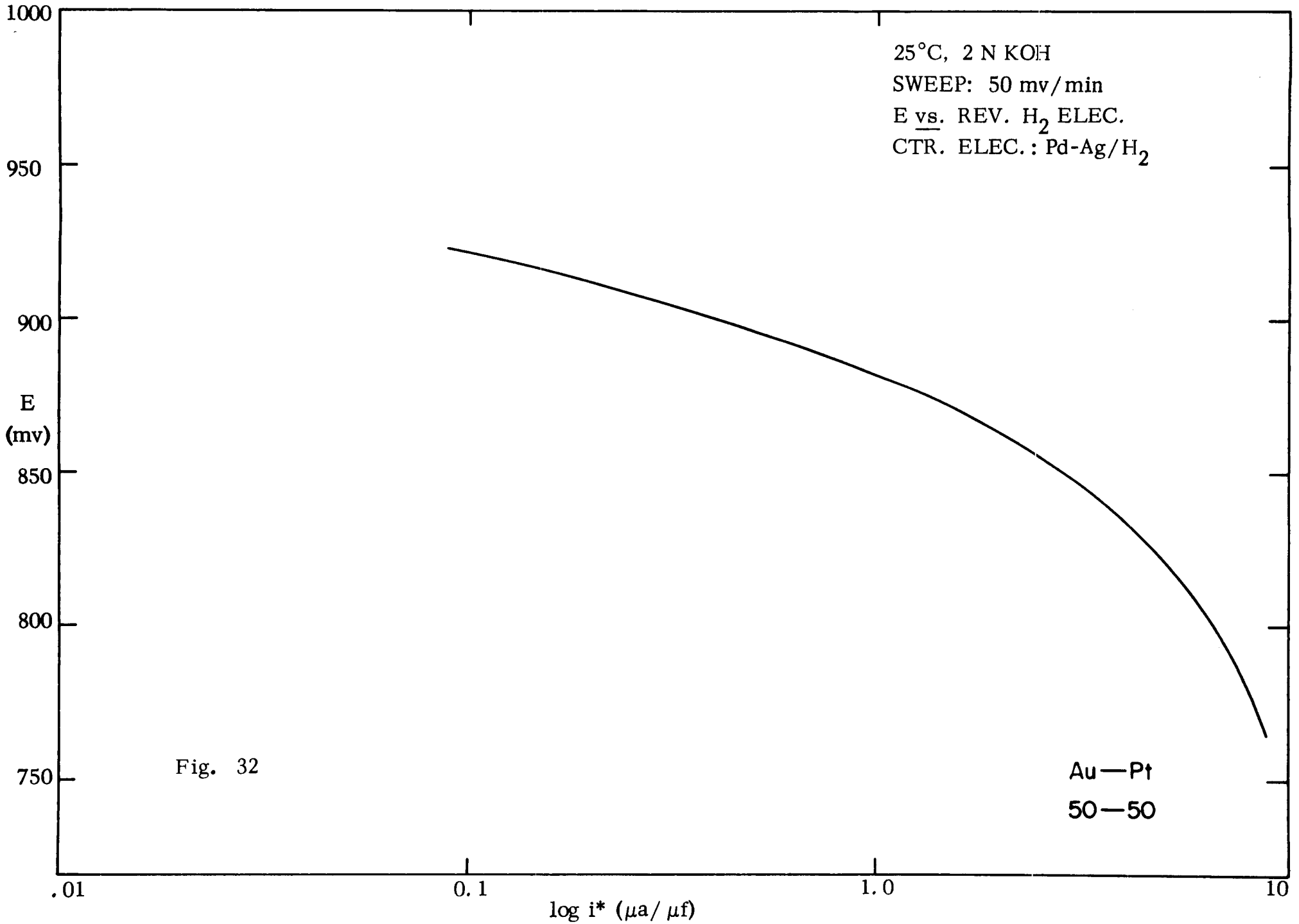
25°C, 2 N KOH
SWEEP: 50 mv/min
E vs. REV. H2 ELEC.
CTR. ELEC.: Pd-Ag/H2
1000
950
900
850
800
750
E
(mv)
.01
0.1
1.0
10
log i* (μa/μf)
Au—Pt
50—50

Fig. 32

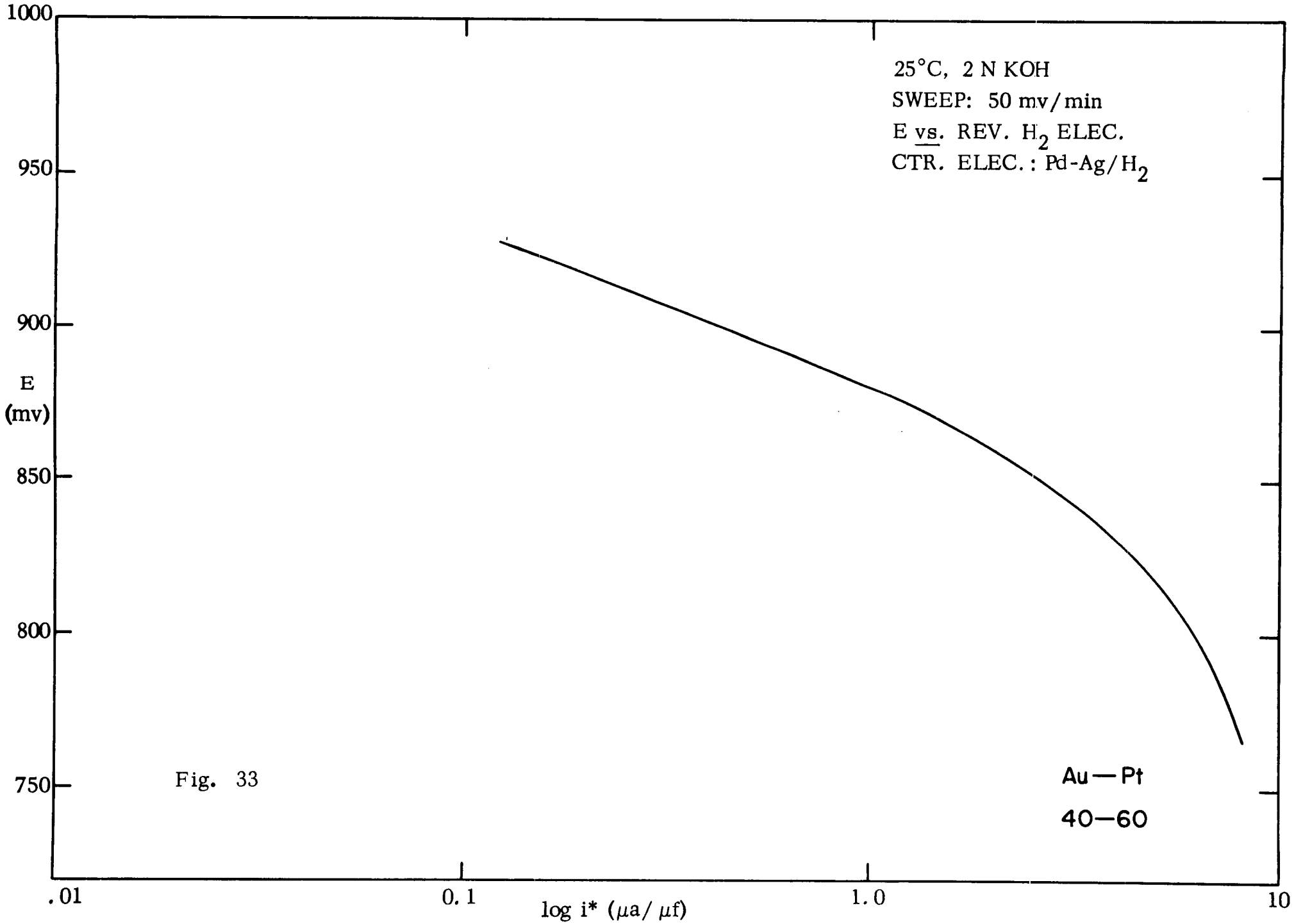
1000
950
900
E
(mv)
850
800
750
25°C, 2 N KOH
SWEEP: 50 mv/min
E vs. REV. H_2 ELEC.
CTR. ELEC.: Pd-Ag/H_2
Au — Pt
40—60
.01
0.1
1.0
10
log i* (μa/ μf)

Fig. 33

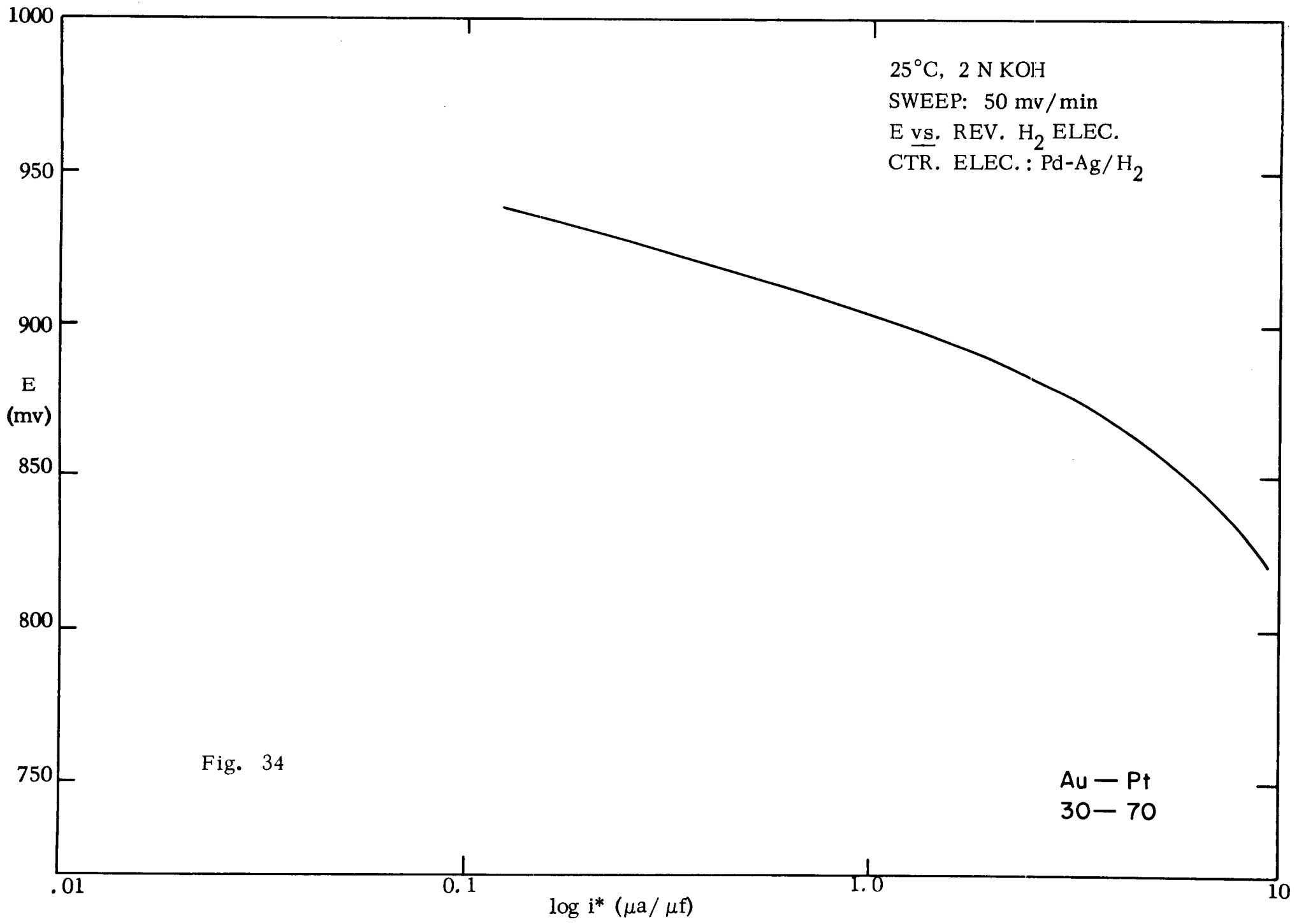
1000
950
900
E
(mv)
850
800
750
25°C, 2 N KOH
SWEEP: 50 mv/min
E vs. REV. H_2 ELEC.
CTR. ELEC.: Pd-Ag/H_2
Au — Pt
30— 70
.01
0.1
1.0
10
log i* (μa/ μf)

Fig. 34

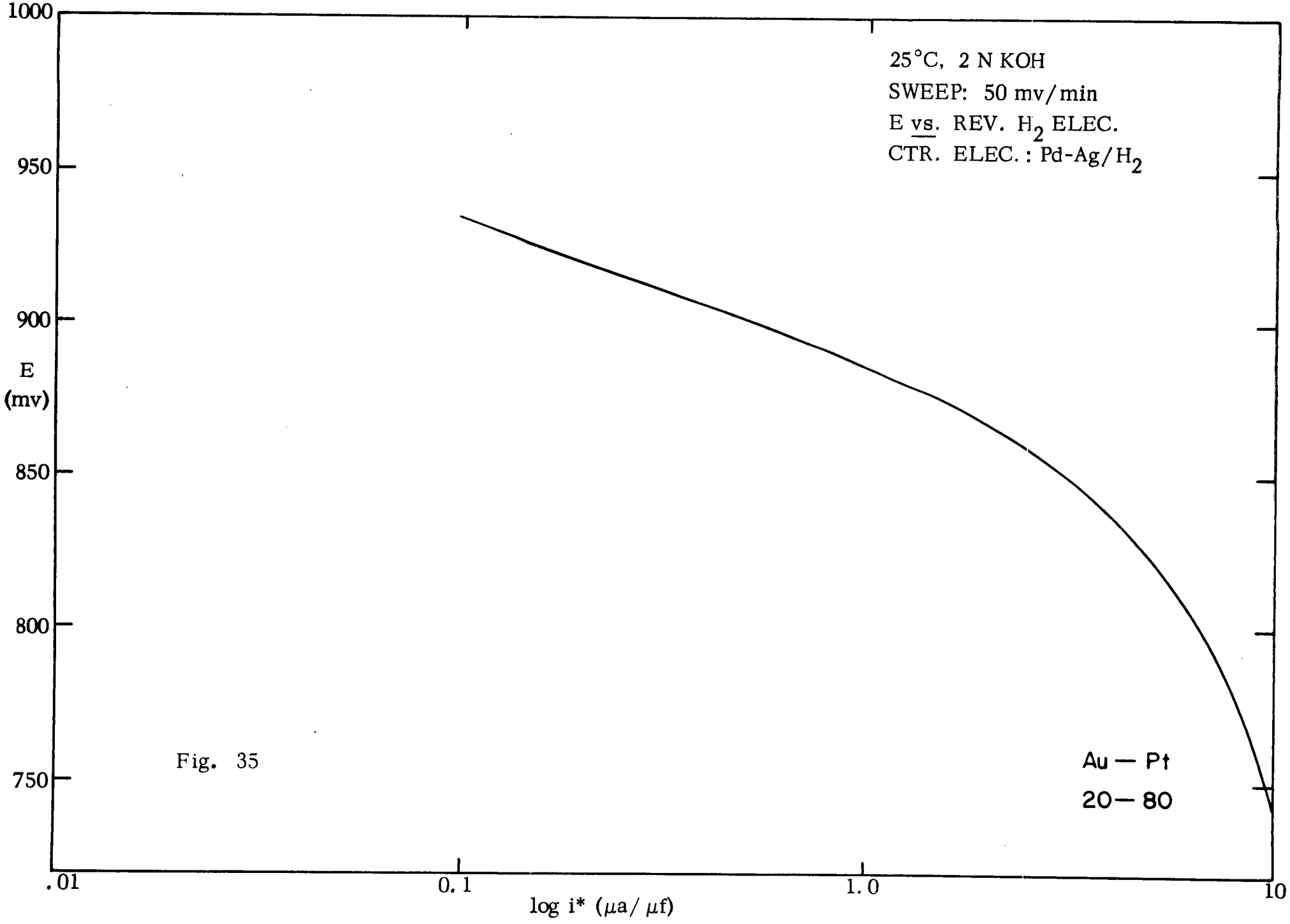
1000
950
900
E
(mv)
850
800
750
25°C, 2 N KOH
SWEEP: 50 mv/min
E vs. REV. H_2 ELEC.
CTR. ELEC.: Pd-Ag/H_2
Au — Pt
20 — 80
.01
0.1
1.0
10
log i* (μa/ μf)

Fig. 35

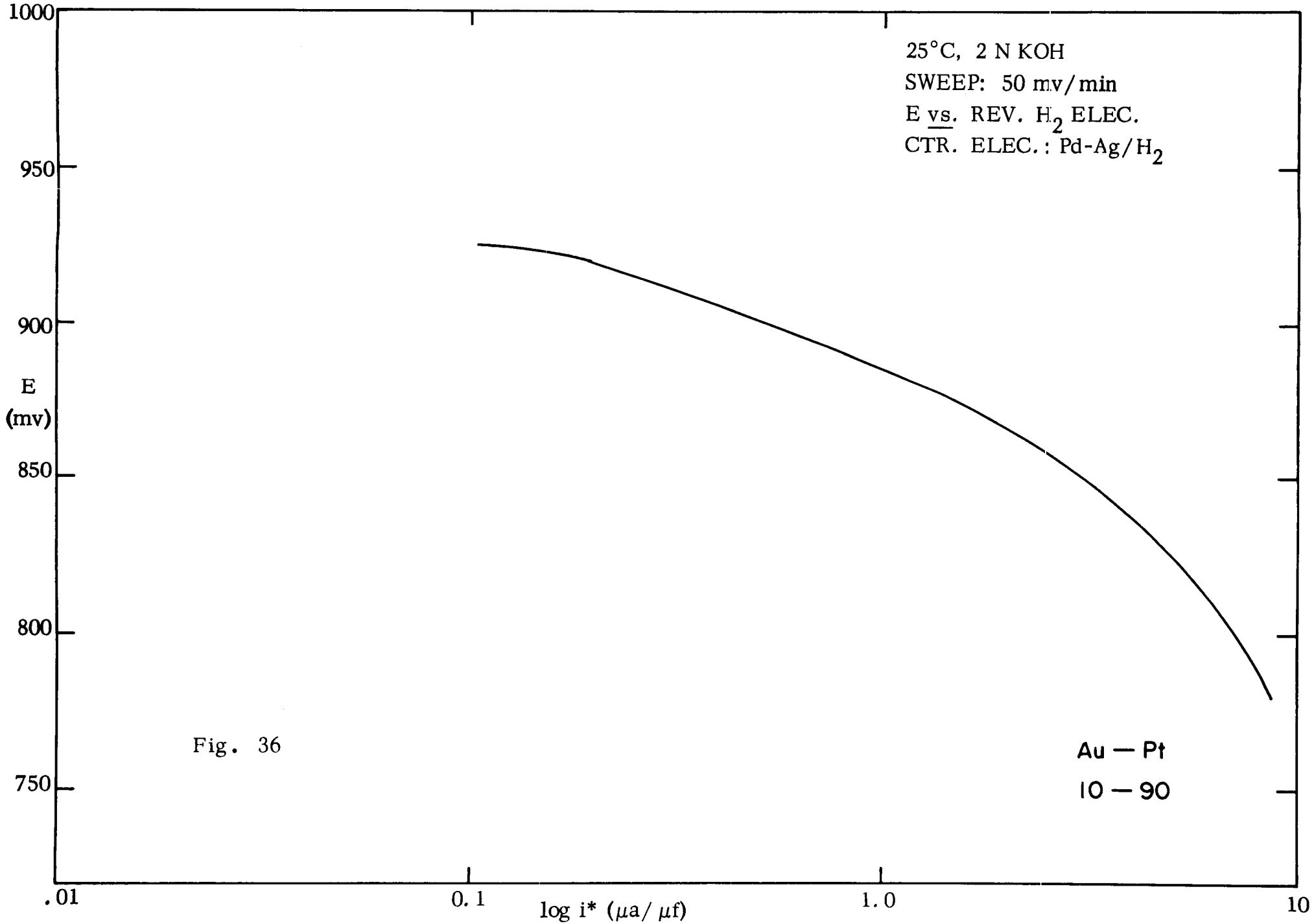
25°C, 2 N KOH
SWEEP: 50 mv/min
E vs. REV. H2 ELEC.
CTR. ELEC.: Pd-Ag/H2
1000
950
900
850
800
750
E
(mv)
.01
0.1
1.0
10
log i* (μa/ μf)
Au — Pt
10 — 90

Fig. 36

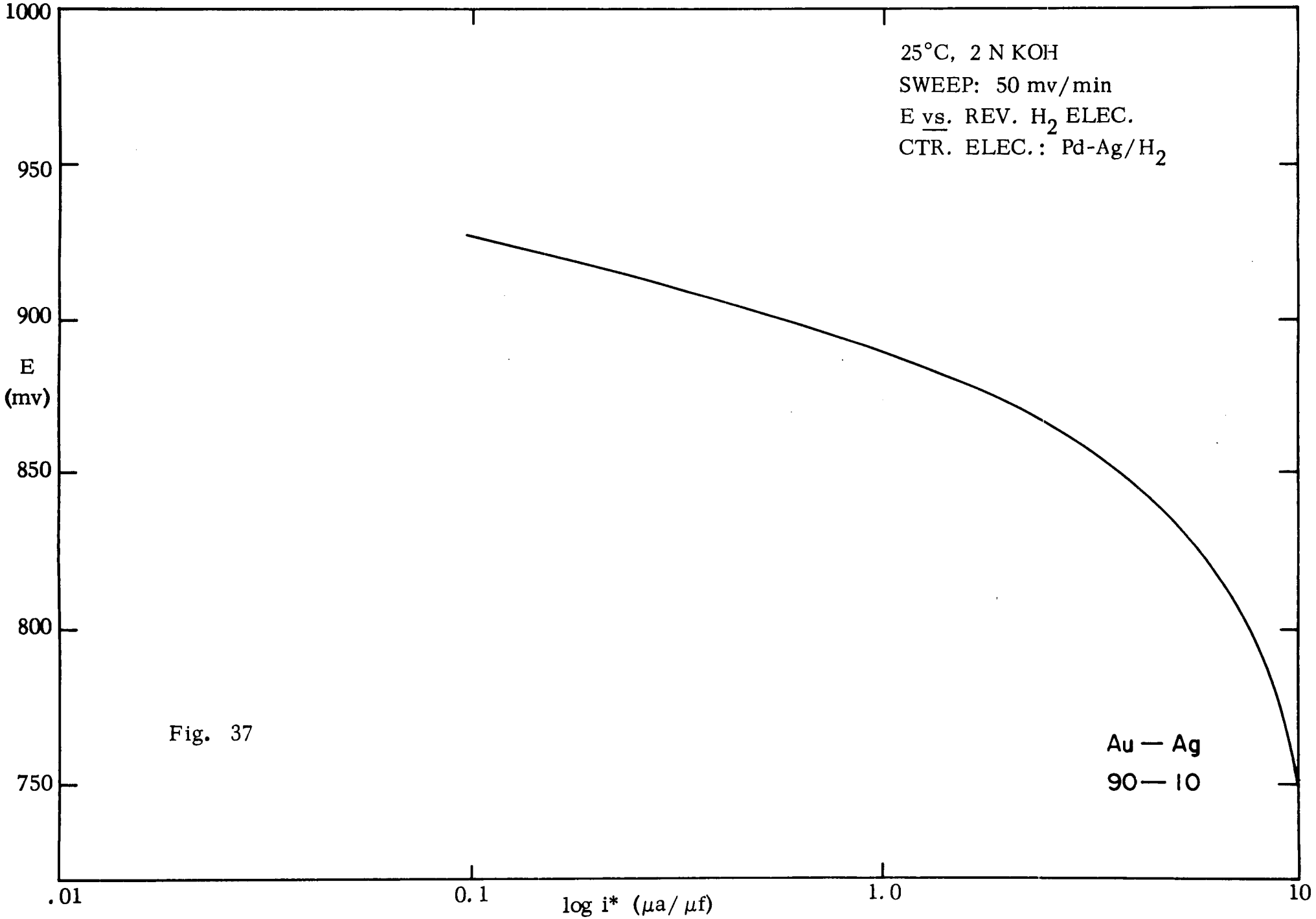
1000
950
900
E
(mv)
850
800
750
25°C, 2 N KOH
SWEEP: 50 mv/min
E vs. REV. H_2 ELEC.
CTR. ELEC.: Pd-Ag/H_2
Au — Ag
90 — 10
.01
0.1
1.0
10
log i* (μa/μf)

Fig. 37

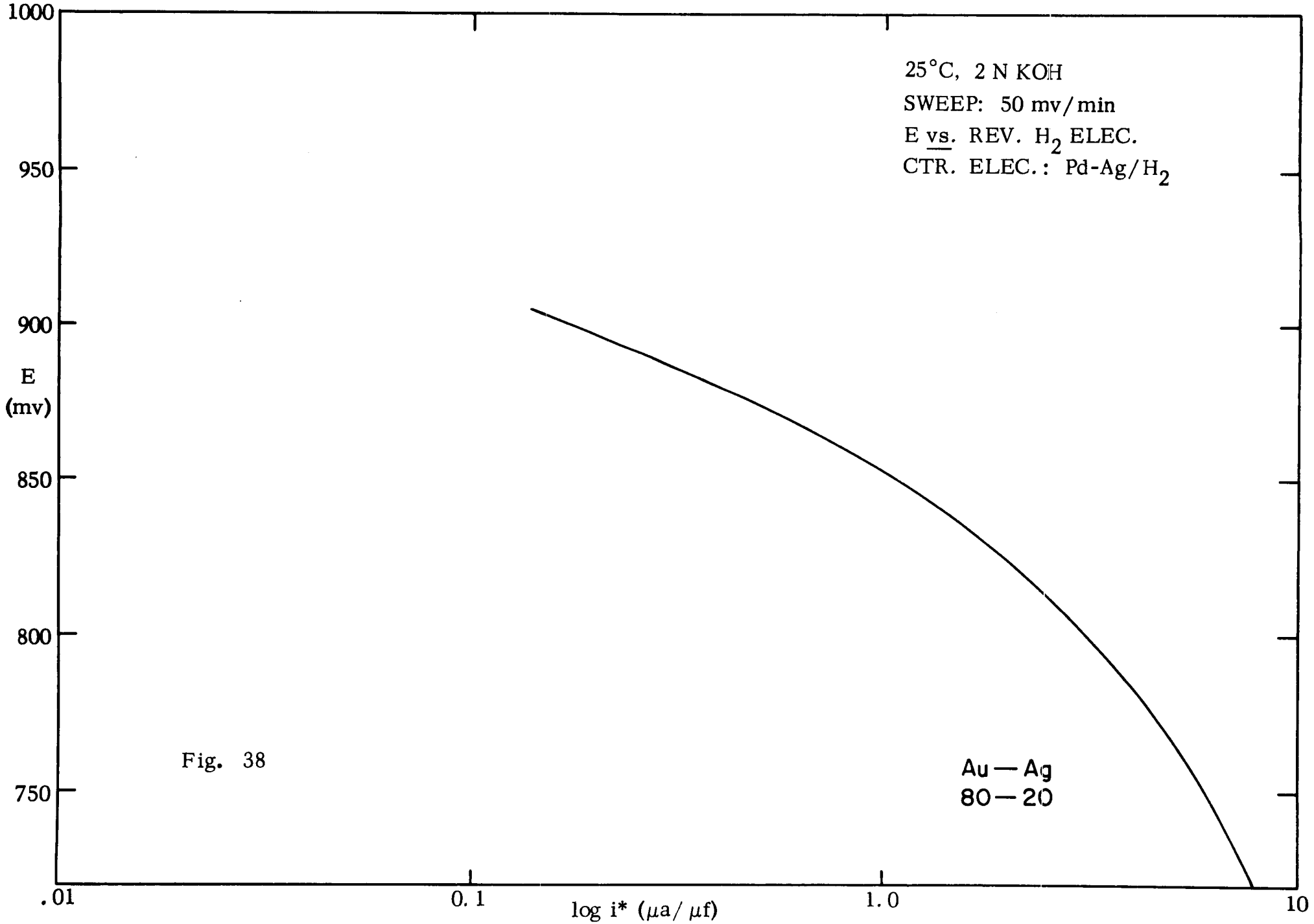
1000
950
900
E
(mv)
850
800
750
25°C, 2 N KOH
SWEEP: 50 mv/min
E vs. REV. H2 ELEC.
CTR. ELEC.: Pd-Ag/H2
Au — Ag
80 — 20
.01
0.1
1.0
10
log i* (μa/μf)

Fig. 38

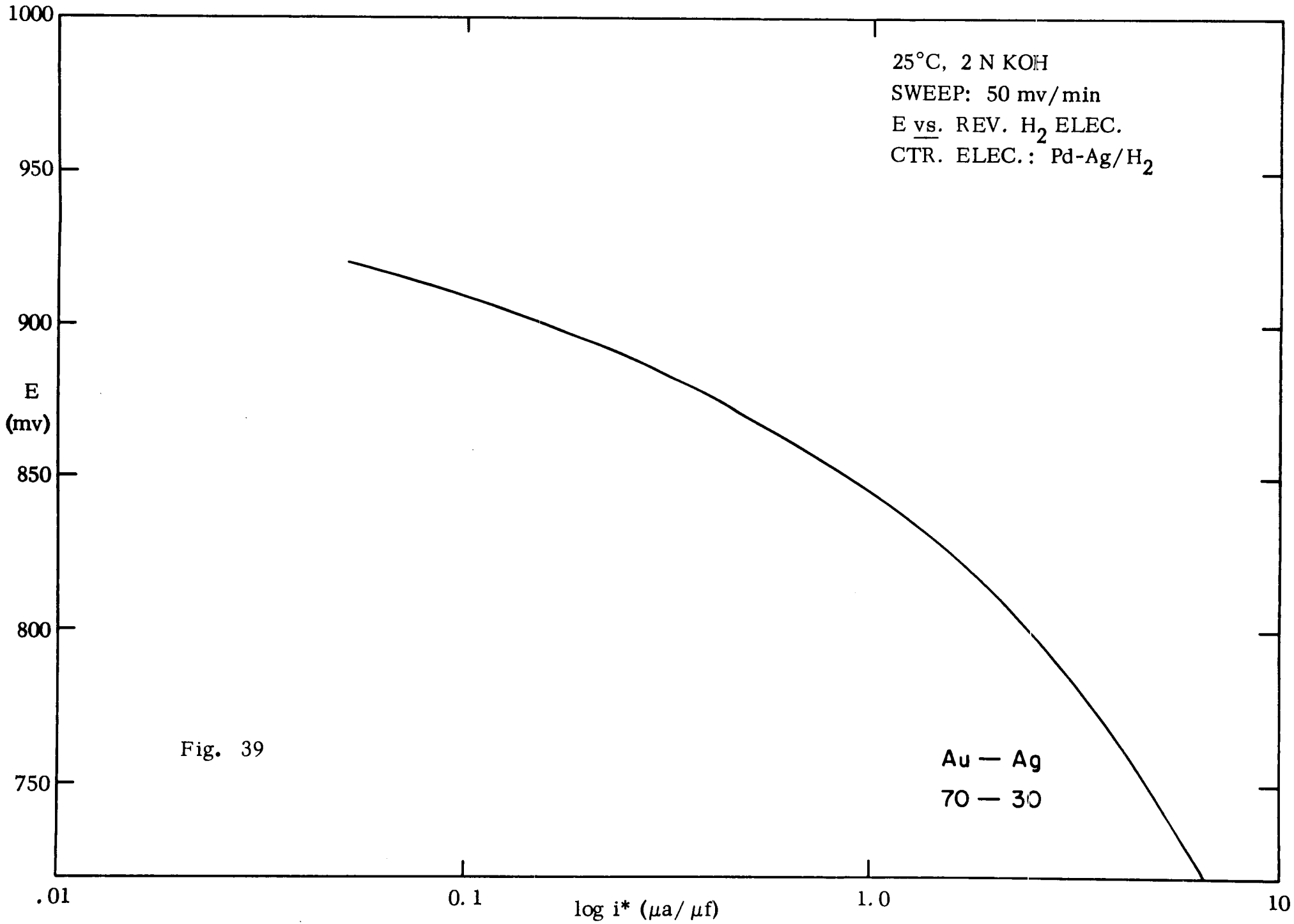
1000
950
900
E
(mv)
850
800
750
25°C, 2 N KOH
SWEEP: 50 mv/min
E vs. REV. H_2 ELEC.
CTR. ELEC.: Pd-Ag/H_2
Au — Ag
70 — 30
.01
0.1
1.0
10
log i* (μa/μf)

Fig. 39

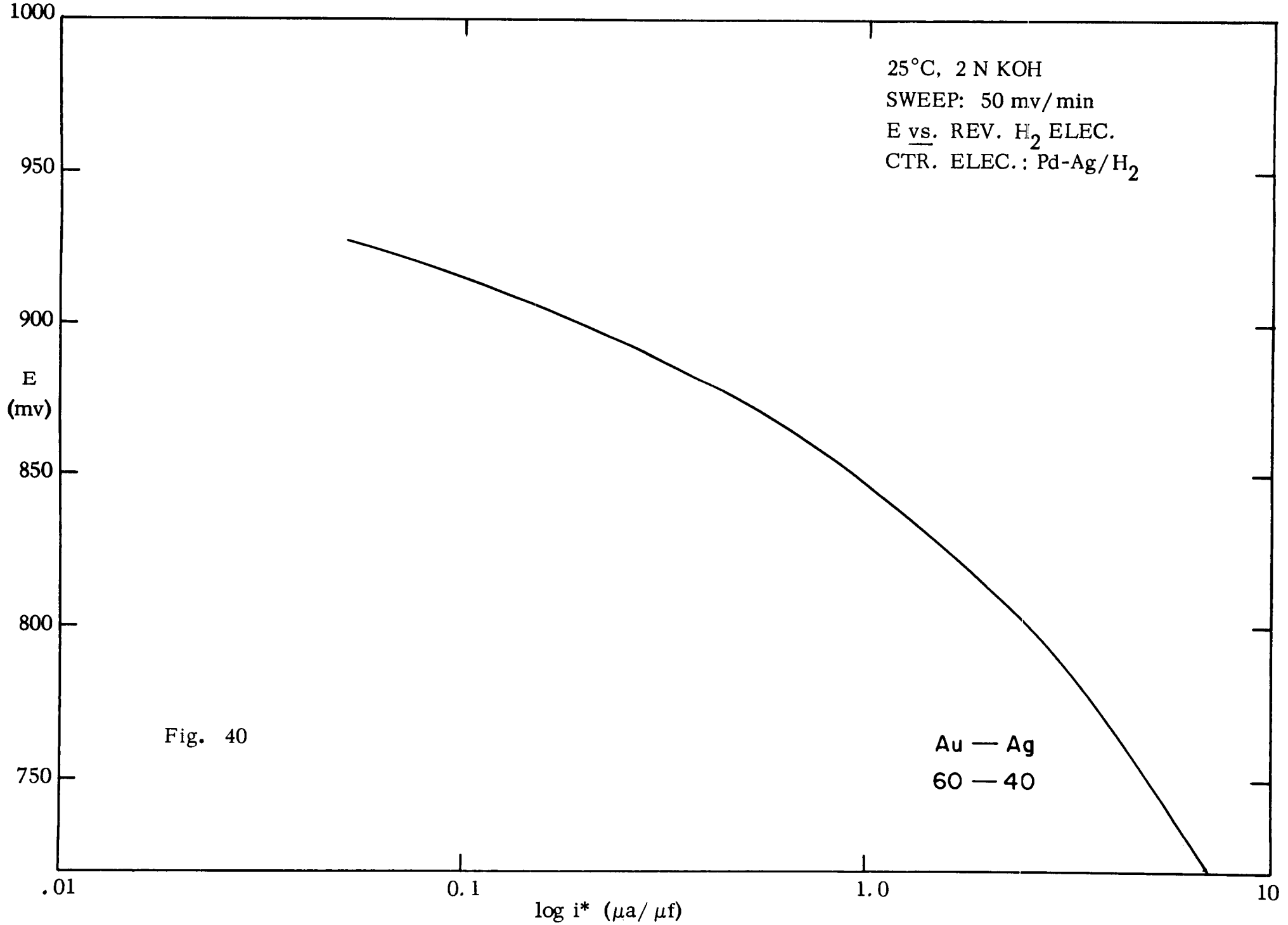
1000
950
900
E
(mv)
850
800
750
25°C, 2 N KOH
SWEEP: 50 mv/min
E vs. REV. H2 ELEC.
CTR. ELEC.: Pd-Ag/H2
Au — Ag
60 — 40
.01
0.1
1.0
10
log i* (μa/μf)

Fig. 40

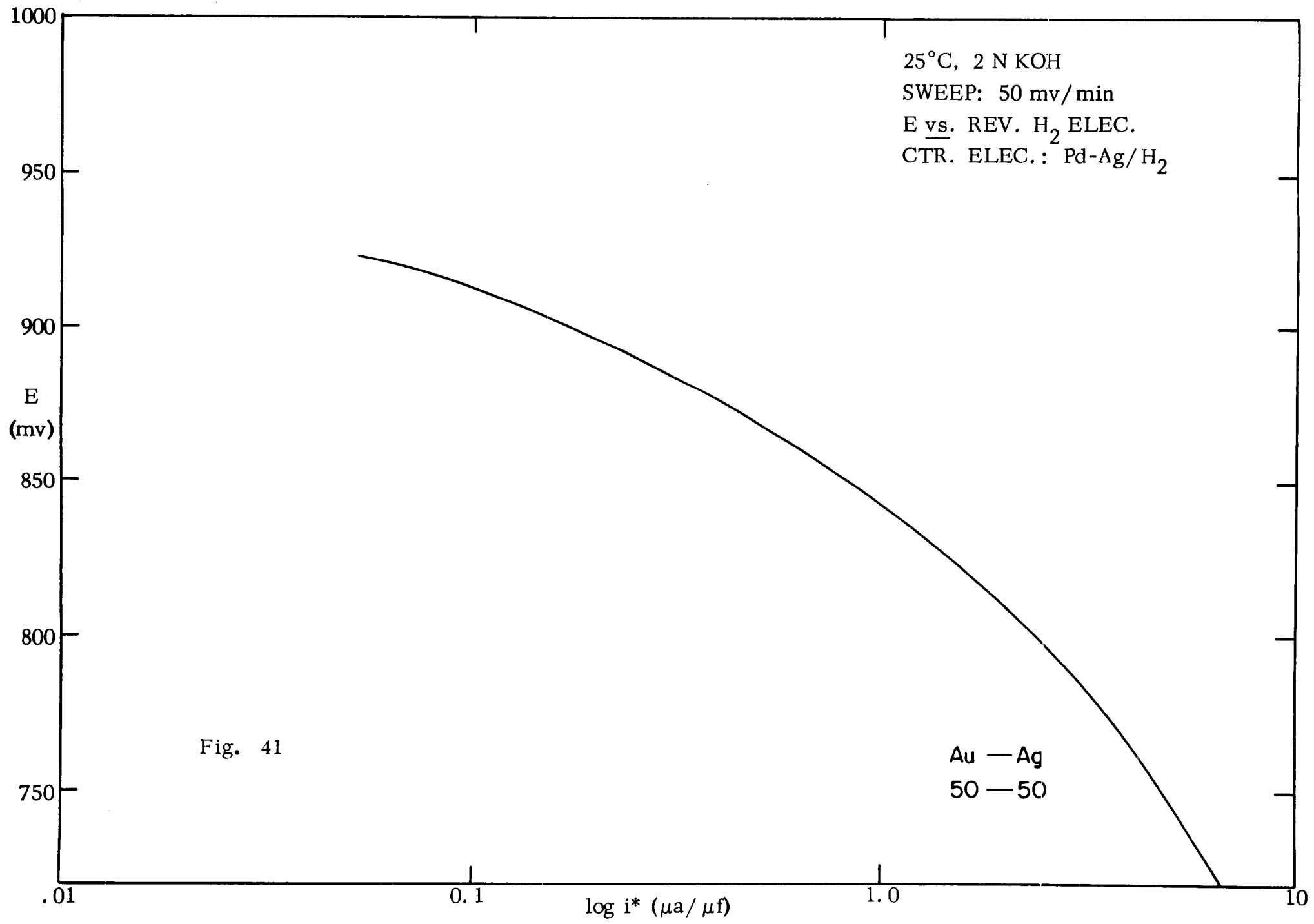
1000
950
900
E
(mv)
850
800
750
25°C, 2 N KOH
SWEEP: 50 mv/min
E vs. REV. H_2 ELEC.
CTR. ELEC.: Pd-Ag/H_2
Au —Ag
50 —50
.01
0.1
1.0
10
log i* (μa/μf)

Fig. 41

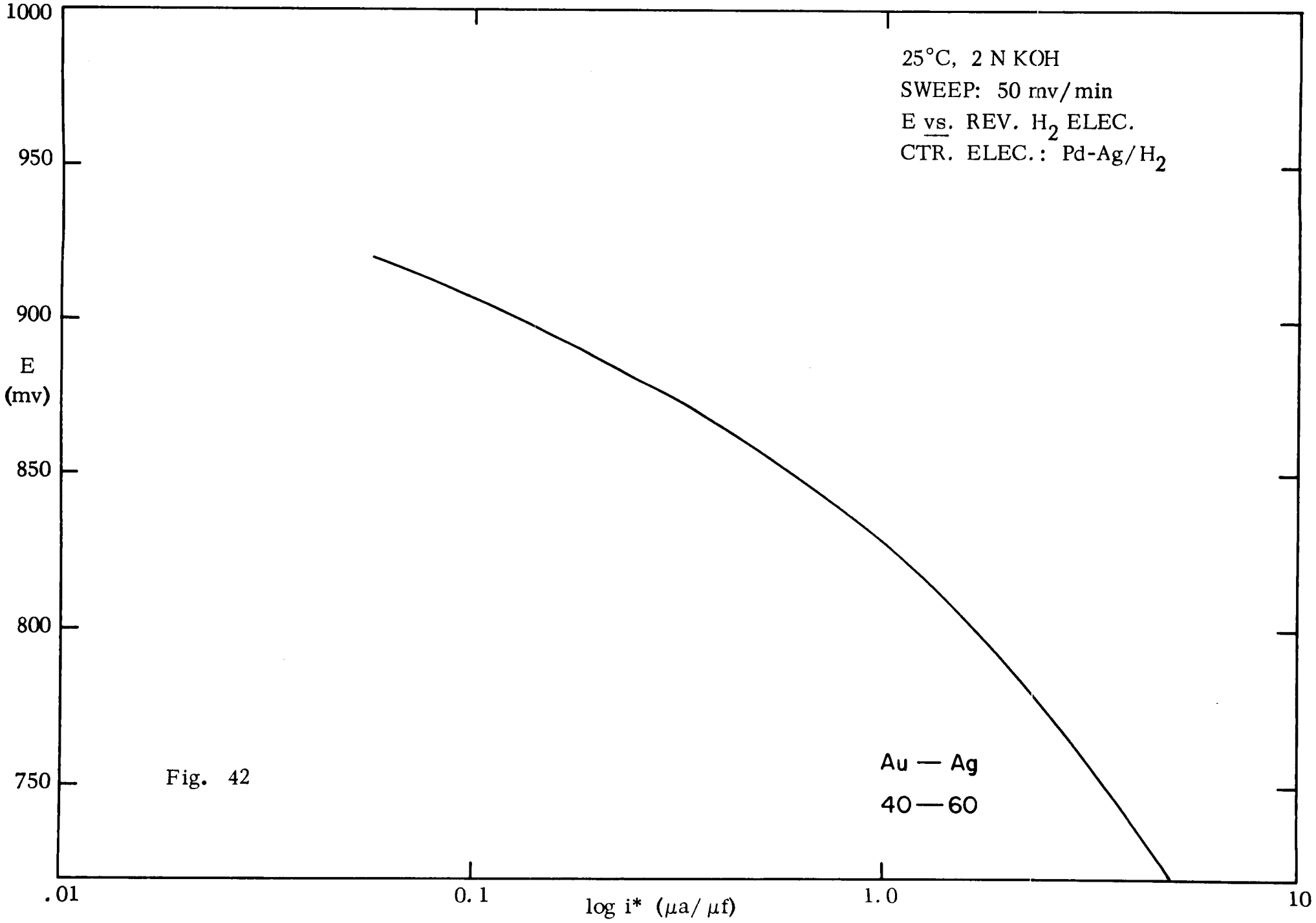
1000
950
900
E
(mv)
850
800
750
25°C, 2 N KOH
SWEEP: 50 mv/min
E vs. REV. H2 ELEC.
CTR. ELEC.: Pd-Ag/H2
Au — Ag
40—60
.01
0.1
1.0
10
log i* (μa/μf)

Fig. 42

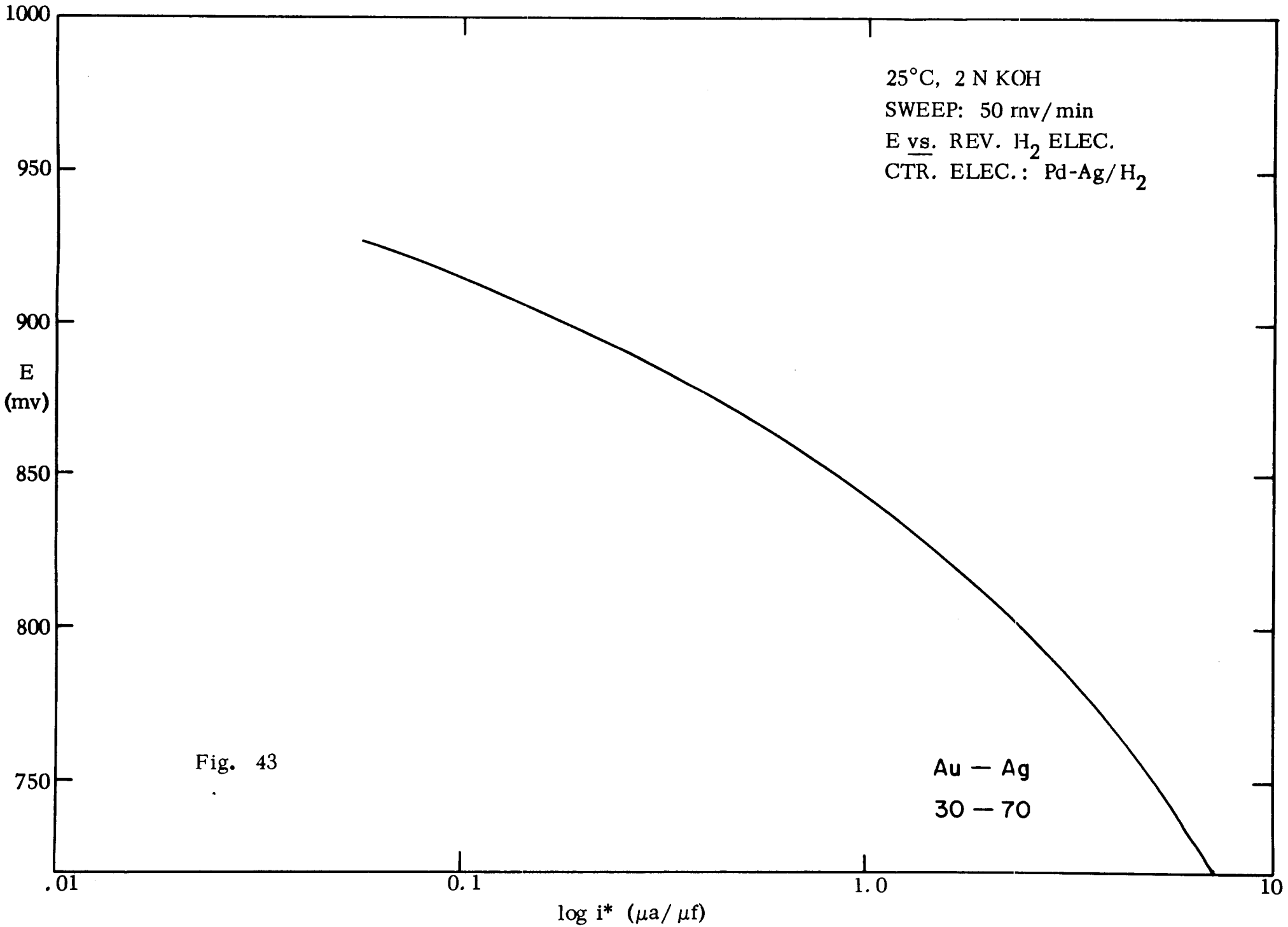
1000
950
900
E
(mv)
850
800
750
25°C, 2 N KOH
SWEEP: 50 mv/min
E vs. REV. H2 ELEC.
CTR. ELEC.: Pd-Ag/H2
Au — Ag
30 — 70
.01
0.1
1.0
10
log i* (μa/μf)

Fig. 43

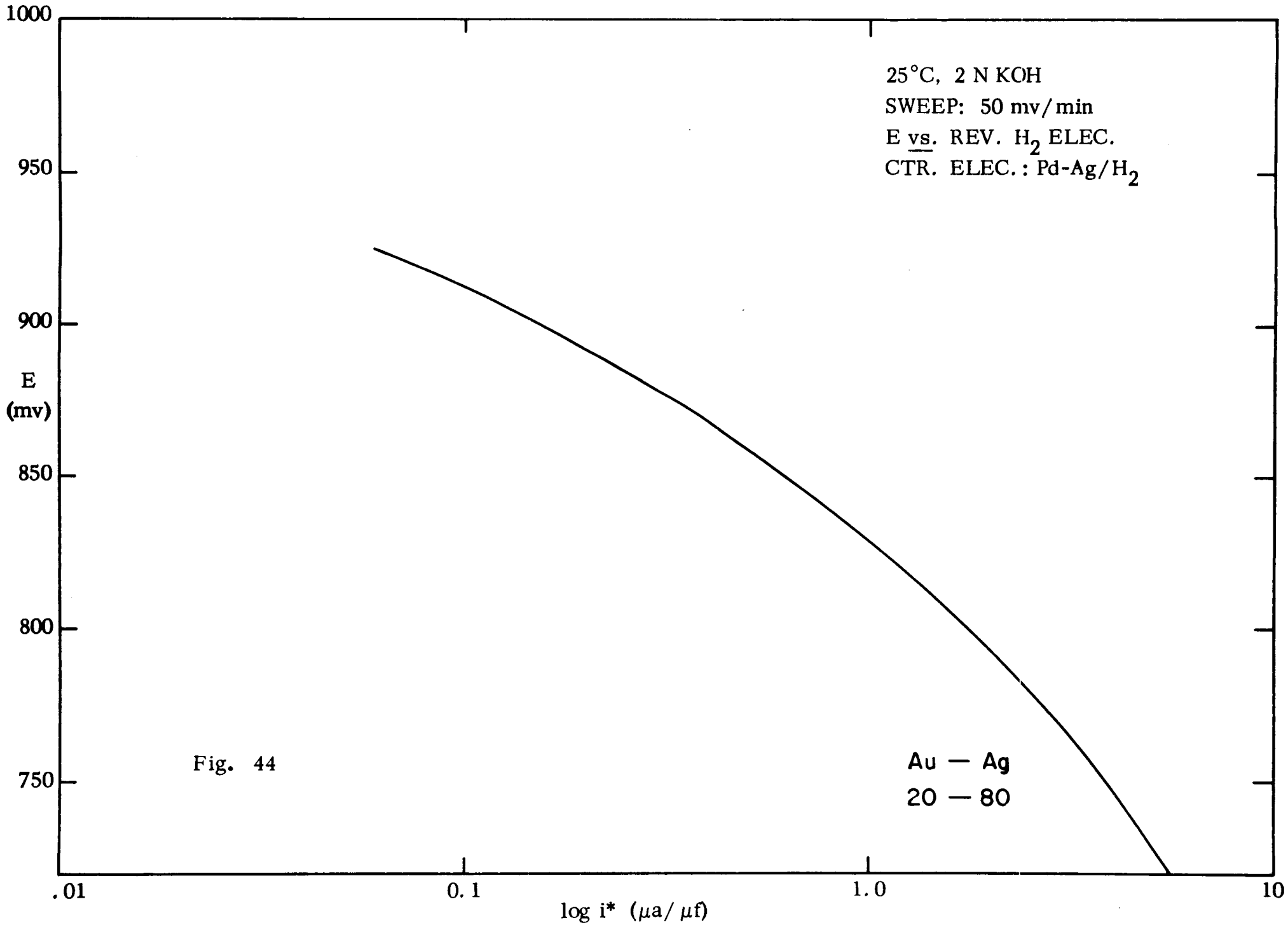
1000
950
900
E
(mv)
850
800
750
25°C, 2 N KOH
SWEEP: 50 mv/min
E vs. REV. H2 ELEC.
CTR. ELEC.: Pd-Ag/H2
Au — Ag
20 — 80
.01
0.1
1.0
10
log i* (μa/μf)

Fig. 44

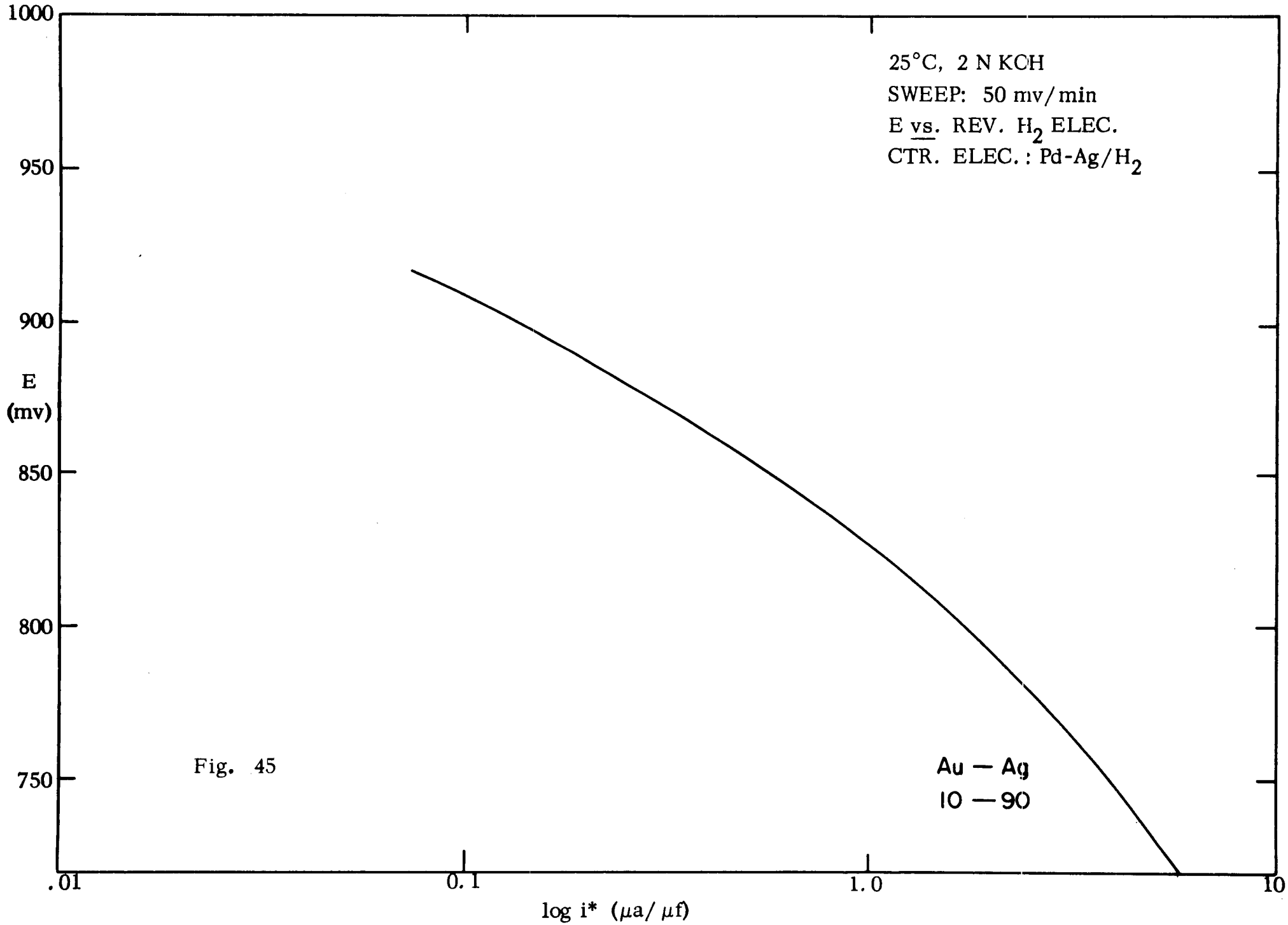
1000
950
900
E
(mv)
850
800
750
25°C, 2 N KOH
SWEEP: 50 mv/min
E vs. REV. H2 ELEC.
CTR. ELEC.: Pd-Ag/H2
Au — Ag
10 — 90
.01
0.1
1.0
10
log i* (μa/μf)

Fig. 45

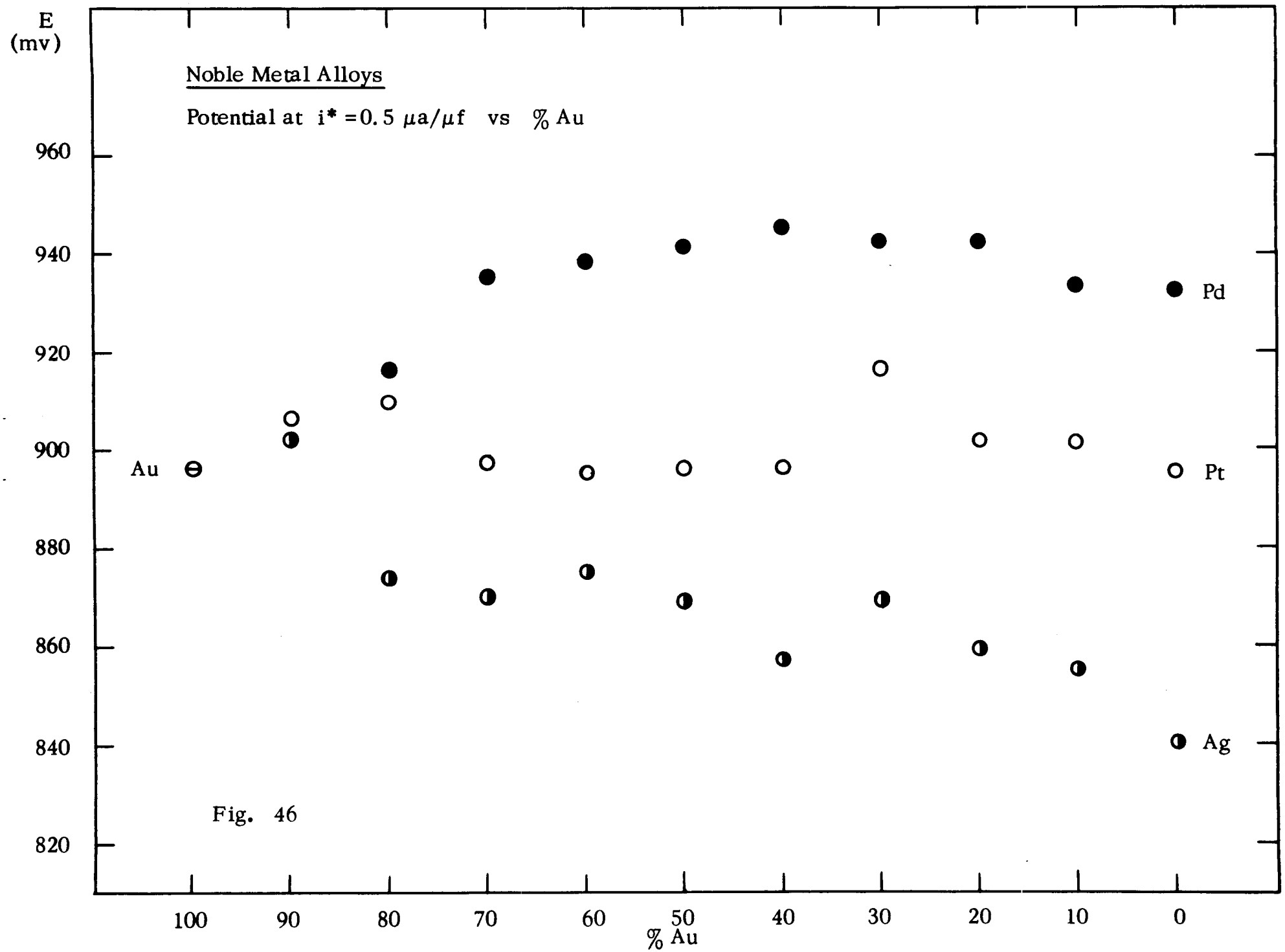
E
(mv)
Noble Metal Alloys
Potential at i* = 0.5 μa/μf vs % Au
960
940
920
900
880
860
840
820
Au
Pd
Pt
Ag
100
90
80
70
60
50
40
30
20
10
0
% Au

Fig. 46

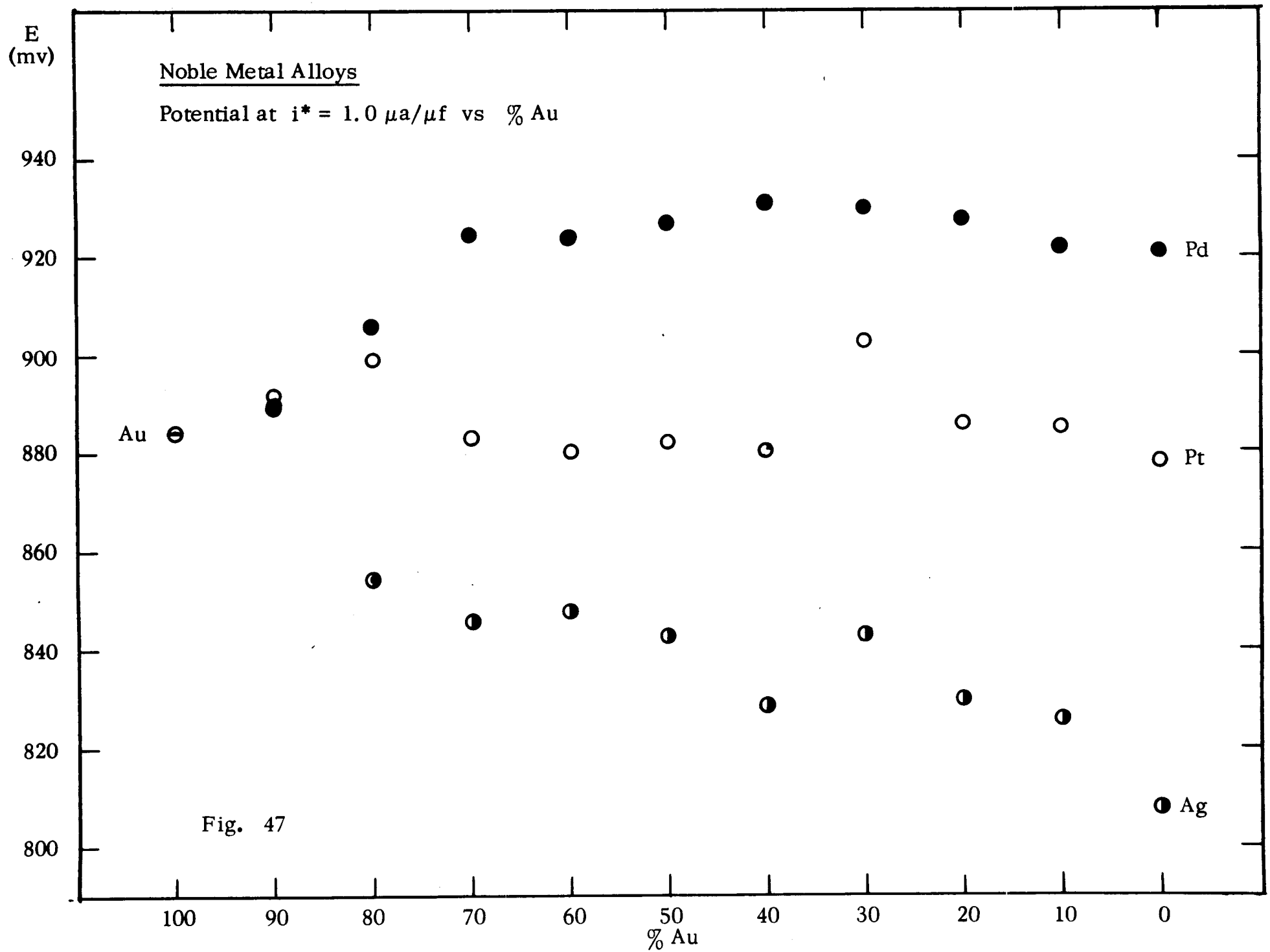
E
(mv)
Noble Metal Alloys
Potential at i* = 1.0 μa/μf vs % Au
940
920
900
880
860
840
820
800
Au
Pd
Pt
Ag
100
90
80
70
60
50
40
30
20
10
0
% Au

Fig. 47

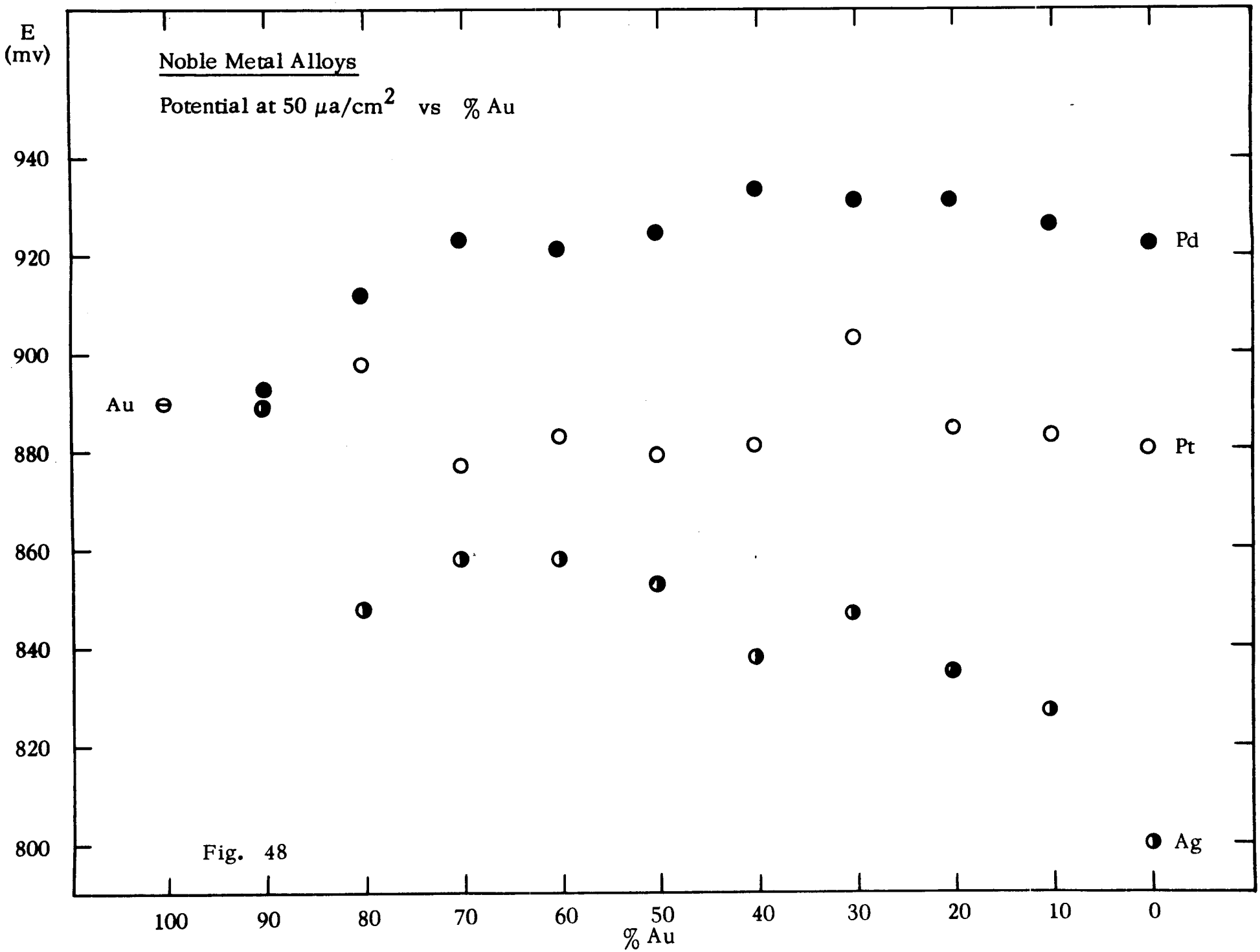
E
(mv)
Noble Metal Alloys
Potential at 50 μa/cm2 vs % Au
940
920
900
880
860
840
820
800
Au
Pd
Pt
Ag
100
90
80
70
60
50
40
30
20
10
0
% Au

Fig. 48

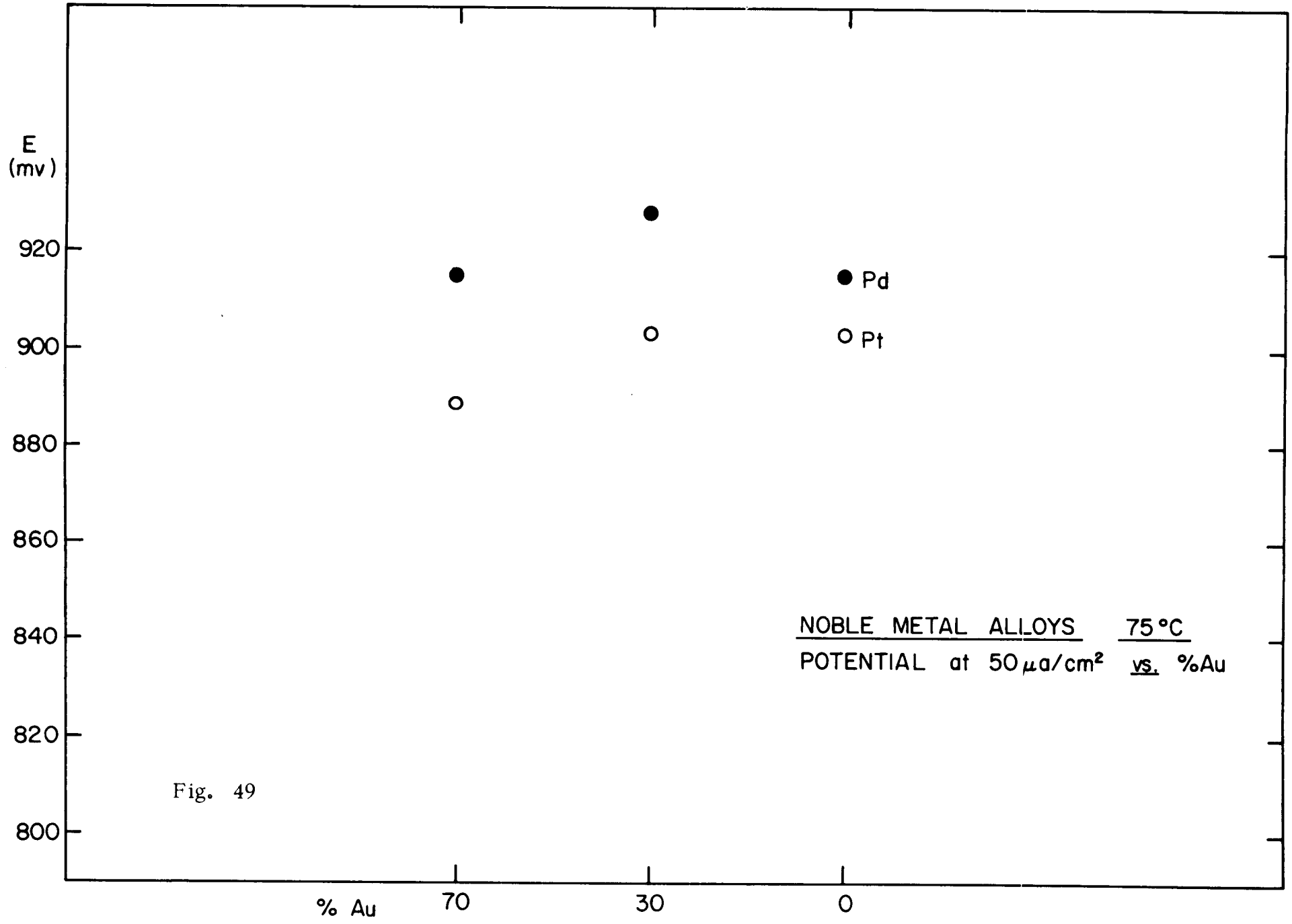
E
(mv)
920
900
880
860
840
820
800
Pd
Pt
NOBLE METAL ALLOYS 75°C
POTENTIAL at 50 μa/cm² vs. %Au
% Au
70
30
0

Fig. 49

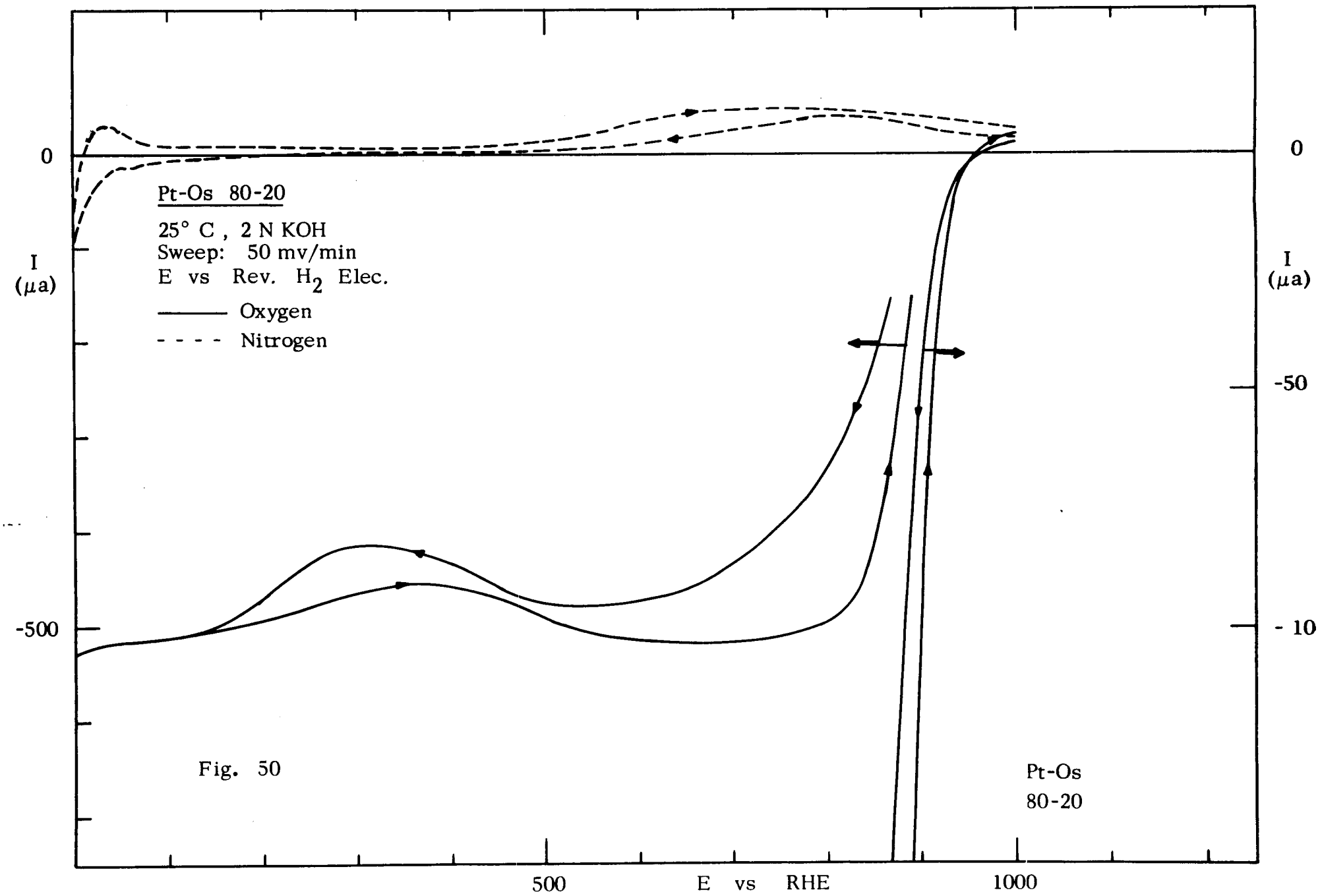
0
I
(μa)
Pt-Os 80-20
25° C , 2 N KOH
Sweep: 50 mv/min
E vs Rev. H2 Elec.
Oxygen
Nitrogen
-500
0
-50
- 10
I
(μa)
500
E vs RHE
1000
Pt-Os
80-20

Fig. 50

OFFICIAL DISTRIBUTION LIST
FOR FUEL CELL REPORTS

December 1, 1966

NASA and JPL

National Aeronautics & Space Admin.
Scientific and Technical Information Facility
College Park, Maryland 20740
Attn: NASA Representative
Send 2 copies plus 1 reproducible

National Aeronautics & Space Admin.
Washington, D.C. 20546
Attn: RNW/E. M. Cohn

National Aeronautics & Space Admin.
Washington, D. C. 20546
Attn: MAT/G. F. Esenwein

National Aeronautics & Space Admin.
Washington, D.C. 20546
Attn: FC/A. M. Greg Andrus

National Aeronautics & Space Admin.
Washington, D.C. 20546
Attn: MLT/T. Albert

National Aeronautics & Space Admin.
Goddard Space Flight Center
Greenbelt, Maryland 20771
Attn: Thomas Hennigan, Code 716.2

National Aeronautics & Space Admin.
Langley Research Center
Langley Station
Hampton, Virginia 23365
Attn: John Patterson

National Aeronautics & Space Admin.
Lewis Research Center
21000 Brookpark Road
Cleveland, Ohio 44135
Attn: Mr. Robert Miller

National Aeronautics & Space Admin.
Washington, D.C. 20546
Attention: Office of Technology Utilization

National Aeronautics & Space Admin.
Lewis Research Center
21000 Brookpark Road
Cleveland, Ohio 44135
Attn: M. J. Saari
MS 500-202

National Aeronautics & Space Admin.
Lewis Research Center
21000 Brookpark Road
Cleveland, Ohio 44135
Attn: Mr. N. D. Sanders

National Aeronautics & Space Admin.
Marshall Space Flight Center
Huntsville, Alabama 35812
Attn: Mr. Richard Boehme
R-ASTR-E

National Aeronautics & Space Admin.
Marshall Space Flight Center
Huntsville, Alabama 35812
Attn: Mr. Charles Graff
R-ASTR-EAP

National Aeronautics & Space Admin
Ames Research Center
Pioneer Project
Moffett Field, California 94035
Attn: Mr. John Rubenzer

National Aeronautics & Space Admin.
Manned Spacecraft Center
Houston, Texas 77001
Attn: Mr. William R. Dusenbury

National Aeronautics & Space Admin.
Manned Spacecraft Center
Houston Texas 77001
Attn: Mr. Hoyt McBryar
EP-5, Building 16

National Aeronautics & Space Admin.
Manned Spacecraft Center
Houston, Texas 77001
Attn: Mr. Forrest Eastman

National Aeronautics & Space Admin.
Electronics Research Center
575 Technology Square
Cambridge, Mass. 02139
Attn: Dr. Sol Gilman

Jet Propulsion Laboratory
4800 Oak Grove Drive
Pasadena, California 91103
Attn: Mr. Aiji Uchiyama

Department of the Army

U. S. Army Engineer R&D Labs.
Fort Belvoir, Virginia 22060
Attn: Energy Conversion Research Lab.

Commanding General
U. S. Army Electronics R&D Labs
Attn: Code AMSEL-KL-P
Fort Monmouth, New Jersey 07703

Harry Diamond Labs.
Room 300, Building 92
Conn. Ave. & Van Ness Street, N. W.
Washington, D.C. 20438
Attn: Mr. Nathan Kaplan

U.S. Army Natick Laboratories
Clothing & Organic Materials Div.
Natick, Massachusetts 01760
Attn: Leo A. Spano

Department of the Navy

Office of Naval Research
Department of the Navy
Washington, D.C. 20300
Attn: Dr. Ralph Roberts/H.W. Fox

U. S. Naval Research Laboratory
Washington, D.C. 20390
Attn: Dr. J. C. White
Code 6160

Commander, Naval Ship System Command
Department of the Navy
Washington, D.C. 20350
Attn: Mr. Bernard B. Rosenbaum

Commander, Naval Ship System Command
Department of the Navy
Washington, D.C. 20350
Attn: Mr. C. F. Viglotti

Naval Ordnance Laboratory
Department of the Navy
Corona, California 91720
Attn: Mr. William C. Spindler
Code 441

Naval Ordnance Laboratory
Silver Spring, Maryland 20910
Attn: Mr. Philip B. Cole
Code 232

U. S. Navy Marine Engineering Lab.
Special Projects Division
Annapolis, Maryland 21402
Attn: J. H. Harrison

Department of the Air Force

Wright-Patterson AFB
Aeronautical Systems Division
Dayton, Ohio 45433
Attn: James E. Cooper, APIP-2

AF Cambridge Research Lab.
Attn: CRE
L.G. Hanscom Field
Bedford, Massachusetts 01731
Attn: Francis X. Doherty
Edward Raskind (Wing F)

Rome Air Development Center
Griffiss AFB, New York 13442
Attn: Mr. Frank J. Mollura
(RASSM)

Other Government Agencies

Mr. Donald A. Hoatson
Army Reactor, DRD
U. S. Atomic Energy Commission
Washington, D.C. 20545

Office, DDR&E: Sea Warfare Systems
The Pentagon
Washington, D.C. 20301
Attn: G. B. Wareham

Mr. D. Bienstock
Bureau of Mines
4800 Forbes Avenue
Pittsburgh, Pa., 15213

Private Organizations

Aeronutronic Division of Philco Corp.
Technical Information Services
Ford Road
Newport, California 92663

Allis-Chalmers Mfg. Co.
1100 S. 70th St.
Milwaukee, Wisconsin 53214
Attn: John W. McNeil
Mgr, Marketing Research Div.
#3349

Allison Division of General Motors
Indianapolis, Indiana 46206
Attn: Dr. Robert E. Henderson

American Cyanamid Company
1937 W. Main Street
Stamford, Connecticut 06901
Attn: Dr. R. G. Haldeman

American Machine & Foundry
689 Hope Street
Springdale, Connecticut 06879
Attn: Dr. L. H. Shaffer
Research Division

Arthur D. Little, Inc.
Acorn Park
Cambridge, Mass., 02140
Attn: Dr. Ellery W. Stone

Aerospace Corp.
P. O. Box 95085
Los Angeles, California 90045
Attn: Tech. Library Acquisitions Group

Atomics International Division
North American Aviation, Inc.
8900 De Soto Avenue
Canoga Park, California 91304
Attn: Dr. H. L. Recht

Battelle Memorial Institute
505 King Ave.
Columbus, Ohio 43201
Attn: Dr. C. L. Faust

Bell Telephone Laboratories, Inc.
Murray Hill, New Jersey 07971
Attn: U. B. Thomas

ChemCell Inc.
150 Dey Road
Wayne, New Jersey 07470
Attn: Peter D. Richman

Clevite Corporation
Mechanical Research Division
540 East 105th Street
Cleveland, Ohio 44108
Attn: D. J. Berger

Consolidated Controls Corporation
15 Durant Avenue
Bethel, Connecticut 06801
Attn: Miss Carol R. Naas
(NsG-325 reports only)

G. & W. H. Corson, Inc.
Plymouth Meeting,
Pennsylvania 19462
Attn: Dr. L. J. Minnick

Douglas Aircraft Company, Inc.
Astropower Laboratory
2121 Campus Drive
Newport Beach, California 92663
Attn: Dr. Carl Berger

Electrochimica Corp.
1140 O'Brien Drive
Menlo Park, California 94025
Attn: Dr. Morris Eisenberg

Electro-Optical Systems, Inc.
300 North Halstead Street
Pasadena, California 91107
Attn: Martin Klien

Engelhard Industries, Inc.
497 Delancy Street
Neward, New Jersey 07105
Attn: Dr. J. G. Cohn

Esso Research and Engineering Co.
Government Division
P. O. Box 8
Linden, New Jersey 07036
Attn: Dr. C. E. Heath

The Franklin Institute
Philadelphia, Pennsylvania 19103
Attn: Mr. Robert Goodman

Garrett Corporation
1625 Eye St., N.W.
Washington, D.C. 20013
Attn: Mr. Bowler

General Dynamics/Convair
P. O. Box 1128
San Diego, California 92112
Attn: Mr. R. P. Mikkelson
Electrical Systems Dept. 988-7

General Electric Company
Direct Energy Conversion Operation
930 Western Ave.
Lynn, Massachusetts 01901
Attn: P. Schratter

General Electric Company
Research & Development Center
P. O. Box 8
Schenectady, New York 12301
Attn: Dr. H. Liebhafsky

General Electric Company
777-14th St., N. W.
Washington, D.C. 20005
Attn: Philip C. Hargraves

General Motors Corp.
Box T
Santa Barbara, California 93102
Attn: Dr. C. R. Russell

Globe-Union, Inc.
P. O. Box 591
Milwaukee, Wisconsin 53201
Attn: J. D. Onderdonk,
V.P., Marketing

Ionics, Incorporated
65 Grove Street
Watertown, Massachusetts 02172
Attn: Dr. Werner Glass

Institute for Defense Analyses
Research & Engineering Support Div.
400 Army Navy Drive
Arlington, Virginia 22202
Attn: Dr. George C. Szego

Institute for Defense Analyses
Research & Engineering Support Div.
400 Army Navy Drive
Arlington, Virginia 22202
Attn: Dr. R. Briceland

Institute of Gas Technology
State and 34th Streets
Chicago, Illinois 60616
Attn: Dr. B. S. Baker

Johns Hopkins University
Applied Physics Laboratory
8621 Georgia Avenue
Silver Spring, Maryland
Attn: Richard Cole

LTV Research Center
P. O. Box 5907
Dallas, Texas 75222
Attn: Madison Reed
(Contract W12,300 only)

Johns-Manville R&E Center
P. O. Box 159
Manville, New Jersey 08835
Attn: J. S. Parkinson

Leesona Moos Laboratories
Lake Success Park
Community Drive
Great Neck, New York 11021
Attn: Dr. A. Moos

Livingston Electronic Corporation
Route 309
Montgomeryville, Pennsylvania 18936
Attn: William F. Meyers

Lockheed Missiles & Space Company
Technical Information Center
3251 Hanover Street
Palo Alto, California 93404

McDonnell Aircraft Corporation
Attn: Project Gemini Office
P. O. Box 516
St. Louis, Missouri 63166

Midwest Research Institute
425 Volker Boulevard
Kansas City, Missouri 64110
Attn: Physical Science Library

Monsanto Research Corporation
Boston Laboratories
Everett, Massacusetts 02149
Attn: Dr. J. O. Smith

Monsanto Research Corporation
Dayton Laboratory
Dayton, Ohio 45407
Attn: Librarian

North American Aviation Co.
S&ID Division
Downey, California 90241
Attn: Dr. James Nash

Oklahoma State University
Stillwater, Oklahoma 74075
Attn: Prof. William L. Hughes
School of Electrical Engineering

Power Information Center
University of Pennsylvania
Moore School Building
200 South 33rd Street
Philadelphia, Pennsylvania 19104

Radio Corporation of America
Astro Division
P. O. Box 800
Hightstown, New Jersey 08540
Attn: Dr. Seymour Winkler

Rocketdyne
6633 Canoga Avenue
Canoga Park, California 91304
Attn: Library, Dept. 086-306-Zone 2

Speer Carbon Company
Research & Development Laboratories
Packard Road at 47th Street
Niagara Falls, New York 14304
Attn: W. E. Parker

Stanford Research Institute
820 Mission Street
So. Pasadena, California 91108
Attn: Dr. Fritz Kalhammer

Texas Instruments, Inc.
P. O. Box 5936
Dallas, Texas 75222
Attn: Mr. Issac Trachtenberg

TRW, Inc.
23555 Euclid Avenue
Cleveland, Ohio 44115
Attn: Dr. R. A. Wynveen

TRW Systems
One Space Park
Redondo Beach, California 90278
Attn: Dr. A. Krausz

Tyco Laboratories, Inc.
Bear Hill
Hickory Drive
Waltham, Massachusetts 02154
Attn: Dr. A. C. Makrides

Unified Science Associates, Inc.
826 S. Arroyo Parkway
Pasadena, California 91105
Attn: Dr. Sam Naiditch

Union Carbide Corporation
Electronics Division
P. O. Box 6116
Cleveland, Ohio 44101
Attn: Dr. George E. Evans

United Aircraft Corporation
400 Main Street
East Hartford, Connecticut 06108
Attn: Library

University of Pennsylvania
Electrochemistry Laboratory
Philadelphia, Pennsylvania 19104
Attn: Prof. John O'M. Bockris

University of Pennsylvania
Institute for Direct Energy Conversion
260 Towne Building
Philadelphia, Pennsylvania 19104
Attn: Dr. Manfred Altman

Western Reserve University
Department of Chemistry
Cleveland, Ohio 44101
Attn: Prof. Ernest Yeager

Research a nd Development Center
Westinghouse Electric Corporation
Churchill Borough
Pittsburgh, Pennsylvania 15235
Attn: Dr. A. Langer

Whittaker Corporation
Narmco R&D Division
3540 Aero Court
San Diego, Calif. 92123
Attn: Dr. M. Shaw

Yardney Electric Corp.
40 Leonard Street
New York, New York 10013
Attn: Dr. George Dalin

Dynatch Corp.,
17 Tudor Street
Cambridge, Mass. 02139

Zaromb Research Corp.
376 Monroe Street
Passaic, N. Y. 07055